

January 2013

Corrosion of Post-Tensioning Strands in UngROUTED Ducts - Unstressed Condition

Michael John Hutchison

University of South Florida, jefrk2@gmail.com

Follow this and additional works at: <http://scholarcommons.usf.edu/etd>



Part of the [Civil Engineering Commons](#), and the [Materials Science and Engineering Commons](#)

Scholar Commons Citation

Hutchison, Michael John, "Corrosion of Post-Tensioning Strands in UngROUTED Ducts - Unstressed Condition" (2013). *Graduate Theses and Dissertations*.

<http://scholarcommons.usf.edu/etd/4905>

This Thesis is brought to you for free and open access by the Graduate School at Scholar Commons. It has been accepted for inclusion in Graduate Theses and Dissertations by an authorized administrator of Scholar Commons. For more information, please contact scholarcommons@usf.edu.

Corrosion of Post-Tensioning Strands
in UngROUTED Ducts – Unstressed Condition

by

Michael Hutchison

A thesis submitted in partial fulfillment
of the requirements for the degree of
Master of Science in Materials Science and Engineering
Department of Chemical and Biomedical Engineering
College of Engineering
University of South Florida

Major Professor: Alberto Sagüés, Ph.D.
Gray Mullins, Ph.D.
Wenjun Cai, Ph.D.

Date of Approval:
November 7, 2013

Keywords: Wire Bending, Relative Humidity,
Seven-wire Steel Strand, Shallow Pitting, Marine Exposure

Copyright © 2013, Michael Hutchison

ACKNOWLEDGMENTS

I would like to express my deepest gratitude to Dr. Alberto Sagüés for his guidance, advice, and encouragement. I would also like to thank Dr. Gray Mullins and Dr. Wenjun Cai for their participation in the committee, as well as Dr. Kingsley Lau for valuable technical discussions.

I would like to thank the Florida Department of Transportation for their sponsorship, participation, and particularly Richard DeLorenzo and Mark Conley for their assistance in mechanical testing.

The opinions, findings, and conclusions expressed here are those of the author and not necessarily those of the Florida Department of Transportation or the University of South Florida.

TABLE OF CONTENTS

LIST OF TABLES.....	iii
LIST OF FIGURES.....	iv
ABSTRACT.....	viii
INTRODUCTION.....	1
Background.....	1
Corrosion.....	3
Objective.....	6
Literature Review.....	7
Corrosion During the UngROUTED Period.....	7
Corrosion in Subsequent Service.....	9
Summary.....	20
APPROACH.....	22
METHODOLOGY.....	24
Facility Design.....	24
Testing Design.....	27
Environment.....	27
Duct Conditions.....	27
Exposure Lengths.....	28
Strand Material.....	29
Evaluation Methods.....	30
Relative Humidity.....	30
Visual Inspection.....	30
Tensile Testing.....	31
Metallography.....	32
Experimental Setup of Prior Study.....	34
RESULTS.....	35
Relative Humidity and Temperature.....	35
Temperature.....	36
Closed and Dry Ducts.....	37
One End Open Ducts.....	38
Both Ends Open Ducts.....	39

Closed and Wet Ducts	40
Visual Inspection	41
Tensile Testing	43
Load at Failure	45
Total Elongation	47
Load at 1% Extension	49
Statistics	51
Fracture Surface	54
Metallography	56
DISCUSSION	62
Relative Humidity and Temperature	62
Water Availability	64
Visual Inspection	65
Environment	66
Duct Conditions	66
Exposure Length	67
Tensile Testing	67
Metallography	69
Discussion on Limit Conditions Associated with Corrosion	70
General (Uniform) Corrosion Approximation	70
Pitting	72
Comparison with Prior Study	73
CONCLUSIONS	75
FUTURE WORK	77
REFERENCES	78
APPENDIX 1 PHOTOGRAPHIC EVALUATION	82
Typical Strand As Received	82
Duct Condition Comparison - SSK Strands	83
Duct Condition Comparison – USF Strands	84
Exposure Length Comparison – SSK Strands	85
Exposure Length Comparison – USF Strands	86
Environment Comparison – As Extracted	87
Environment Comparison – Cleaned	88
APPENDIX 2 STRAND MANUFACTURER STRENGTH REPORT	89
APPENDIX 3 TENSILE TESTING DATA	90

LIST OF TABLES

Table 1 Duct Environment Conditions	28
Table 2 Strand Extraction Dates and Approximate Extraction Times	35
Table 3 Standard Deviation Values for Each Experiment Variable	51
Table 4 Mean Values for Each Experiment Variable	51

LIST OF FIGURES

Figure 1 Anodic Polarization Curve of a Metal Which Can Passivate (Source: Gellings, Modified by Hutchison)	5
Figure 2 USF Duct Facility in the Open Position	25
Figure 3 SSK Duct Facility in the Closed Position - Sunshine Skyway Bridge Main Span and Generator Control Room in the Background	25
Figure 4 Relative Humidity & Temperature Probe Housings Attached to Ducts via Vent Port and Secured with Wood Boards and Zip-Ties	26
Figure 5 Water Reservoir Attached via Vent Port (left) and Closed Vent Port Covered with Bug Shield (Right).....	26
Figure 6 Strand Group Ready for Duct Insertion with Galvanized Spike Secured with Stainless Steel Hose Clamp.....	27
Figure 7 Schematic of Strand Cross Section.....	29
Figure 8 Strand Identification Code.....	30
Figure 9 Locations of Cut Sections for Tensile Testing from Exposed Strands.....	31
Figure 10 Strand Ends' Grip Material Configuration.....	32
Figure 11 "U" Bend Illustration	33
Figure 12 Typical Wire After Bending.....	34
Figure 13 Temperature of 2-End Open Ducts at USF (Black) and SSK (Red) Locations	36
Figure 14 Relative Humidity of Duct 1 at SSK.....	37
Figure 15 Relative Humidity of Duct 5 at SSK.....	37
Figure 16 Relative Humidity of Duct 1 at USF.....	37
Figure 17 Relative Humidity of Duct 5 at USF.....	37

Figure 18 Relative Humidity of Duct 2 at SSK.....	38
Figure 19 Relative Humidity of Duct 6 at SSK.....	38
Figure 20 Relative Humidity of Duct 2 at USF.....	38
Figure 21 Relative Humidity of Duct 6 at USF.....	38
Figure 22 Relative Humidity of Duct 4 at SSK.....	39
Figure 23 Relative Humidity of Duct 8 at SSK.....	39
Figure 24 Relative Humidity of Duct 4 at USF.....	39
Figure 25 Relative Humidity of Duct 8 at USF.....	39
Figure 26 Relative Humidity of Duct 3 at SSK.....	40
Figure 27 Relative Humidity of Duct 7 at SSK.....	40
Figure 28 Relative Humidity of Duct 3 at USF.....	40
Figure 29 Relative Humidity of Duct 7 at USF.....	40
Figure 30 Outer Wire of 9-Month SSK Wet Exposure Sample - Before Bending (1/3).....	41
Figure 31 Outer Wire of 9-Month SSK Wet Exposure Sample - Before Bending (2/3).....	41
Figure 32 Outer Wire of 9-Month SSK Wet Exposure Sample - Before Bending (3/3).....	41
Figure 33 Outer Wire of 8-Week SSK 2-Open Exposure Sample - Before Bending.....	41
Figure 34 Outer Wire of 8-Week USF 2-Open Exposure Sample - Before Bending.....	42
Figure 35 Sample Strands' Ends Coated in Grit Material Awaiting Tensile Testing	44
Figure 36 Sample Strand Break and Fully Engaged Grip.....	44
Figure 37 Total Cumulative Fraction of Load at Failure.....	45
Figure 38 Cumulative Fraction of Load at Failure - Environment Comparison	46
Figure 39 Cumulative Fraction of Load at Failure - Duct Condition Comparison.....	46

Figure 40 Cumulative Fraction of Load at Failure - Exposure Length Comparison	47
Figure 41 Total Cumulative Fraction of Total Elongation at Failure.....	47
Figure 42 Cumulative Fraction of Total Elongation at Failure - Environment Comparison	48
Figure 43 Cumulative Fraction of Total Elongation at Failure - Duct Condition Comparison	48
Figure 44 Cumulative Fraction of Total Elongation at Failure - Exposure Length Comparison	49
Figure 45 Total Cumulative Fraction of Load at 1% Extension.....	49
Figure 46 Cumulative Fraction of Load at 1% Extension - Environment Comparison	50
Figure 47 Cumulative Fraction of Load at 1% Extension - Duct Condition Comparison	50
Figure 48 Cumulative Fraction of Load at 1% Extension - Exposure Length Comparison	51
Figure 49 Average Load at Failure by Experiment Variable - Error Bars are 2 Standard Deviations Tall (Red Line Indicates ASTM A416 Minimum Requirement).....	52
Figure 50 Average Elongation to Failure by Experiment Variable - Error Bars are 2 Standard Deviations Tall (Red Line Indicates ASTM A416 Minimum Requirement).....	53
Figure 51 Average Load at 1% Extension by Experiment Variable - Error Bars are 2 Standard Deviations Tall (Red Line Indicates ASTM A416 Minimum Requirement)	53
Figure 52 Typical Fracture Surface (1/4).....	54
Figure 53 Typical Fracture Surface (2/4).....	55
Figure 54 Typical Fracture Surface (3/4).....	55
Figure 55 Typical Fracture Surface (4/4).....	56
Figure 56 9-Month SSK Wet Exposure Sample - Exterior of Bend Surface	57
Figure 57 9-Month SSK Wet Exposure Sample - Unetched (Field Width- 2 mm)	57

Figure 58 9-Month SSK Wet Exposure Sample - Etched with Nital (Field Width- 2 mm)	57
Figure 59 9-Month SSK Wet Exposure Sample - Unetched.....	58
Figure 60 9-Month SSK Wet Exposure Sample – Etched with Nital.....	58
Figure 61 8-Week SSK 2-Open Exposure Sample - Exterior of Bend Surface	58
Figure 62 8-Week SSK 2-Open Exposure Sample - Unetched (Field Width- 2 mm)	59
Figure 63 8-Week SSK 2-Open Exposure Sample - Etched with Nital (Field Width- 2 mm).....	59
Figure 64 8-Week SSK 2-Open Exposure Sample - Unetched.....	59
Figure 65 8-Week SSK 2-Open Exposure Sample - Etched with Nital.....	60
Figure 66 8-Week USF 2-Open Exposure Sample - Exterior of Bend Surface	60
Figure 67 8-Week USF 2-Open Exposure Sample - Unetched (Field Width- 2 mm)	60
Figure 68 8-Week USF 2-Open Exposure Sample - Etched with Nital (Field Width- 2 mm).....	61
Figure 69 8-Week USF 2-Open Exposure Sample - Unetched.....	61
Figure 70 8-Week USF 2-Open Exposure Sample - Etched with Nital.....	61
Figure A1.71 Typical As Received Condition of Strands Prior to Exposure	82
Figure A1.72 Duct Condition Comparison of Exposed SSK Strands.....	83
Figure A1.73 Duct Condition Comparison of Exposed USF Strands.....	84
Figure A1.74 Exposure Length Comparison of Exposed SSK Strands	85
Figure A1.75 Exposure Length Comparison of Exposed USF Strands	86
Figure A1.76 Environment Comparison of Exposed Strand - As Extracted.....	87
Figure A1.77 Environment Comparison of Exposed Strand – Cleaned.....	88

ABSTRACT

Recent failures and severe corrosion distress of post-tensioned (PT) bridges in Florida have revealed corrosion of the 7-wire strands in tendons. Post-tensioned duct assemblies are fitted with multiple 7-wire steel strands and ducts are subsequently filled with grout. During construction, the length of time from the moment in which the strands have been inserted into the ducts, until the ducts are grouted, is referred to as the 'ungROUTED' period. During this phase, the steel strands are vulnerable to corrosion and consequently the length of this period is restricted (typically to 7 days) by construction guidelines. This investigation focuses on determining the extent of corrosion that may take place during that period, but limited to strands that were in the unstressed condition. Visual inspections and tensile testing were used to identify trends in corrosion development. Corrosion induced cracking mechanisms were also investigated via wire bending and metallographic cross section evaluation. Corrosion damage on unstressed strands during ungrouted periods of durations in the order of those otherwise currently prescribed did not appear to seriously degrade mechanical performance as measured by standardized tests. However the presence of stress in the ungrouted period, as is normally the case, may activate other mechanisms (e.g., EAC) that require further investigation. As expected in the unstressed condition, no evidence of transverse cracking was observed.

INTRODUCTION

The durability of reinforced concrete structures is of paramount concern. Buildings, bridges, dams, nuclear containment vessels and other critical infrastructure components are constructed with reinforced concrete. Not only is replacement cost of high concern but more importantly safety. Sudden failure of any of these systems would not only be costly, but lethal. Understanding these failure modes and degradation mechanisms affords the owners of these structures the ability to plan financially for repair/replacement and to prevent a sudden failure scenario.

Background

Reinforced concrete is a composite material comprised of steel (the reinforcement) and concrete. Steel reinforcement in concrete is traditionally referred to as 'rebar'. Concrete, which performs well under compressive loading, fails with little tensile stress - about one-tenth of its compressive strength (Mindess, Young and Darwin 2003). The reinforcement, which is chosen because of its high tensile strength, is placed inside the concrete in the area of the structure which will be in tension under service conditions, the steel rebar then takes the load which the concrete could not (Andrew 1987), this results in more efficient usage of both steel and concrete. Prestressed concrete increases the efficiency of this composite. Steel strands are stressed in a casting bed prior to the concrete being poured. The concrete is then poured into the bed and once cured, the strands are relaxed. The steel, when relaxed

from its prestressed loading, forces the concrete into compression (Gerwick 1993). This prestressed compressive force must be overcome before any tensile stresses can develop. Where standard reinforced concrete would fail or crack in the tensile zone long before the compressive zone could develop its full structural capacity, prestressed concrete takes nearly full advantage of the extremely high compressive strength of concrete.

Post-tensioning, a form of prestressed concrete, is characterized by stressing the reinforcing steel after the concrete has set or cured, through the use of tendons which run the length of the concrete element(s) and with the aid of anchors at each end which then stress the concrete into compression before the service load is applied (Prestressed Concrete Institute 1972). For Florida bridge structures, post-tension tendons are typically composed of a high density polyethylene (HDPE) ducts, steel strands, and a grouted matrix that binds the strands. Typically this matrix is cement grout. Other less prevalent systems use galvanized spiral ribbed ducts and grease or oil as the matrix material (Corven and Moreton 2004). The structural steel is 7-wire high strength carbon steel strand conforming to ASTM A416 which is cold-drawn and 6 wires are helically wrapped together around a center wire to form the strand. The strand material is a very fine pearlitic structure with less than 0.8% carbon. The matrix material is placed within the duct to provide corrosion protection for the reinforcing strand (American Concrete Institute 1990). Grout is preferable than oil or grease because in addition to protecting the steel from corrosion by passivating the steel, it also provides additional stability in the event of strand failure. Should a strand fail in service, the grout will prevent the strand from breaking free and damaging other components, the grout

will take the stress which was supported by the strands and distribute it to the other strands further along the tendon.

During construction, the HDPE ducts are placed through concrete elements, the strands are then fed through the ducts, attached to anchorage systems, and stressed. Unhydrated cementitious (uncured) grout is then pumped into the ducts through grouting ports and completely fills all of the remaining space. Vent ports along the tendon length allow air to evacuate the duct during grouting. Once the grout has cured, the tendon is then complete.

Corrosion

All engineering materials will ultimately return to their original state to the forms which are found in nature. Corrosion is an electrochemical process by which materials degrade by means of a reaction with their environment (Gellings, 2005). Corrosion necessitates four crucial components: an anodic reaction, a cathodic reaction, an electrolyte, and an electronic path. All four of these criteria must be met for corrosion to take place. For corrosion of steel (commonly known as rusting), the oxidation of iron is the anodic reaction. The cathodic reaction is normally the reduction of oxygen. The water also serves as an electrolyte, and the electronic path is provided by the conductive iron. The reaction of paramount interest is the anodic reaction which is given by the following chemical equation:



Multiple other reactions subsequently take place to eventually form the corrosion product $Fe(OH)_3$. The specific reactions and their rates are dependent on the particular

solution which the iron is exposed, but predominantly the cathodic reaction is oxygen reduction:



More information on this process is expounded on within the discussion. Steel placed in basic solutions (high pH) steel forms a protective oxide or oxyhydroxide film on its surface which impedes corrosion. This is called passivation. The protective film is referred to as a passive film or passive layer. This layer breaks direct contact from the steel and the electrolyte and thus stops or severely slows corrosion. As corrosion is an electrochemical process, corrosion rate is often expressed in terms of a current density. If the specific reactions are known, as well as the specimen size and current, a simple relationship relates the metal loss with the corrosion current density. Figure 1 demonstrates the corrosion reactions for a metal which can passivate. In Figure 1, the abscissa is the logarithm of the current density, where the ordinate is the electrical potential. The black curve is the anodic reaction which has a stable passive behavior above E_p . The red line represents the anodic reaction following passivity breakdown. The blue curve denotes the cathodic reaction (oxygen reduction). Without the use of an externally applied current, corrosion reactions must occur at intersections of these reaction lines. The current of the cathodic reaction must perfectly balance with the anodic reaction. From the figure it is demonstrated above that the corrosion current density, and consequently, the corrosion rate, is exponentially reduced when the metal becomes passive. Aggressive elements, such as chlorides, present in marine or deicing salt service environments, have been known to break down this passive layer in steels.

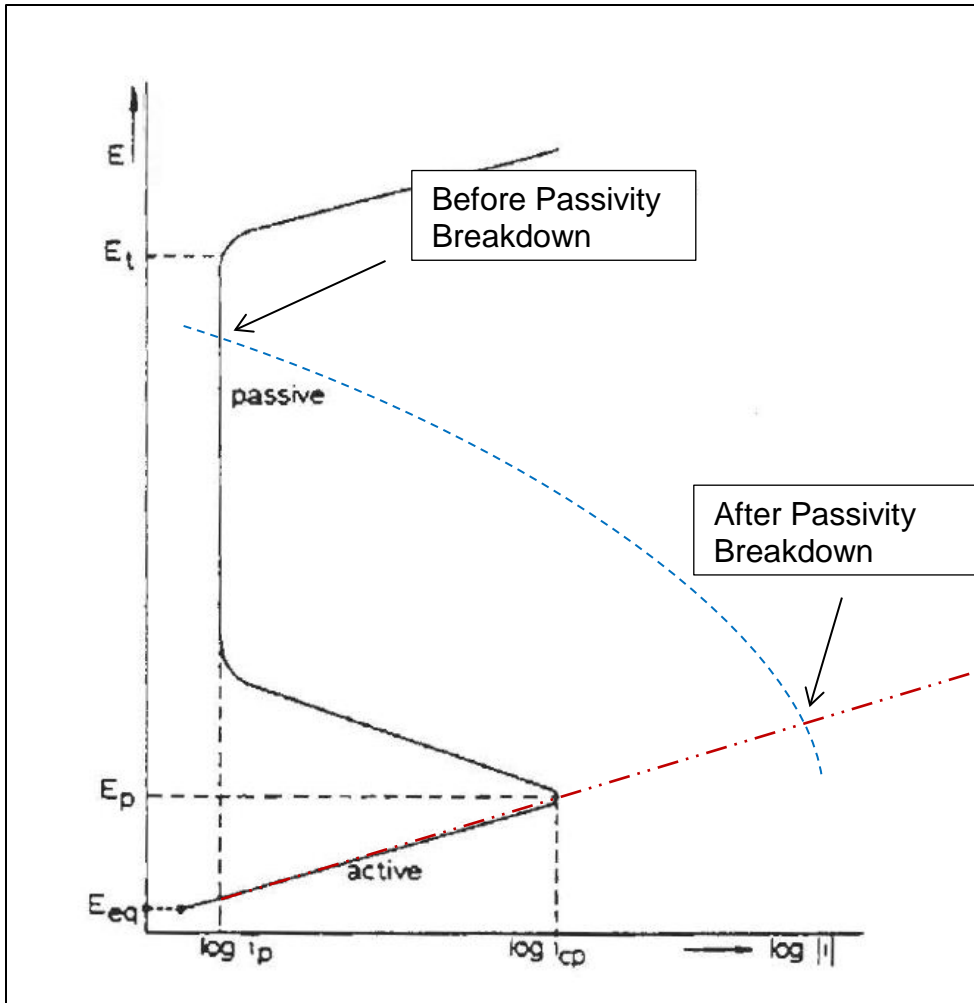


Figure 1 Anodic Polarization Curve of a Metal Which Can Passivate (Source: Gellings, Modified by Hutchison)

The estimated corrosion protection of post-tensioned concrete structures is excellent. The high pH of the grout facilitates the conditions needed for carbon steel to become passive (Fontana and Greene 1978). The grout also acts as a diffusion barrier to aggressive elements, and the intact HDPE duct acts as an impermeable layer as well. Additionally, the whole tendon is embedded or otherwise commonly encased within yet another concrete element. By all of these methods there should not be any corrosion of the strand, or any performance degradation of the tendon. Because of this, post-tensioned bridges have expected service lives of 75-100 years (Corven and

Moreton 2004). However, recent failures in Florida bridges within as little as seven (7) years of construction indicate that this prediction is not always valid (Wang, Sagüés and Powers 2005). There is an increasing body of research, addressed in the next section, conducted to understand the reason for these failures and control future occurrences. It is generally acknowledged too that any deterioration of the strands prior to grouting may be an important aggravating factor in any subsequent corrosion. During construction, the length of time from the moment in which the strands have been inserted into the ducts, until the ducts are grouted, is referred to as the 'ungROUTED' period. During this phase, the steel strands are vulnerable to corrosion and consequently the length of this period is restricted (typically to 7 days) by construction guidelines. This investigation focuses on determining the extent of corrosion that may take place during that period, by extending a prior study in the subject (Sagüés, Karins, & Lau, 2011). Possible aggravation of future corrosion damage due to corrosion during the ungrouted period is addressed as well.

Objective

Based on the above introduction, the primary goal of this investigation is to broaden the information available on the extent of corrosion development on the strand that may take place during the ungrouted period of PT tendon construction, as a basis toward determining if that damage can facilitate potential early failure, or lead to subsequent failure of these critical structural elements.

A review of the relevant issues pertaining to this objective is presented in the following section.

Literature Review

Corrosion During the UngROUTED Period

Recent studies conducted around the world have attempted to understand the accelerated degradation of tendons in PT bridges. The literature is dominated by investigations into failure of PT tendons which are grouted whereas little research has been conducted attempting to understand what effect the ungrouted period has on long-term performance.

The San Francisco-Oakland Bay Bridge (SFOBB) underwent a period during its erection which halted construction and caused tendons with stressed strands to be left without protective grout for as long as 15 months. A study was conducted by Robert Reis to determine the corrosion damage on strands which were left in ungrouted tendon ducts for this period (Reis, 2007). The results from the investigation showed that most strands had nominal damage and met the specified requirements for strength according to ASTM A416. Borescope exploration of internal tendons revealed strands had considerable corrosion products including pits which were visible with the unaided eye. Darker corrosion products were apparent at pit initiation sites. Little corrosion was found near the points where strands intersected with the galvanized duct. One crack 0.0049 inches, found on a moderately corroded wire, emanated from the base of a corrosion pit. The crack had a branching morphology suggestive of Environmentally Assisted Cracking (EAC). On mechanical testing of exposed strands extracted from the ducts, the majority were found to meet the specified strength requirements, with few exceptions which only fell 6% below specification. The findings suggest that that corrosion damage in strands left ungrouted even for times much in excess of typically

specified periods may still not be sufficient to cause severe degradation of strength as tested by conventional methods. Caution is in order however as indicated in the phase III project report (Reis, 2007) where Appendix B contains a cautionary implication: “It is emphasized that the apparently limited corrosion observed in the present case should in no way be viewed as dismissing the adverse consequences of delayed grouting in future projects. Small variations in environmental conditions or system configuration could have easily resulted instead in severe corrosion” (Sagüés A. A., 2007).

The Florida Department of Transportation (FDOT) sponsored an investigation to evaluate the seven (7) day ungrouted period requirement, and the extent to which it may be overly conservative or otherwise (Sagüés, Karins, & Lau, 2011). This project simulated duct conditions at test stations located both the University of South Florida (inland conditions) and the Sunshine Skyway Bridge (marine-shore conditions).

Exposure lengths were set to 1, 2, 4, and 8 weeks. The simulated duct conditions were Dry and closed, dry and open at one end, wet (meaning water was intentionally added to ducts) and closed, and another wet and closed but with a vapor-phase inhibitor.

Exposure runs were in the late fall. Strands exposed in ducts as long as eight (8) weeks showed no appreciable loss of strength, and the vapor-phase inhibitor did not appear to have any well-defined effect on the corrosion progression on the strands. Importantly, given that the test exposures were conducted at a time of the year where temperature and humidity were moderate for the test locations involved, the authors indicated that additional and potentially valuable information could be obtained by reproducing the experiment “... by exposing a new set of strands, with the existing facilities, during the summer” (Sagüés, Karins, & Lau, 2011) where corrosion vulnerabilities that might have

been missed in that study could have a better chance to be manifested. The present investigation was conducted largely in consequence of that recommendation to broaden the information available in this issue. The report on the FDOT-sponsored investigation also summarizes other studies on pre-grouting corrosion prevention, mostly dealing with the application of inhibitors and protective agents; the reader is referred to that publication for further detail.

Corrosion in Subsequent Service

A study by Nürnberger in 2002 addresses corrosion mechanism issues (Nürnberger, 2002). He states that prestressing steels, because of their much higher tensile strength, have an increased susceptibility to corrosion. Thusly, extra precautions should be taken to ensure that the strand is protected, not only in service, but also in construction: namely, enforcing a limit on the maximum time allowed for the strand to be left in the ungrouted condition. Nürnberger suggests that the failure incidents can be attributed to poor construction, poor workmanship, or poor materials. Poor workmanship, such as the improper execution of the grouting procedure was the most noticeable reason for later tendon corrosion-induced failure. Impurities in grouting materials, such as sulphate and chloride can compromise the corrosion protection offered by the grout. "Unsuitable" prestressing steel, can lead to increased hydrogen embrittlement; which can cause the steel to become brittle, and fail from the presence of a very small crack. Stress corrosion cracking (SCC) is possible as a failure mode for these steels as SCC affects higher strength steels. Very little corrosion on the surface is needed to create the conditions necessary to facilitate SCC. This small amount of corrosion could be generated during the construction phase of the structure.

In direct response to recent tendon failures of Florida PT Bridges, Wang and Sagüés set out to determine the corrosion characteristics of the post-tensioned strand-anchorage system in grouted assemblies (Wang, Sagüés, & Powers, 2005). They simulated two grout types, an expansive grout and a low-bleed grout. Failures were observed in bridges with the former. Unstressed strands were placed and then grouted with the anchorage assembly. Voids were intentionally added to simulate poor grouting procedure. A mixed metal oxide coated titanium wire was also inserted to serve as a counter electrode and a reference electrode for Electrochemical Impedance Spectroscopy (EIS). Both fresh and NaCl contaminated water was intentionally added periodically, simulating leaks in the anchorage seals. Recharge events with salt solutions showed immediate drop to lower potentials indicating that the steel had depassivated, accompanied with an increased macrocell current. Recharging using fresh water could also initiate corrosion if the chloride content of the grout exceeded 500 ppm. Corrosion products visible at the grout-void interface confirmed these findings. Carbonation of the grout had a negligible effect on the depassivation of the steel compared with the effect of the recharge events. Increased corrosion susceptibility at the grout-void interface was observed as expected. The galvanic coupling between the strand and the anchorage system caused the strand to become the net anode, and the anchorage the net cathode, aggravating the corrosion of the strands. These factors combined to produce extensive corrosion in the void space with high internal relative humidity. The estimated corrosion rates are consistent with a 7-year failure as observed in some of Florida's PT bridges.

Proverbio and Longo attempted to determine if carbonated solutions similar to those experienced in some grouted conditions can promote SCC and cause brittle fracture modes (Proverbio & Longo, 2003). High-strength steels, while also subjected to general corrosion issues, are also highly susceptible to stress corrosion cracking. Carbonation of the grout causing a local pH drop thus leading to depassivation of the strand is not uncommon in bridge structures. Strands were held at ~80% of their ultimate tensile strength while immersed in a bicarbonate solution with a platinum mesh counter electrode, as well as a calomel reference electrode for EIS measurements. The machine which applied the load was also set up to a lever system which, when the steel strand system failed, would drop and stop a timer which was set at the beginning of the test to determine time to failure. After failure, the strands were cleaned and metallographically evaluated. Normal failure times were ~45-50 days. A control specimen, not immersed, was also tested and showed ductile failure, indicated by dimples in the central region of the fracture surface. For the immersed strands, the failure mechanism was brittle, surface cracks were distributed throughout the strand, a stepwise pattern of cracks was observed towards the flap, typical in SCC failures. Surface voids on the longitudinal surface of the metal were evaluated with EDX and found to be manganese sulphide, elongated in the stressing direction; this was postulated to be due to hydrogen entrapment, observed in other conditions.

Following the advent of multiple early failures of bridges within the United States and Europe, Pillai et al. developed a probabilistic model to predict the time-variant tensile capacity of PT tendons (Pillai, Gardoni, Trejo, Hueste, & Reinschmidt, 2010). Using 384 unstressed and 162 stressed specimens in varying moisture, void, and

chloride contamination conditions, five void conditions were simulated with respect to the longitudinal axis: no void, parallel, bleed-water, inclined, and orthogonal. These orientations were used to simulate what could and has occurred in PT segmental box bridges. Strands were in the “as-received” condition from the manufacturer, indicating that there was minor but negligible surface corrosion on the strands. Strands under aggressive environments and high stress can be susceptible to stress corrosion cracking (SCC). More unstressed strands were tested because of the ease of experiment construction versus that of the stressed condition. The effective size of the anode compared with the cathode has a dramatic effect of the corrosion progression. Smaller anodic regions in the voids can accelerate corrosion of the strand. Water may intrude and become trapped in the tendons. Because of the effects of SCC, the relationship between the model of the unstressed strands and the stressed follow a power relationship. The experiment lasted over 21 months. The investigators warn that the relationship does not hold for field applications, as the strands in field investigations are in the stressed condition and thus the stressed model must be used, because it includes the effects of SCC. The proposed model showed good agreement (within 3.2%) with the data obtained from early failures in both Florida and Virginia PT segmental box girder bridges.

Toribio, Kharin and Vergara considered the failures from a different perspective, high-strength steel strands are formed through a cold drawing process And the residual stresses formed during this procedure may have a considerable effect of the hydrogen embrittlement properties of this material (Toribio, Kharin, & Vergara, 2011). High strength steels, such as 7-wire strand used in post-tensioned structures are subjected to

extremely high stresses and “particularly susceptible to fracture phenomena”. The diffusion of hydrogen through the metal is dependent on the stress. Local variations in the stress distribution caused by residual stresses in the drawing process may change the diffusion rate of hydrogen and current models may not be conservative enough when predicting the hydrogen ingress, if they do not include these effects. A numerical model with a finite element mesh was used to estimate the residual stress in the wire. The cold drawing process is normally composed of six (6) stages, where the diameter of the wire is reduced by drawing the steel through a die which has a specified opening. The values from the computer model of the stress fields in the strand, ignoring hydrostatic pressure from the atmosphere, also modeled the effective diffusion coefficient of the strand at any point on the mesh. Coupled with a Fickian diffusion model Toribio estimated the hydrogen ingress through the steel surface. The results showed that, when accounting for the stress fields induced from cold drawing, the hydrogen diffusion through the wire was faster and resulted in higher concentrations in the steel.

Bertolini and Carsana looked at a phenomenon which was observed in conjunction with several failures: grout segregation (Bertolini & Carsana, 2011). Prestressing steels used in post-tensioned bridges is ensured through a passive layer facilitated by the high pH of the grout and lack of chloride ion presence. However recent failures in PT bridges have launched several investigations as to the cause of failure. Initial investigations showed that the grout in the ducts had segregated. The segregation was characterized by X-ray diffractometry (XRD), thermogravimetric analysis (TGA), and scanning electron microscopy (SEM). While the pH remained high enough to

facilitate a passive layer and the amount of chlorides were not enough to cause depassivation, failure still occurred; the cause of which remains unknown. The segregated grout showed higher than expected values of sulphate concentrations. The source of which is a main constituent of cement: gypsum. Failure of the strands was evaluated to be ductile, removing the possibility of failure through stress corrosion cracking or hydrogen embrittlement. Corrosion tests were made on pickled specimens removed from bridges. Placed in both simulated and actual solutions obtained from the bridges with an addition of sodium sulphate to some samples, corrosion rates were obtained through the polarization resistance method. While general corrosion of the strands was not severe enough to cause the damage seen in bridge tendons, crevice corrosion was observed underneath a plastic O-ring which was intentionally added to promote this. Because of the high pH, and the lack of chlorides in the grout, normal corrosive mechanisms attributed to these failures are not applicable. The Pourbaix diagram for steel in high pH environments does contain a small section, at certain electrical potential ranges, of passivity breakdown and steel corrosion. However, despite deaeration and the addition of sulphate, this potential was not able to reach the necessary values to obtain this condition without the use of an impressed current. The macrocell coupling from local crevice corrosion and the region unaffected could be why the attacks in bridges were so severe. While not addressed within his paper, perhaps the anodic polarization from the anchorage assembly observed by Wang & Sagues would be enough to drive the steel potential to this range.

A comparison of the results obtained by a simulated accelerated marine exposure with those results from an actual marine exposure on the Atlantic coast at

Kennedy Space Center (KSC) is presented by Montgomery, et al. Current exposure testing requires 3-5 years of exposure; an accelerated timeframe would certainly be industrious (Montgomery, Curran, Calle, & Kolody, 2012). Salt deposition, temperature, precipitation, wave height, and relative humidity were monitored on site. Salt deposition was evaluated through the use of a 'wet-candle'. A length of gauze is wrapped around a nonporous cylinder. The ends of the gauze are dipped in an amount of water, normally stored in a plastic Erlenmeyer flask beneath the cylinder, to ensure the gauze remains wet for adherence of salt spray on the continually damp gauze. In addition to mass loss measurements to determine corrosion rates, visual comparisons between both exposure regimes were presented. The visual comparison concluded that there was a "distinct physical difference" between corrosion products formed by the accelerated tests and the real marine exposure. Further planned testing will determine if there are chemical differences between products.

Coronelli, et al. comments that compared with the vast available information on the failure mechanisms of reinforced concrete, there is strikingly little information of the failure mechanisms for post-tensioned systems, including brittle failure and bonded tendons (Coronelli, Castel, Vu, & François, 2009). Post-tensioned beams were made with encouraged brittle failure by sawing a single bonded wire, generating an induced crack. Cavities were introduced via polystyrene. After concrete curing (28 days) the polystyrene was removed and provided direct access to the strand. Two locations of access were made: one at a region of low bending moment, and the other at an area of high bending moment. To compare the results, a finite element model was made to simulate the actual tendons. In addition to being reasonably consistent with the small

mock up tests, the numerical model also showed good agreement with a large scale element which was removed from a decommissioned bridge. The results showed that this model would be consistent to bridge element failures due to stress corrosion cracking and brittle shear failures. Future work includes the influence of improper grouting and voids on the structural response of the strand.

Jaeger, Sansalone and Poston described that bonded post-tensioned structures in use for bridges are susceptible to failure from improper grouting and the presence of voids (Jaeger, Sansalone, & Poston, 1996). Several existing methods to detect voids may be unsuitable. Radiographic methods have been used to detect voids, but these methods are often bulky, expensive, require direct access, and specially trained personnel to use X-ray equipment. A cheaper and simpler method is presented: the impact echo method. The method consists of a heavy spherical weight being impacted on the surface and measuring the vibrational response of the structure. Theoretically, identifiable characteristics of the response should indicate the presence of either voids or fully bonded tendons. The resonant response was measured and a fast Fourier transform technique was used on-site to convert the response into the frequency domain. A mock slab with varying conditions was used to calibrate the method, comprised of three conditions: fully grouted, and empty duct, and a void created at a known location. The thin metal duct would provide a negligible interference to the response of the grout and internal strands. This assumption was confirmed through a computer model and experimental results. Estimated characteristic frequency peaks for both the internal steel and the grout from the ducts were identified with experimental results, and thusly were able to identify the presence of grout, or voids. A field study to

confirm the results showed through testing and subsequent excavation that the impact echo method could determine the presence of voids in a bonded PT structure.

Prospective future work includes the detection of water within the voids, honeycombing and more complex structural geometries.

Kovac, Leban and Legat developed a new method using multiple techniques for determining cracking of the strand. Pitting corrosion of steel is extremely difficult to measure or detect with available methods (Kovac, Leban, & Legat, 2007). Traditionally it has been treated solely as a statistical phenomenon, manifesting itself under certain corrosive conditions for passive steels. Prestressing steel wire, while passivated, is susceptible to this mode of corrosion. Similarly, stress corrosion cracking (SCC) is not fully understood, and failures are brittle, sudden, and without warning. Detection is nearly impossible, as little or no visible corrosion products form at the surface of the crack. Current methods are insufficient; however, minute indications provided from multiple techniques may elucidate the presence of pitting and/or SCC. Acoustic emission (AE), electrochemical noise (Echem noise), and elongation measurements combined may provide insight and possible detection of these corrosion modes. Several samples were immersed in a corrosion-promoting environment namely, ammonium thiocyanate and mechanically stressed. Some failures were brittle, indicating SCC had occurred, which was later confirmed metallographically and with scanning electron microscopy. Transgranular SCC was the primary SCC process. Pitting was also observed on tested specimens. Cracks originated from the surface and traveled perpendicular to the applied stress. Ultimately detection of individual events was unreliable. Because of the transient nature of both pitting and SCC, initiations of both

pits and cracks may be sudden, indicating a spike in both AE and Echem noise methods. However, the vast majority of these events would quickly die. Most pits and cracks do not cause significant degradation of performance of the material.

Minh, Mutsuyoshi and Niitani observed visible cracking on the exterior surface in several Japanese post-tensioned structures. The most prominent source of this degradation is chloride attack from sea spray (Minh, Mutsuyoshi, & Niitani, 2007). It is assumed that the source of the cracks is from the circumferential pressure generated by corrosion of the duct itself. (Note: nowhere within the article do the authors mention the material the duct is made of; an assumption of steel could be made, possibly galvanized steel as is normally used in the United States) Two PT systems were built, one straight, and the other with curvature of the duct. Accelerated corrosion tests were made on both setups, which were placed in tanks with a 5% sodium chloride solution. Salt was also intentionally added to the concrete mix to further accelerate corrosion, and an impressed current was added to both corrode the steel and accelerate diffusion of chlorides to the steel surface. Several grouting conditions were also simulated. During loading tests, crack development was monitored. Ducts which were fully grouted developed cracks more rapidly than those which were partially filled. No cracks were observed in the ducts without grout. The explanation for this is that the pressure generated from the expansive corrosion products would be alleviated by the freedom offered by the available airspace within the duct. Improper grouting in the curved ducts showed a considerable decrease in strength. It was also concluded that the bond between the concrete and the corroded duct would be significantly weakened, as was shown by its reduced load-bearing capacity.

Darmawan and Stewart describe that prestressing wires embedded in concrete are subjected to the same corrosion characteristics of regular reinforced concrete, including pitting which is normally treated in a statistical manner. Salt spray from the ocean or deicing salts may penetrate through the concrete and cause local passivity breakdown and pitting. Pits may be an initiation site for stress corrosion cracking (SCC) or hydrogen embrittlement (HE) (Darmawan & Stewart, 2007). Accelerated corrosion tests were assumed to be a realistic simulation of real conditions as X-ray diffractometry (XRD) revealed that similar morphological details in longer-term structures were similar to those found in the accelerated test. SCC and HE were a more prominent problem with “old-type” quenched and tempered steels. High strength steels used in bridge construction today normally use a cold drawing process. A 5% sodium chloride solution was used in addition to an impressed current through a stainless steel plate to accelerate corrosion and develop pitting on the strands embedded within the concrete. Using a statistical analysis and assuming a hemispherical morphology of pit growth, a linear elastic fracture mechanical approach was used to determine the reduction of strength through an assumed stress intensity factor ‘K’. Scanning electron microscopy did not reveal any evidence of stress corrosion cracking. The use of this method of fracture mechanics was not valid as the plane strain condition was not met. Also pits do not have a sharp tip as in the case of a crack. While neither SCC nor brittle fracture was observed, the authors warn that this mechanism should not be ignored.

Mietz cautions that defects in the grouting condition of post-tensioned ducts in the form of voids can lead to failure of these structures (Mietz, 2000). Evidence of hydrogen induced stress corrosion cracking (SCC) was observed during failure analysis

of existing structures. Failures can still occur if the steel is no longer passive due to the presence of voids. "Old-type" quenched and tempered steels show appreciable susceptibility to this mode of failure. Corrosion damage during the construction phase of a project, including transportation and installation, can play a major role in the SCC favoring conditions needed for failure. Anodic SCC is limited by the dissolution of metal at the crack tip, and cathodic SCC is limited by the amount of adsorbed hydrogen at the crack tip. Hydrogen embrittlement is caused by a buildup of adsorbed hydrogen on the surface of the metal which then penetrates into the metal. This occurs in the cathodic region of the metal surface. Sulphides and thiocyanates present within the grout may also contribute to the SCC behavior of high strength prestressing steels. Sulphate solutions, when depleted of oxygen, can cause failure via SCC. The microstructure of the steel has a key role to play in crack propagation, as well as residual stresses.

Summary

Multiple failures modes have been observed in structures with PT tendons. Causes of failure emanated from poor construction, poor materials or poor design. An unavoidable corrosion vulnerability is present however in all instances: the corrosion that may take place in the ungrouted regime during the construction phase. Several of the reviewed papers have indicated that prior corrosion damage to prestressing wires can lead to an increased susceptibility of later damage including SCC and HE. Current construction practice allows some minor corrosion on the surface of the strand, under the assumption that the attack will be immediately halted in the presence of the high pH environment offered by grout. The allotted time and exposure during the ungrouted period may have a significant impact on the strands' durability during its remaining

service in the structure. Aside from the reports cited at the beginning of this review, there is relatively little information in the literature as to the extent and consequences of corrosion damage associated with the ungrouted period. Improving the base of information and its understanding is the aim of the research within this thesis.

APPROACH

This investigation will achieve the objectives by determining, through mechanical and visual inspections, the corrosion damage of steel strands in two representative service environments, and various internal and sealing conditions of PT ducts, and durations of exposure. In contrast to inland environments, coastal locations are expected to have higher humidity, temperature, and salt spray, all of which are aggravating elements towards corrosion; hence both an inland and a coastal setting were evaluated. Realistic PT duct conditions were simulated consistent with construction practice and not necessarily state and federal requirements, ranging from dry to wet, closed and open duct conditions. Multiple durations of exposure were evaluated ranging from one week, to over nine months. Relative humidity and temperature was continually monitored to assess the environment within the ducts. Evaluation of corrosion was determined through mechanical performance testing, and visual photographic documentation. Bending tests and subsequent metallographic evaluation will highlight any transverse cracking in the material following exposure. As noted earlier, the results will expand and will be compared with those of a previous investigation conducted using the same facility during a colder-season exposure (Sagüés, Karins, & Lau, 2011). Notably, these studies were conducted as a preliminary phase limited to strands in the unstressed condition. The results of this investigation

serve as a baseline for a more detailed continuation study using similar exposures in the stressed condition.

METHODOLOGY

Facility Design

Two facilities, one at the University of South Florida (USF) in Tampa, Florida and the other at the north abutment of the Sunshine Skyway Bridge (SSK) in St. Petersburg, Florida were available from the previous investigation (Sagüés, Karins, & Lau, 2011) and used for the present study. The facilities were designed to house eight (8) full sized ducts currently used in practice albeit shorter in length than PT duct used in actual bridges. Each facility consists of a hinged roofing enclosure which house eight (8) ducts each. The ducts were sheltered from direct rain on the top and sides, but open to the outside at the ends. The duct segments consisted of polypropylene corrugated sections (PPEX3 3-in internal diameter, 3.6-in external diameter) and transparent polyvinyl chloride (PVC) sections (3-in Sch-40 Harvel™ Clear PVC). The transparent portions were added for in situ visual inspection. Ducts were approximately 20 feet in length and the roof enclosure extended two feet on each side Figure 2 and Figure 3 display the facility design. Duct sections contained a sag in the center to reproduce conditions used in external PT tendons which have intentional sags secured by deviator blocks. Four vent ports (used in construction for grouting purposes) for each duct were installed at fifth points. One of these central vent ports for each duct housed a relative humidity and temperature probe (Omega OM-EL-USB-2-LCD) as shown in Figure 4



Figure 2 USF Duct Facility in the Open Position



Figure 3 SSK Duct Facility in the Closed Position - Sunshine Skyway Bridge Main Span and Generator Control Room in the Background



Figure 4 Relative Humidity & Temperature Probe Housings Attached to Ducts via Vent Port and Secured with Wood Boards and Zip-Ties

The other would house a separate water reservoir for the ducts which required it.

Water level was marked and refilled as needed, as seen in Figure 5.



Figure 5 Water Reservoir Attached via Vent Port (left) and Closed Vent Port Covered with Bug Shield (Right)

A galvanized nail was attached via a stainless steel hose clamp (Figure 6) to simulate the effects (if any) of a galvanized anchorage system on the corrosion propagation of the strands.



Figure 6 Strand Group Ready for Duct Insertion with Galvanized Spike Secured with Stainless Steel Hose Clamp

Testing Design

Environment

The two (2) duplicate facilities were located at both the University of South Florida and by the North abutment of the Sunshine Skyway Bridge in St. Petersburg Florida; the former to represent a milder inland environment and the latter, a more aggressive shoreline environment.

Duct Conditions

Four (4) ducts conditions duplicated at both facilities, realistic of what may occur during bridge erection, were simulated. 'Dry' ducts indicate that there was no water added to the ducts and were kept dry with the exception of moisture from the outside air

in those ducts which were exposed to the external environment. ‘Wet’ ducts indicate that the duct was kept at 100% relative humidity through an attached water reservoir and additionally ~100cc of deionized water was intentionally splashed in the center two vent ports (50cc each port) of those ducts at the beginning of the experiment. The duct conditions used are listed in Table 1.

Table 1 Duct Environment Conditions

Duct	Dry / Wet	Sealed / Open
Ducts 1 & 5	Dry	Sealed – Both Ends
Ducts 2 & 6	Dry	Open - 1 End
Ducts 3 & 7	Wet	Sealed - Both ends
Ducts 4 & 8	Dry	Open – 2 ends

Exposure Lengths

United States’ construction specifications limit the time from which the strand may be placed in a duct to when grout must be applied. Many state agencies require this time frame to be within seven (7) to ten (10) calendar days (Federal Highway Administration, 2012). At the beginning of the experiment five (5) strands were placed in each of the ducts. One (1) strand from each duct was then extracted after one (1), two (2), four (4), and eight (8) week exposures. The duration periods were intended to straddle a plausible range of exposures, with the 8-week period as a somewhat extreme value. In addition, an opportunity arose to investigate the effects of very prolonged exposure whereby one strand in each duct, left over from the previous project (Sagüés, Karins, & Lau, 2011) and with a total exposure time of 9 months was present at the beginning of the experiment. Those strands were removed for testing before

commencing the present exposures. Some of the 9-Month wet exposed strands were in ducts with a vapor-phase inhibitor. As the results both from the previous study and the present concur that inhibitor presence had no “well-defined effect” on the corrosion propensity for those strands (Sagüés, Karins, & Lau, 2011), the results from all 9-Month wet exposed strands will be designated as such without specifying whether inhibitor was present or not.

Strand Material

Grade 270 0.6” diameter 7-Wire uncoated prestressing strand, conforming to ASTM A416 was used. The strand provenance and an example of mechanical properties test results are given in Appendix 2. Figure 7 shows a schematic cross section of the strand.

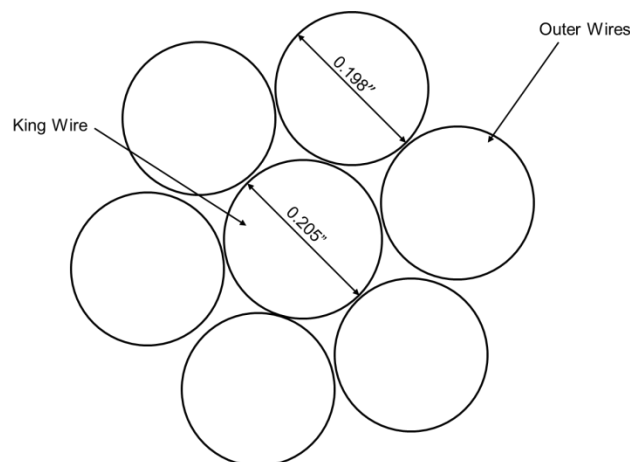


Figure 7 Schematic of Strand Cross Section

Center, or ‘king’, wires are slightly larger than the exterior, or ‘outer’, wires. The strands used had king-wire diameters of 0.205” and outer wire diameters of 0.198”.

Evaluation Methods

A unique identification code was given to each strand to distinctly and quickly identify each strand and from which condition it was exposure to. Figure 8 demonstrates this code.

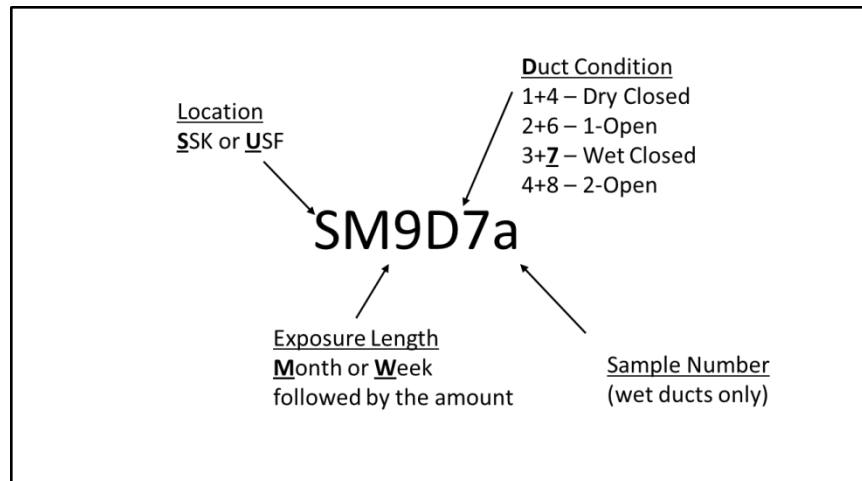


Figure 8 Strand Identification Code

Relative Humidity

Relative humidity and temperature were monitored at both facilities for each of the eight (8) ducts. Omega™ OM-EL-USB-2-LCD Relative Humidity and Temperature probes were used. These data provided an indication of the specific environment conditions that the strands were exposed to and also an indication of available moisture which could condensate on the surface of the strand and provided an electrolyte to enable corrosion.

Visual Inspection

Photographic recording took place before exposure in the 'as-received' condition, as well as after exposure as extracted from the duct and also after cleaning. Photographs of SSK strands were taken following transportation to the laboratory at USF. Cleaning consisted of removing corrosion products from the surface of the strands

by mechanical action through a stainless steel bristle brush. All strands were photographed with a high resolution camera on both sides over the entire length.

Photographic evaluation is presented in Appendix 1.

Tensile Testing

Following photographic evaluation, tensile testing as prescribed by ASTM A416 and ASTM 1061 (ASTM International, 2009) was performed. 50-inch segments from each strand were removed for mechanical testing. Figure 9 illustrates from which portions of the strands for each duct condition sections were removed. Dry duct strand segments (one per strand) were taken from the end of the strands, where two (2) segments from each wet duct strand were taken from both sides of the center portion of the strand.

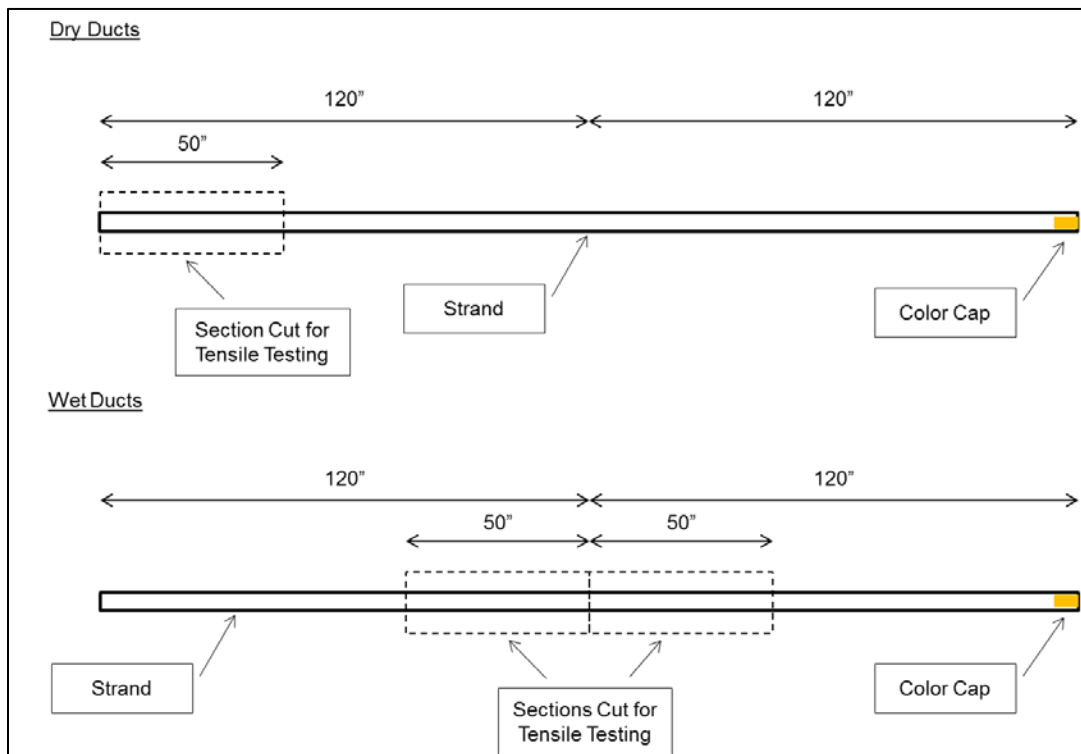


Figure 9 Locations of Cut Sections for Tensile Testing from Exposed Strands

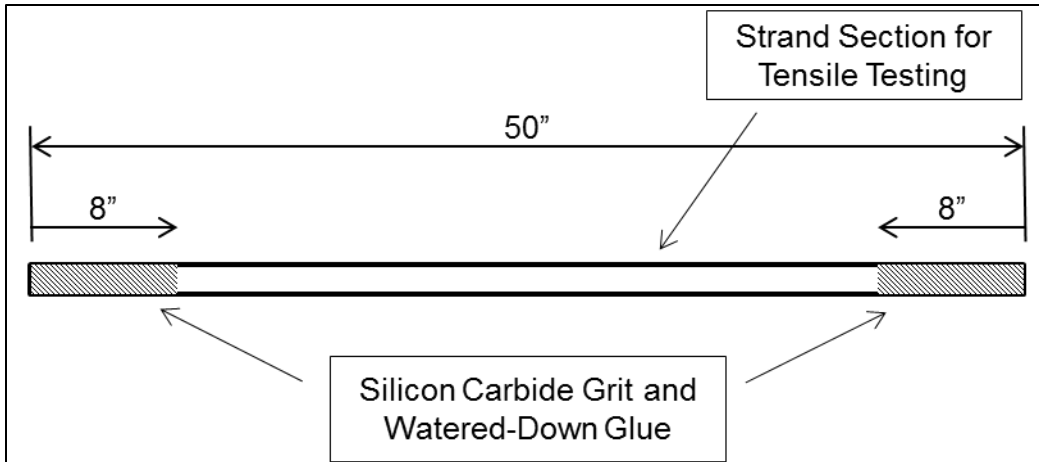


Figure 10 Strand Ends' Grip Material Configuration

Per ASTM 1061 the removed segments were then coated in a watered down Elmer's Glue™ solution at their ends and sprinkled with granulated silicon carbide (80 grit) to form an appropriate surface for gripping during mechanical testing (ASTM International, 2009). Tensile pull tests were performed at the FDOT State Materials Office (SMO) Laboratory in Gainesville, Florida.

Metallography

Sample wires for metallographic evaluation were taken from selected remnants of strands segments which were used for tensile testing, as those segments were from the more heavily corroded areas of each respective strand and any corrosion damage would be more apparent on those sections. The samples were cut from portions of the wires at least 4 in away from the fracture point of the wires. Sample wires were taken only from strands which underwent: 9-Month wet duct exposure, 8-Week wet duct exposure, and 8-Week 2-ends open duct exposures to evaluate representative worst-case conditions. A bend induced on a strand wire was expected to help reveal small pits or other irregularities on the surface by widening those artifacts for further evaluation at

the outer arch of the bend. If causing a crack to form at the base of a pit or other corrosion induced irregularity, bending might also establish the presence of features that could act as detrimental stress concentrators. Only external (non kingwire) wires were evaluated. The wires were cut from the strand segments and bent 180° into a “U” shape with a radius of 0.58” inches and then released. Figure 11 below illustrates this process. After springback the arms of the wire were separated by about 50 degrees.

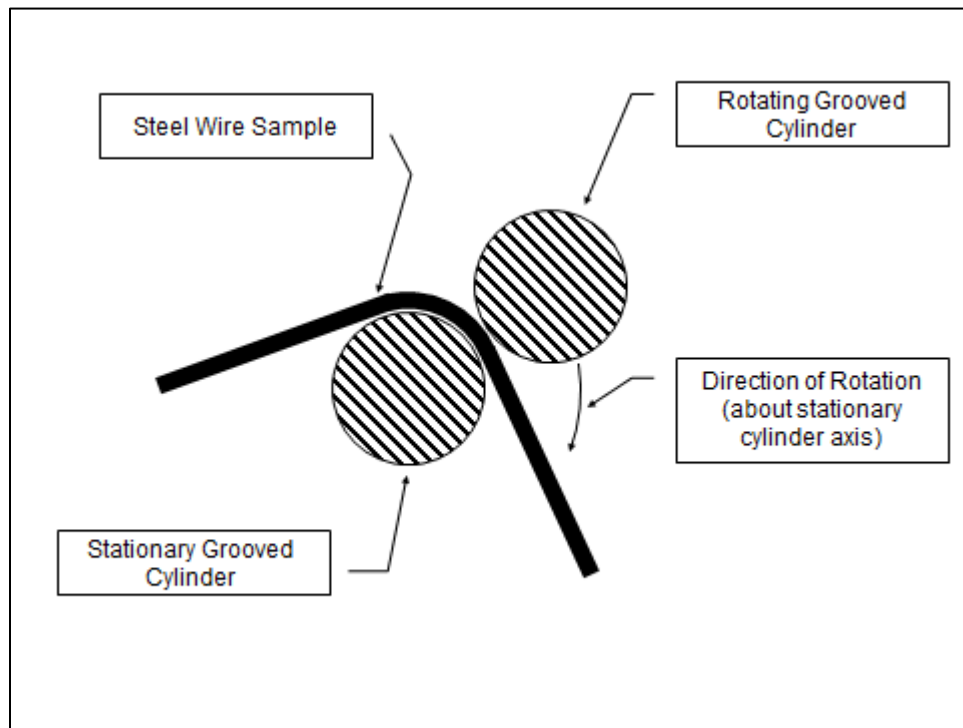


Figure 11 "U" Bend Illustration

The bent wires were then photographed on the exterior of the bend surface to look for any cracks large enough to see which may have been opened up through bending. Wires were subsequently prepared for metallographic examination. Metallographic evaluation was intended to reveal cracks or other features that were not visible to the unaided eye or visual photographic evaluation.



Figure 12 Typical Wire After Bending

Experimental Setup of Prior Study

The facility used for this investigation, as well as the basic structure of exposure were adopted from work by Sagüés (Sagüés, Karins, & Lau, 2011). Major differences in exposures between studies included the elimination of the vapor-phase inhibitor exposure, the addition of the 2-End Open condition, the availability of the 9-Month exposure left from the prior study, and the exposure taking place predominantly over the summer months. The rationale was to subject unstressed strands to more aggressive exposures which might lead to greater corrosion damage, as exposures during the summer months compared with fall will have higher temperatures and both ends being open may allow more air to flow through ducts. Bending and metallographic evaluations (described in the previous section) were added to further assess strand corrosion.

RESULTS

Relative Humidity and Temperature

Temperature results from each location are presented in Figure 13. Temperatures were measured in all ducts, but as there was no major difference in those values obtained between ducts conditions only the temperature for each location are presented. The specific duct conditions in Figure 13 were those open at both ends where the probes were placed near the open end of the ducts.

Table 2 below lists the dates and approximate times of strand extractions.

Table 2 Strand Extraction Dates and Approximate Extraction Times

<u>Week Extracted</u>	<u>SSK</u>	<u>USF</u>
Initial Placement	8/17/11 ~2pm	8/25/11 ~2pm
One (1)	8/24/11 ~12pm	9/1/11 ~12pm
Two (2)	8/31/11 ~1pm	9/8/11 ~1pm
Four (4)	9/14/11 ~12pm	9/22/11 ~10am
Eight (8)	10/12/11 ~12pm	10/20/11 ~10am

Figures 14 to 29 show the RH records for each of the ducts. Each vertical line of the grid in the following graphs denotes a calendar day. Sharp drops or peaks in the graphs correspond to extraction times where the ducts were momentarily opened to remove strand then resealed. Following the two (2) week extraction for the SSK ducts (8/31/11) it was determined that ducts five (5) through eight (8), the duplicate series for both locations, should have the location of the RH probes moved from the center portion within the vent port, to the end of the duct (closed end side of the one-end open ducts) lying alongside the strands. This change would indicate the variability (if any) of the condition between the center portion and the ends, which might be particularly pronounced for those ducts which were in the open condition. Probe 1 from USF failed to record data between the 4-Week extraction and the 8-Week extraction. RH data from the previous 9-Month exposure was not available.

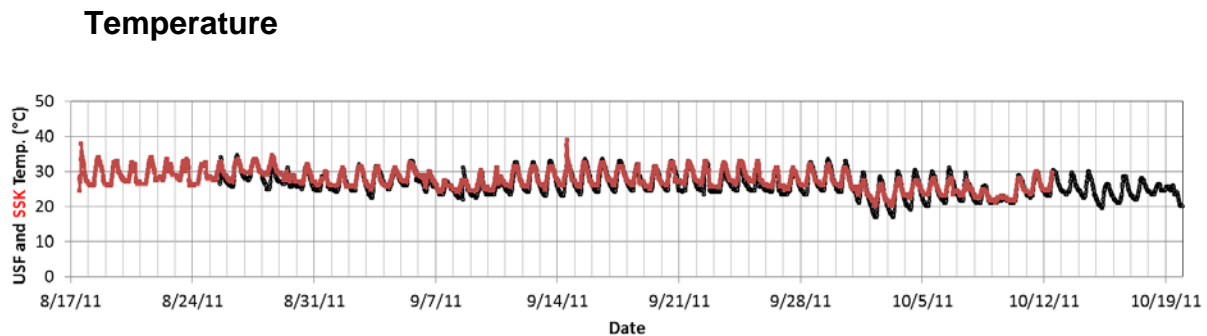


Figure 13 Temperature of 2-End Open Ducts at USF (Black) and SSK (Red) Locations

Closed and Dry Ducts

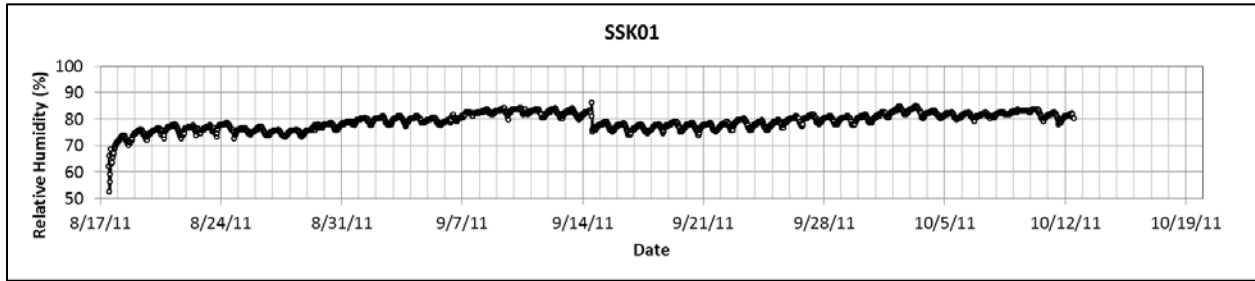


Figure 14 Relative Humidity of Duct 1 at SSK

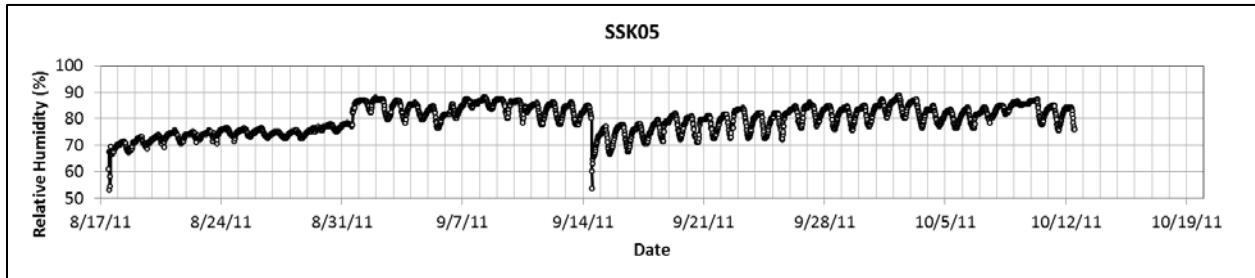


Figure 15 Relative Humidity of Duct 5 at SSK

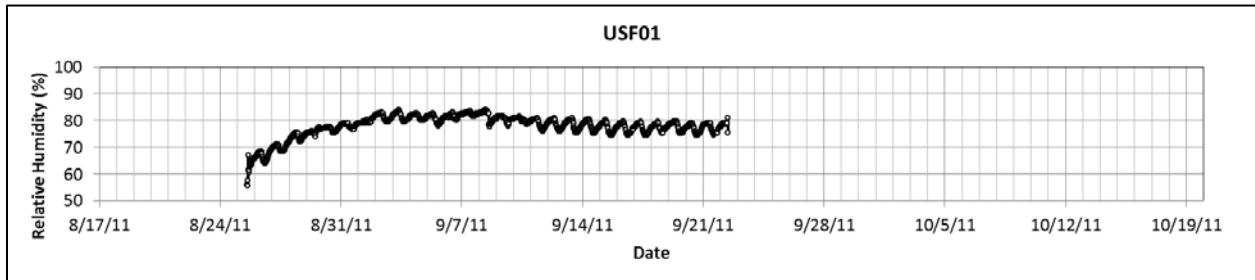


Figure 16 Relative Humidity of Duct 1 at USF

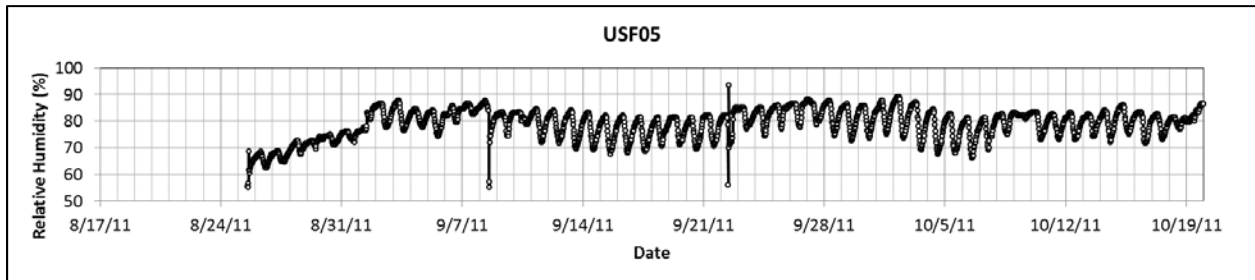


Figure 17 Relative Humidity of Duct 5 at USF

One End Open Ducts

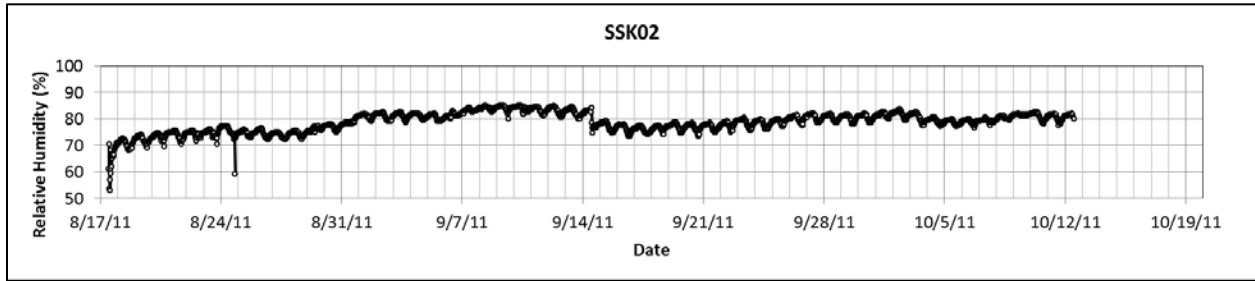


Figure 18 Relative Humidity of Duct 2 at SSK

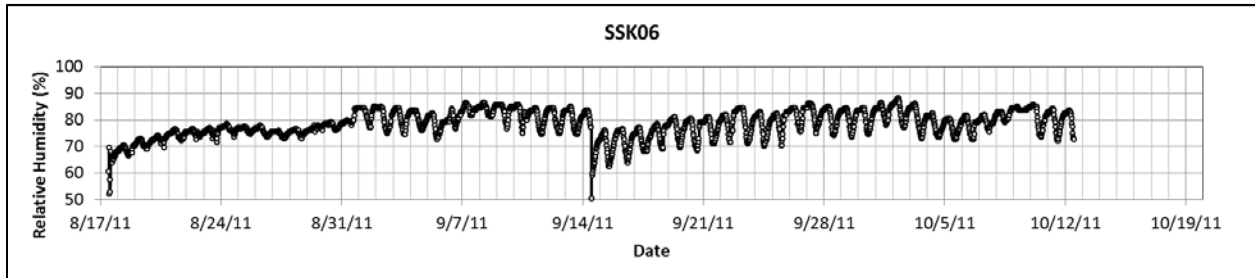


Figure 19 Relative Humidity of Duct 6 at SSK

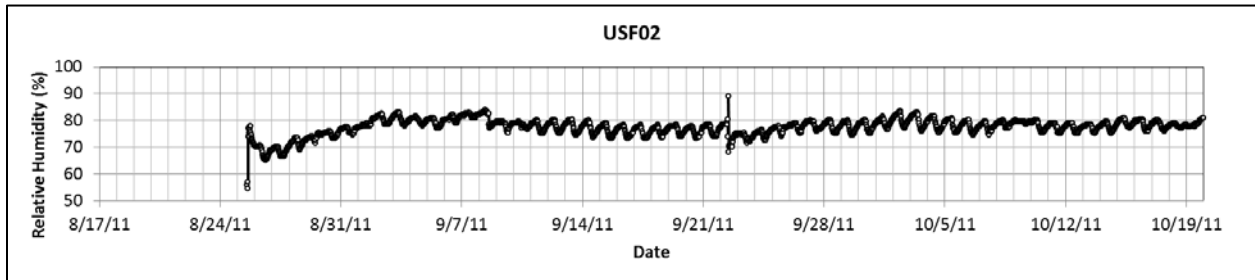


Figure 20 Relative Humidity of Duct 2 at USF

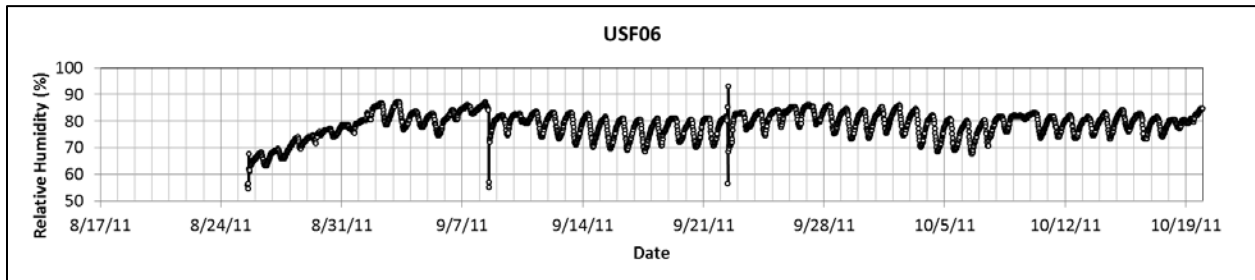


Figure 21 Relative Humidity of Duct 6 at USF

Both Ends Open Ducts

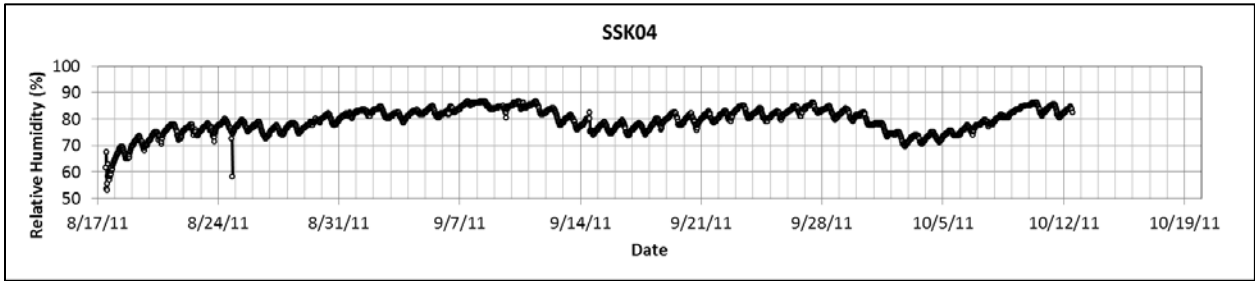


Figure 22 Relative Humidity of Duct 4 at SSK

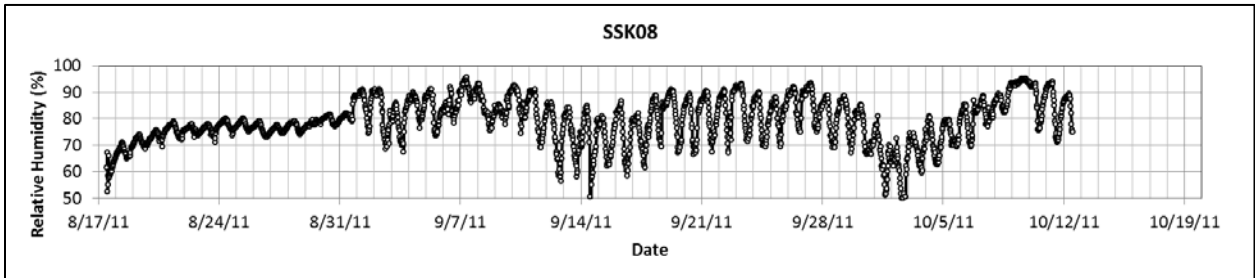


Figure 23 Relative Humidity of Duct 8 at SSK

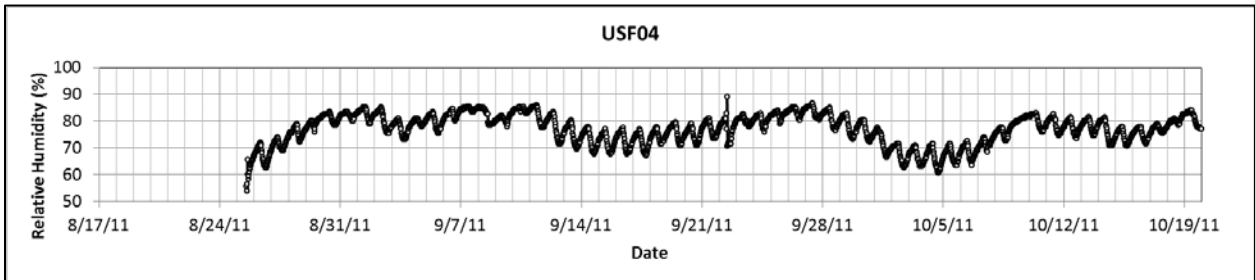


Figure 24 Relative Humidity of Duct 4 at USF

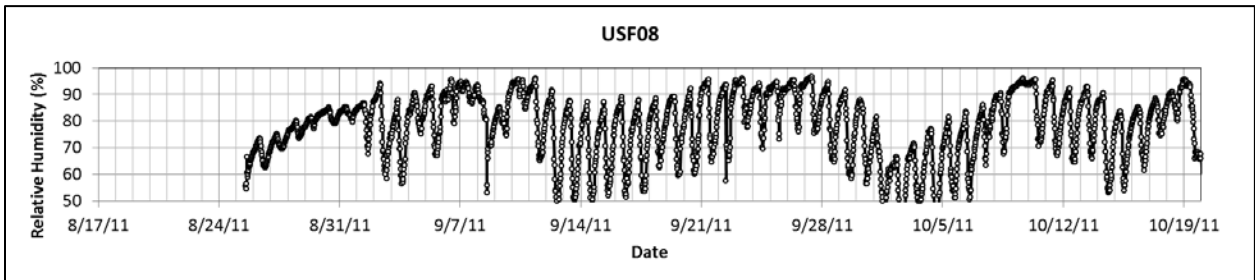


Figure 25 Relative Humidity of Duct 8 at USF

Closed and Wet Ducts

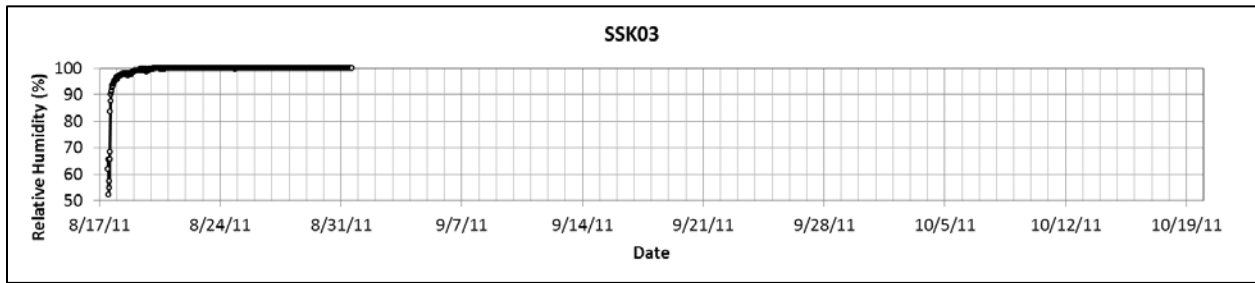


Figure 26 Relative Humidity of Duct 3 at SSK

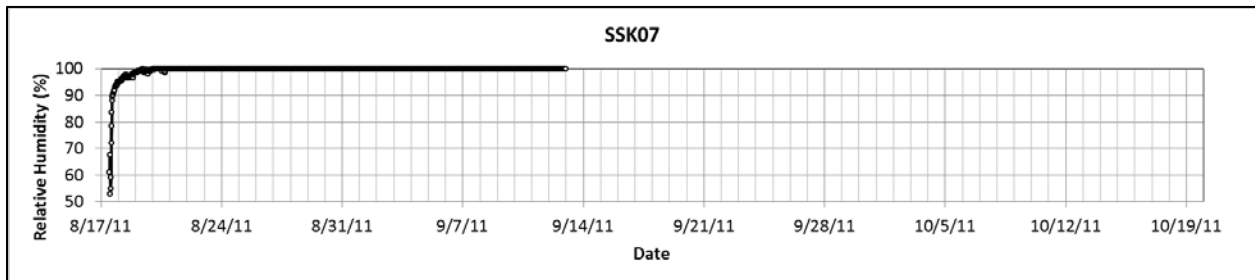


Figure 27 Relative Humidity of Duct 7 at SSK

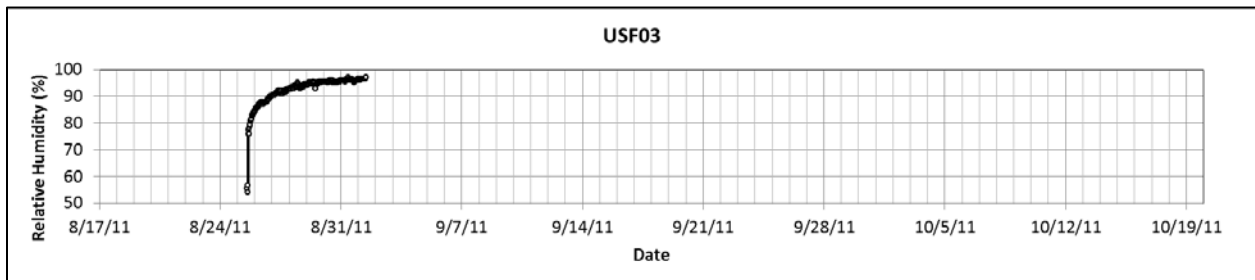


Figure 28 Relative Humidity of Duct 3 at USF

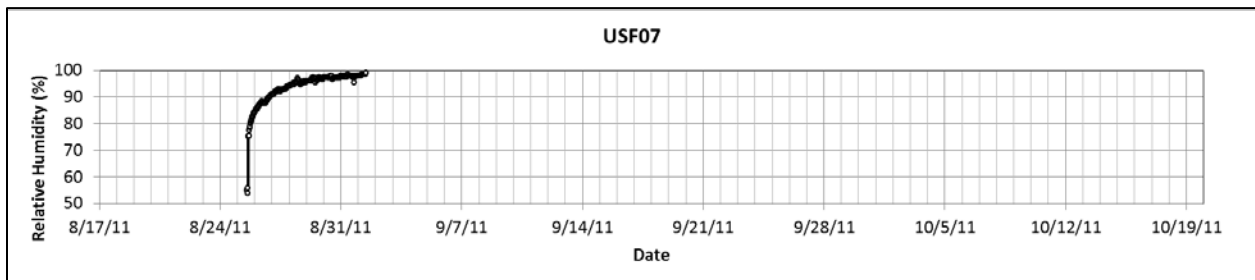


Figure 29 Relative Humidity of Duct 7 at USF

Visual Inspection

Visual inspection provided a rough indication of the corrosion behavior of the strand. The results from photographic documentation of the strand both in the initial, as-extracted, and cleaned condition are presented in Appendix 1. The corrosion observed on the ends of the strands did not appear to be influenced at all by the presence of the galvanized spike. Photographs of outer wires (Figures 30-34, showing the after-cleaning conditions) were taken with a 60mm macro lens; note for scale that wires are 5mm in diameter.



Figure 30 Outer Wire of 9-Month SSK Wet Exposure Sample - Before Bending (1/3)



Figure 31 Outer Wire of 9-Month SSK Wet Exposure Sample - Before Bending (2/3)



Figure 32 Outer Wire of 9-Month SSK Wet Exposure Sample - Before Bending (3/3)



Figure 33 Outer Wire of 8-Week SSK 2-Open Exposure Sample - Before Bending

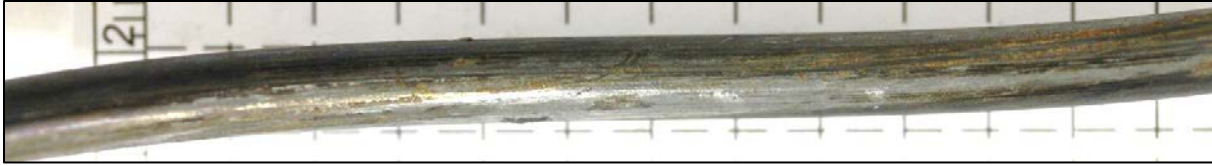


Figure 34 Outer Wire of 8-Week USF 2-Open Exposure Sample - Before Bending

Since conspicuous corrosion was observed only in the wet ducts and the longest term exposures (especially for the supplemental 9-Month exposed samples that became available from the previous investigation), detailed observations addressed mainly those conditions. Wire samples taken from the supplemental 9-Month wet exposed strands (Figures 30-32) showed conspicuous localized corrosion, termed as pitting in the following. That name is used here as a rudimentary term, while recognizing that commonly pitting refers to a phenomenon affecting otherwise passive metals, wherein the passive film is compromised by some means in a localized actively corroding zone coupled with a larger passive region. What was observed in this investigation was likely corrosion in small droplet sized zones where water had condensed on the surface, with electrochemical coupling involving a relatively small domain (Gellings, 2005). Limited pit depth determination was conducted in selected 9-month wet exposed wire samples through the use of a caliper with an attached needle. Corrosion products are still visible within the pits despite cleaning through mechanical abrasion. Corrosion both uniform and pitting, seem to be associating with what appear to be features on the strand formed during manufacturing. The maximum pit depth measured from those selected samples was $\sim 65 \mu\text{m}$. This is consistent with the visual observation of wide, shallow pits where pit width was in the order of one mm (e.g., Figure 31 which shows some of the larger pits). Assuming that only the outer wires contained pits, the pit density in those samples averaged ~ 150 pits per linear foot of

strand, whereas the pit density of strands of all the other conditions sampled was much less and hardly quantifiable. This is illustrated by the appearance of the samples pictured in Figures 32 and 33. 8-Week marine exposed samples (Figure 33) showed very light pitting, far milder than that seen from the supplemental strands exposed for 9 months (Figure 30 -Figure 32). Figure 34 from USF, also 8-Week exposure shows comparable corrosion condition as that in Figure 32, with corrosion appearing to preferentially initiate and progress around what again appear to be manufacturing features. In this instance, there does not seem to be any manifestation of pitting-like damage.

Tensile Testing

Three performance descriptors were evaluated from the results of the tensile pull test: total load at failure, total elongation, and load at 1% elongation. These values were then compared to the mechanical performance criteria as specified by ASTM A416 (ASTM International, 2006). The graphs in Figure 37 through Figure 48 show the cumulative fractions of each respective category. The vertical red lines indicate the ASTM specified requirement for satisfactory performance. Major slippage occurred when testing some strands. The cause was loss of gripping due to either improper application of the silicon carbide at the ends, or failure to suitably clean the jack grips before each sample was tested. Samples which displayed obvious grip slippage are not represented in the following data. Figure 35 shows the samples ready for testing with SiC coated ends. Figure 36 shows a sample break and the fully engaged grips used for testing.



Figure 35 Sample Strands' Ends Coated in Grit Material Awaiting Tensile Testing

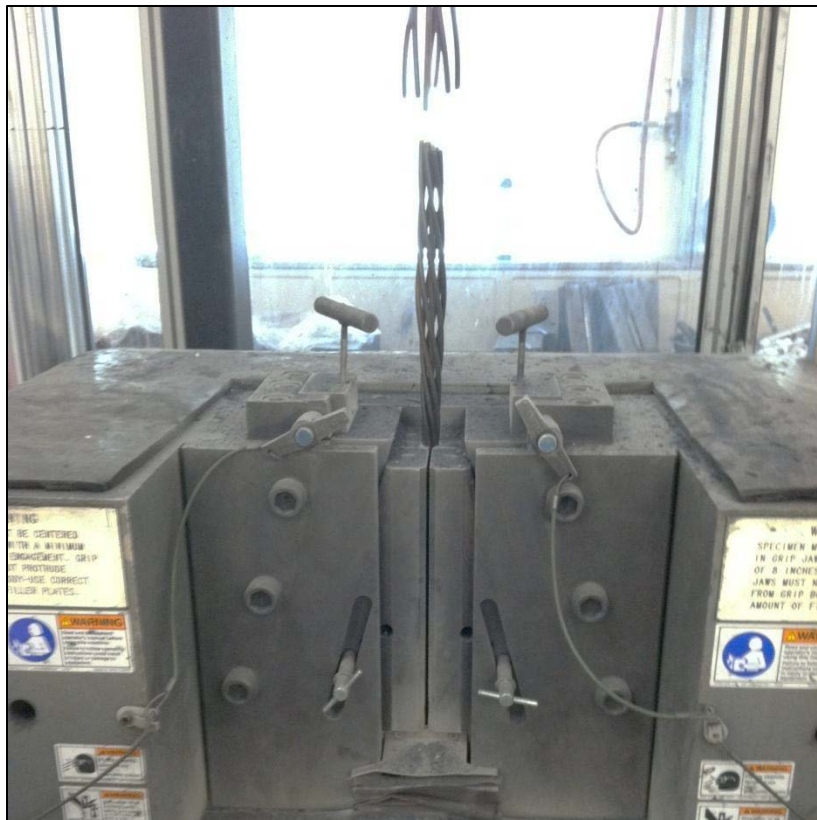


Figure 36 Sample Strand Break and Fully Engaged Grip

One strand, SW2D2, showed a satisfactory load to failure, however, it did not satisfy the 3.5% total elongation requirement. The cause is most likely a reported problem with the extensometer used during testing. Normal practice condoned by ASTM 416 is to test two (2) additional specimens from the same batch, should either of the other two (2) fail, the batch is to then be rejected, otherwise the failure may be ascribed to a testing irregularity (ASTM International, 2006). As multiple strands from the same exposure duration, environment, and duct condition did not show any trend towards this reduction in elongation it may be assumed that this specimen's failure to meet standards was due to a testing irregularity.

Load at Failure

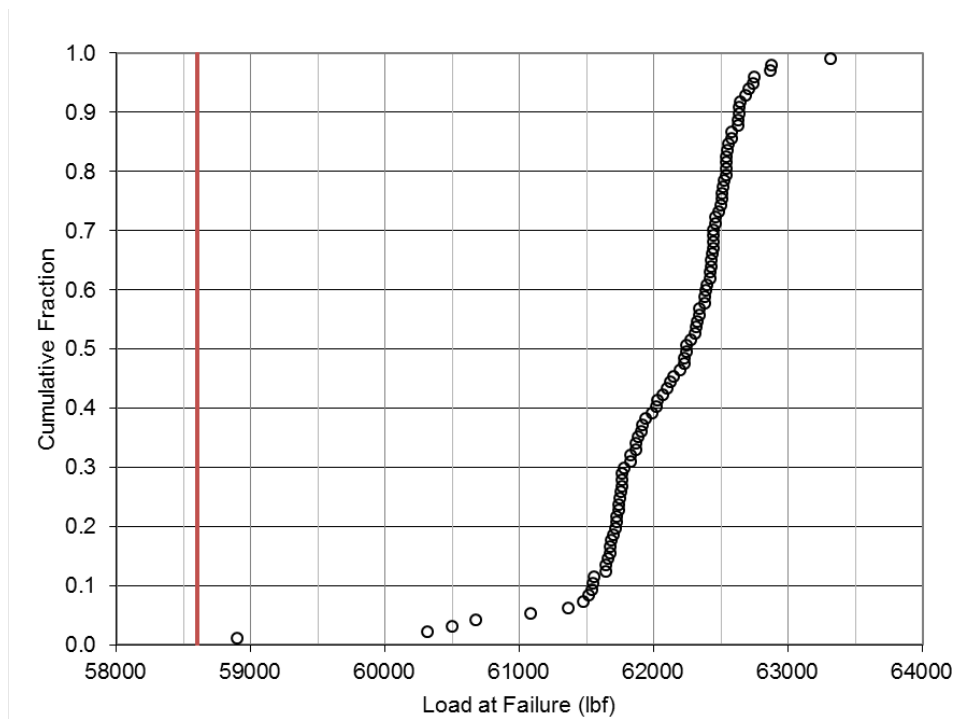


Figure 37 Total Cumulative Fraction of Load at Failure

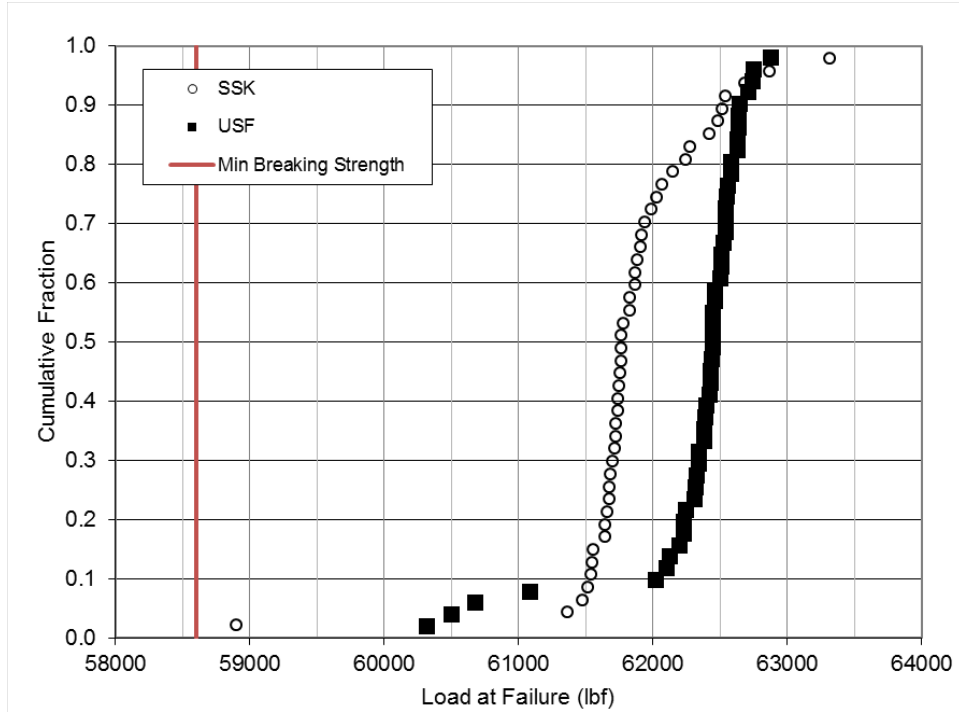


Figure 38 Cumulative Fraction of Load at Failure - Environment Comparison

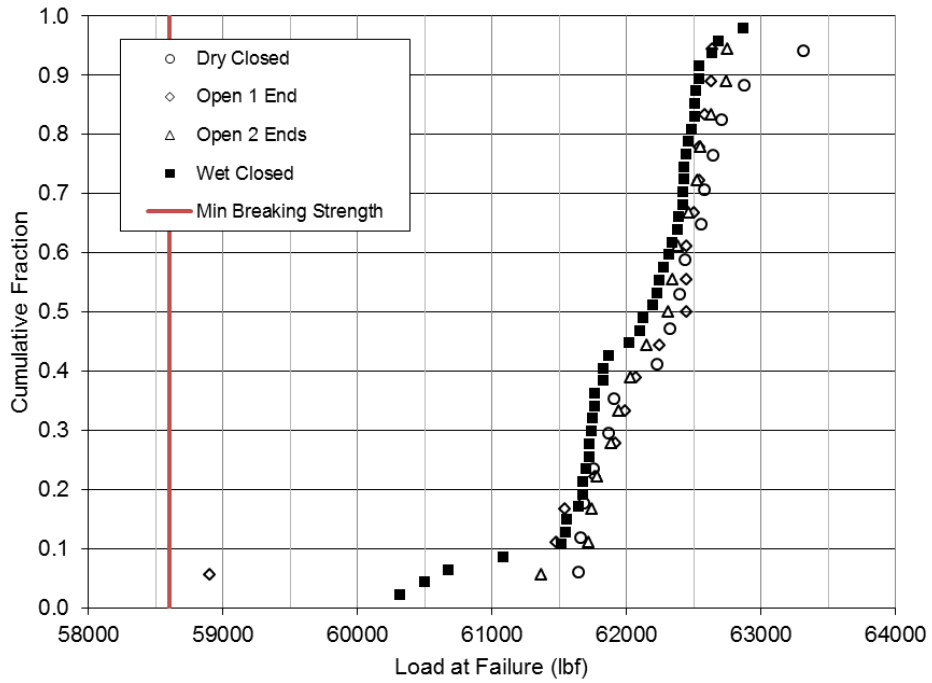


Figure 39 Cumulative Fraction of Load at Failure - Duct Condition Comparison

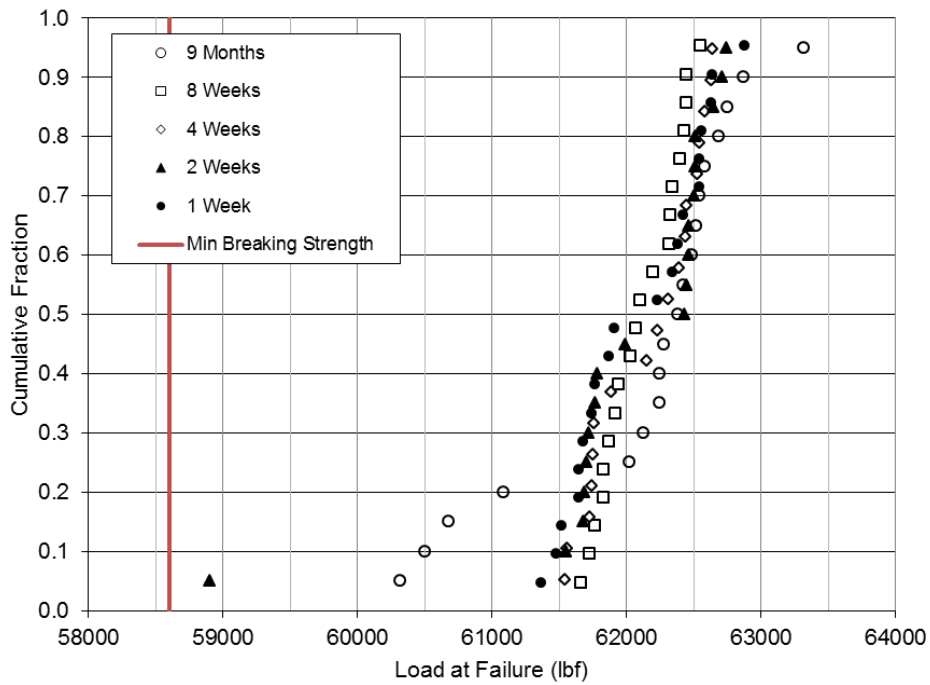


Figure 40 Cumulative Fraction of Load at Failure - Exposure Length Comparison

Total Elongation

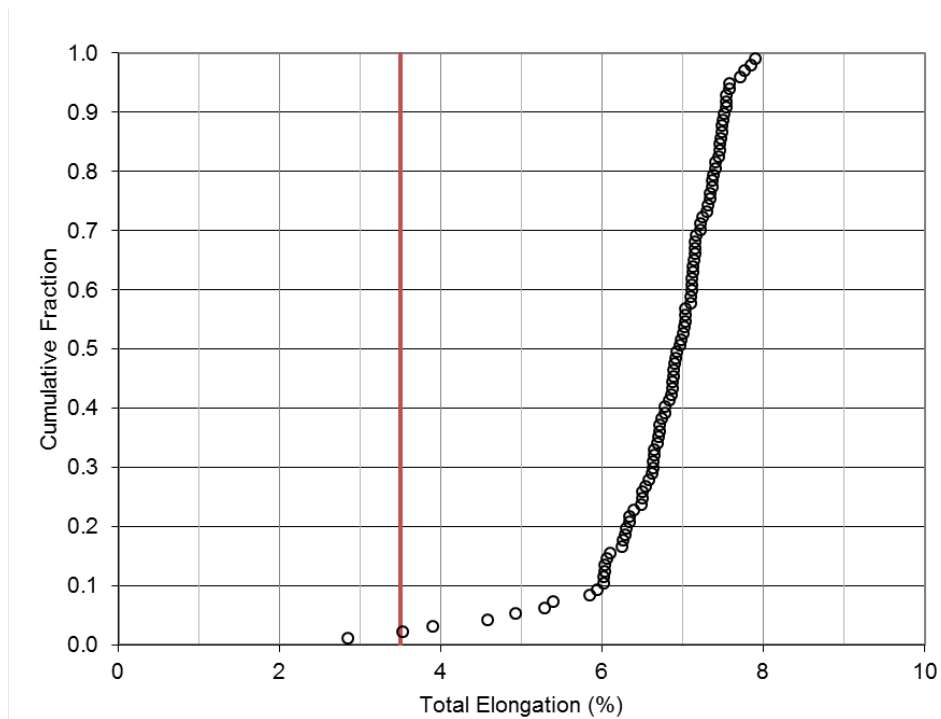


Figure 41 Total Cumulative Fraction of Total Elongation at Failure

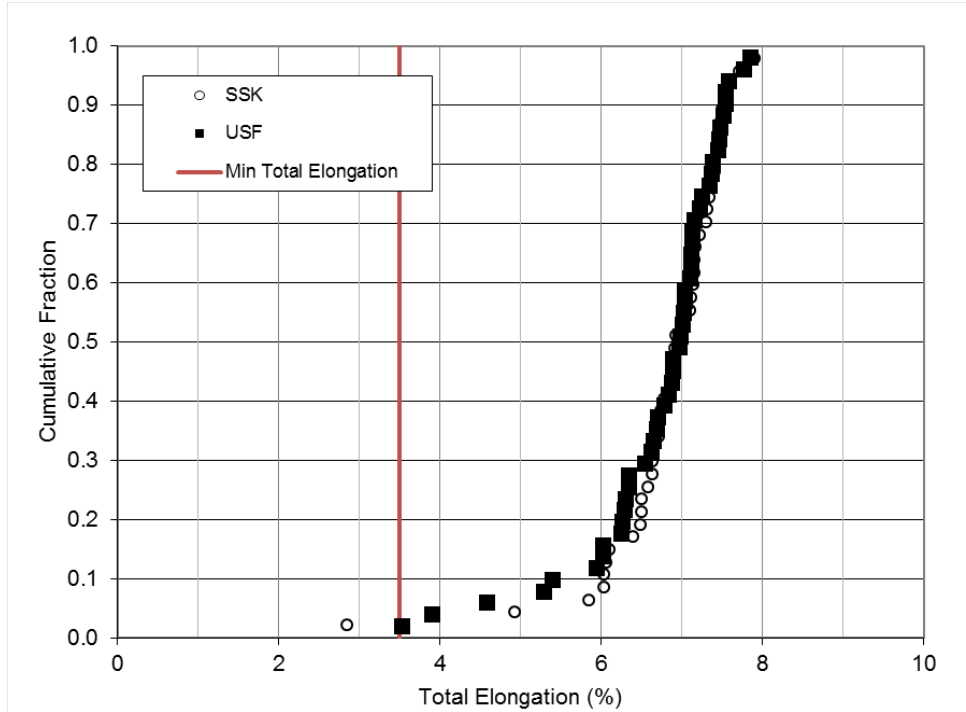


Figure 42 Cumulative Fraction of Total Elongation at Failure - Environment Comparison

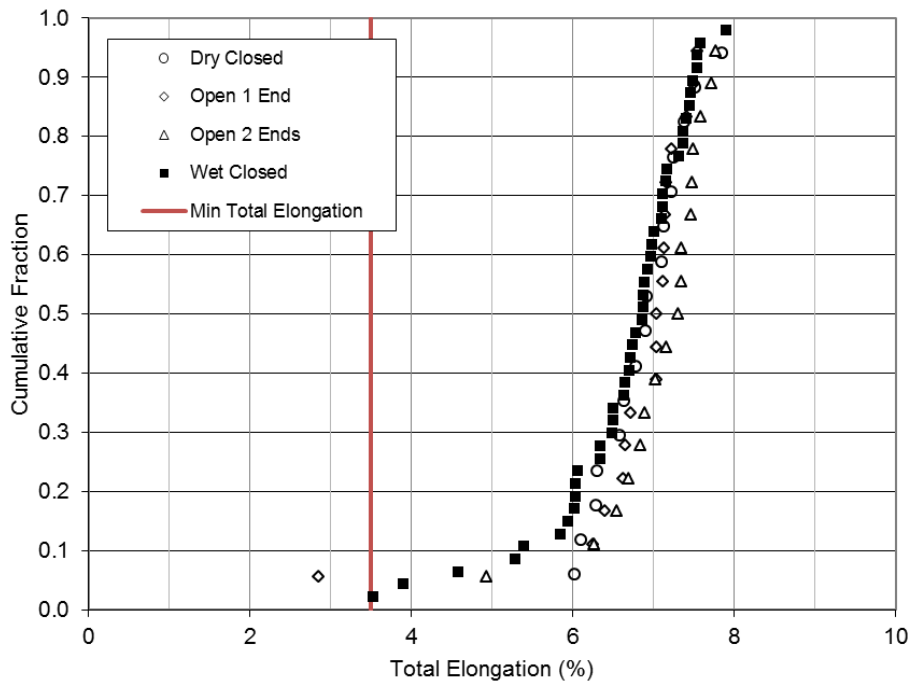


Figure 43 Cumulative Fraction of Total Elongation at Failure - Duct Condition Comparison

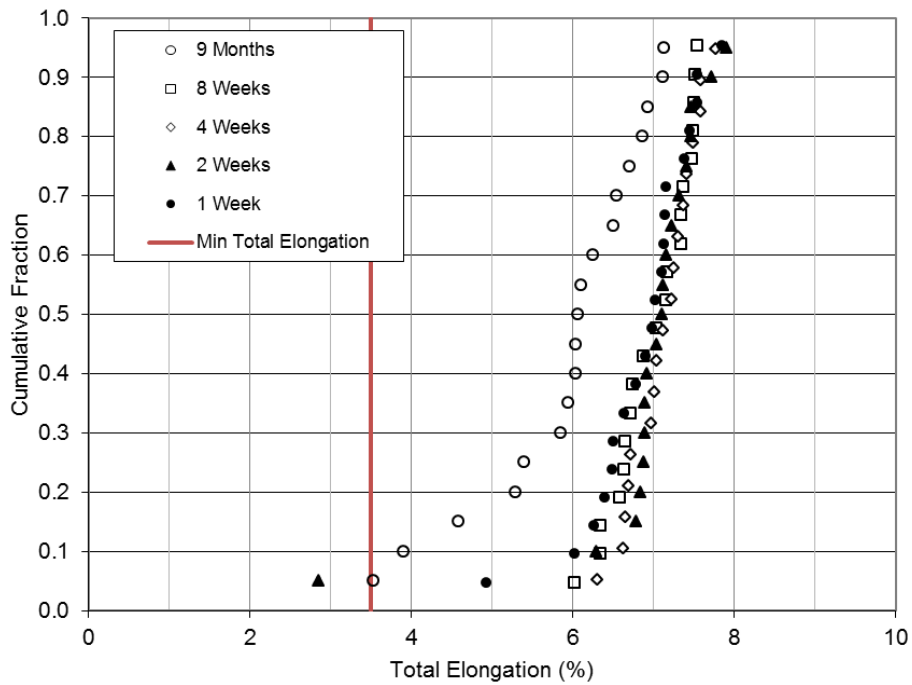


Figure 44 Cumulative Fraction of Total Elongation at Failure - Exposure Length Comparison

Load at 1% Extension

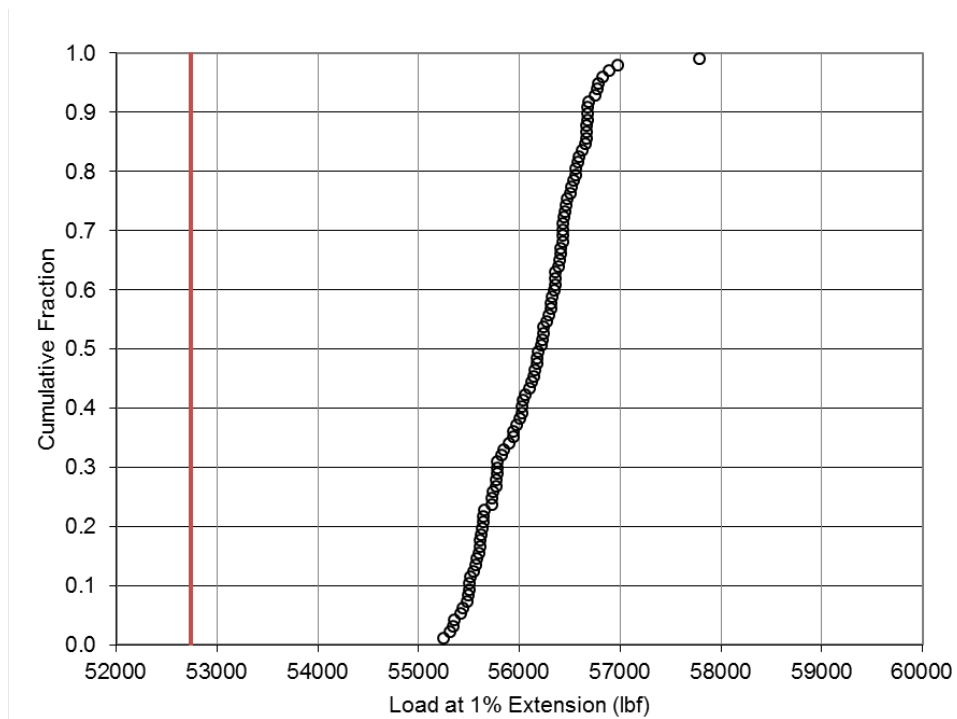


Figure 45 Total Cumulative Fraction of Load at 1% Extension

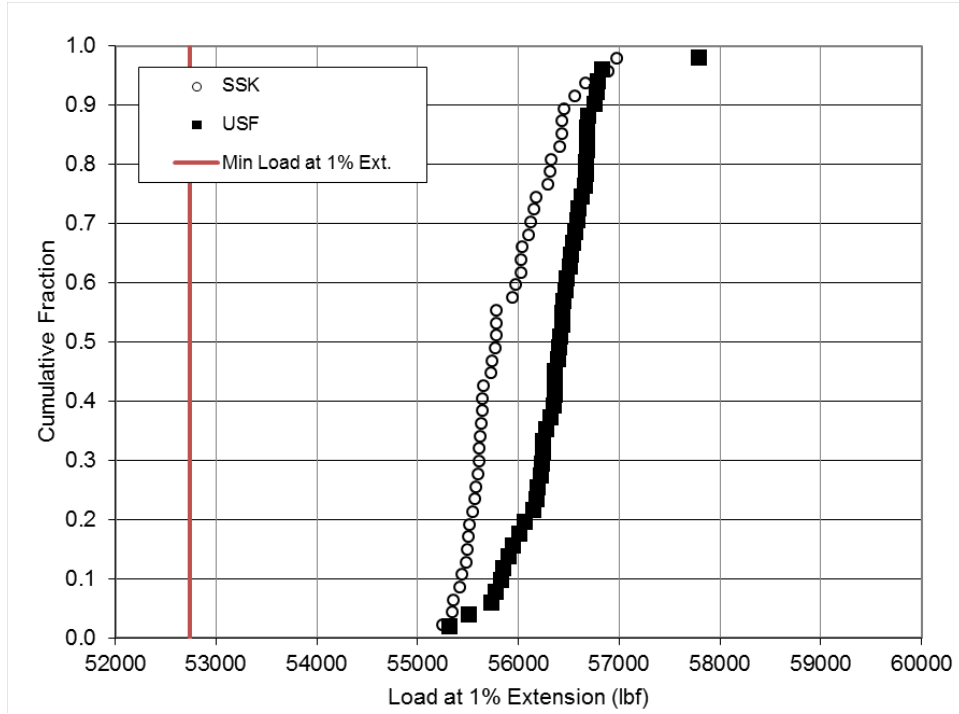


Figure 46 Cumulative Fraction of Load at 1% Extension - Environment Comparison

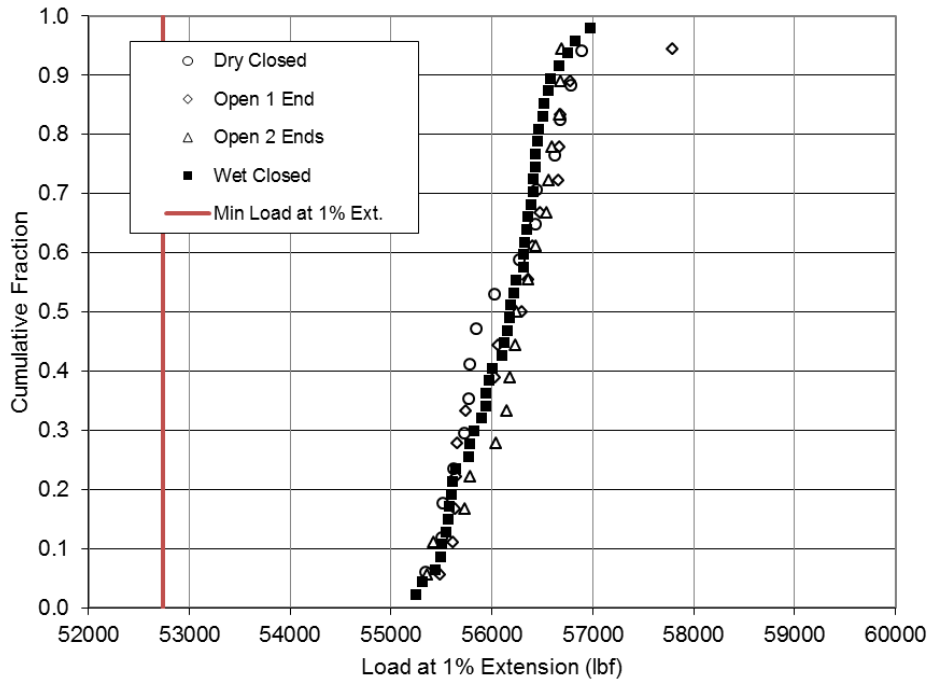


Figure 47 Cumulative Fraction of Load at 1% Extension - Duct Condition Comparison

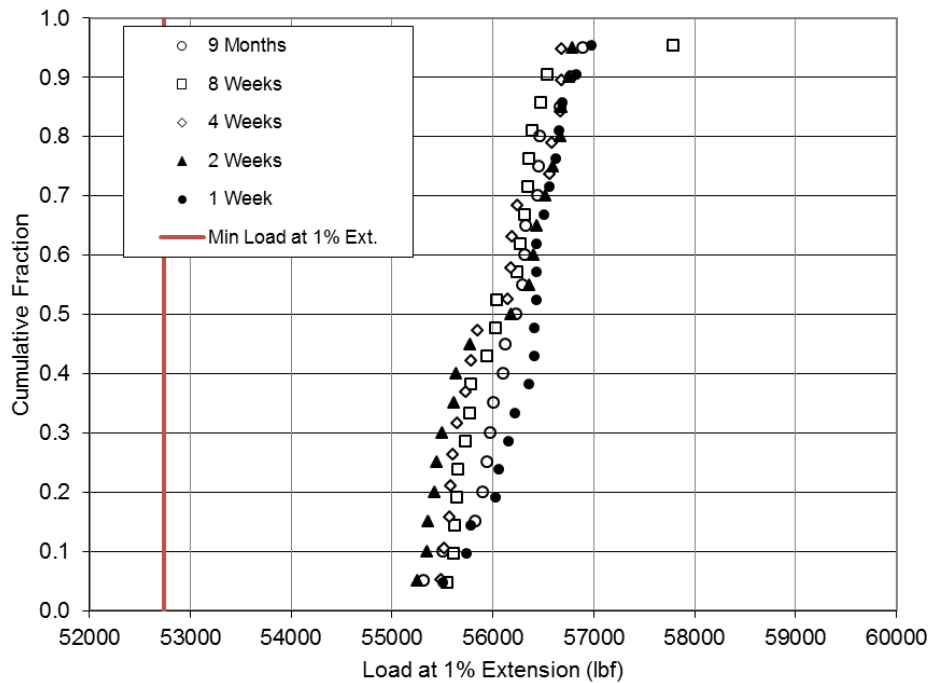


Figure 48 Cumulative Fraction of Load at 1% Extension - Exposure Length Comparison

Statistics

Table 3 Standard Deviation Values for Each Experiment Variable

<i>Experiment Variable</i>	<i>Load at Failure (lbf)</i>	<i>Elongation to Failure (%)</i>	<i>Load at 1% Ext. (lbf)</i>
Total	600	0.86	470
USF	525	0.89	393
SSK	588	0.82	424
Dry	480	0.51	492
1-Open	867	1.04	578
2-Open	394	0.67	414
Wet	558	0.91	427
1-Week	458	0.64	365
2-Week	838	1.02	555
4-Week	384	0.39	436
8-Week	275	0.45	503
9-Month	815	0.99	393

Table 4 Mean Values for Each Experiment Variable

Experiment Variable	Load at Failure (lbf)	Elongation to Failure (%)	Load at 1% Ext. (lbf)
Total	61956	6.87	56437
USF	62493	7.03	56437
SSK	61956	6.87	55924
Dry	62196	6.92	55997
1-Open	62288	7.04	56289
2-Open	62189	7.06	56272
Wet	62038	6.35	56191
1-Week	62148	6.89	56406
2-Week	62212	7.15	56102
4-Week	62223	7.14	56106
8-Week	62147	7.02	56158
9-Month	62013	5.86	56142

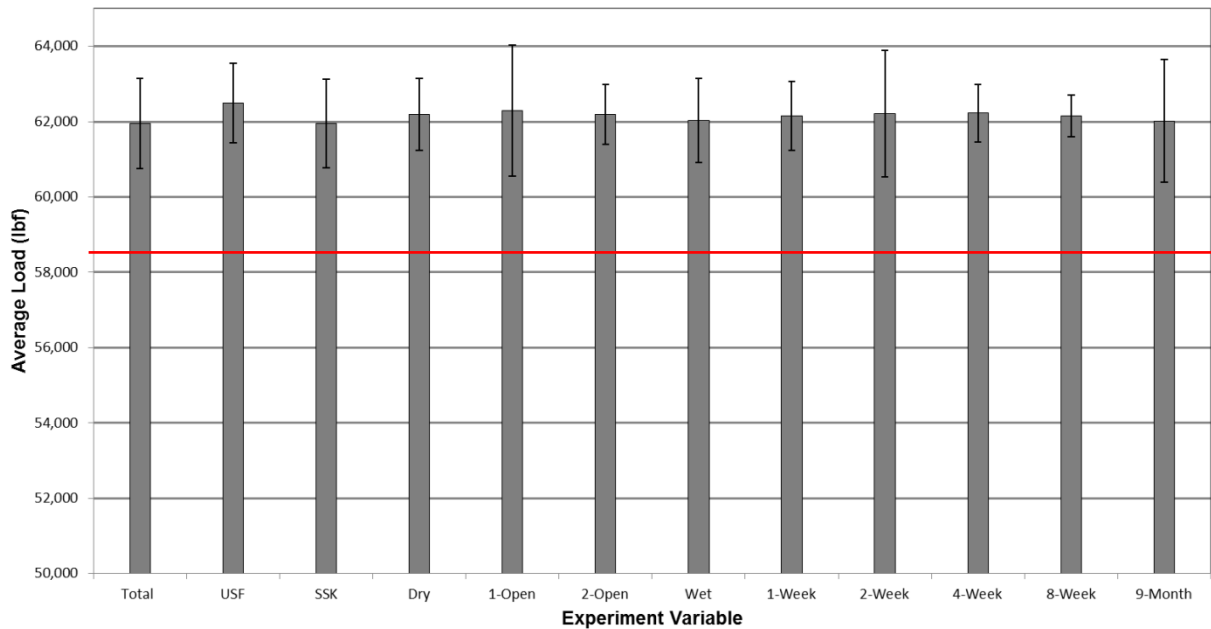


Figure 49 Average Load at Failure by Experiment Variable - Error Bars are 2 Standard Deviations Tall (Red Line Indicates ASTM A416 Minimum Requirement)

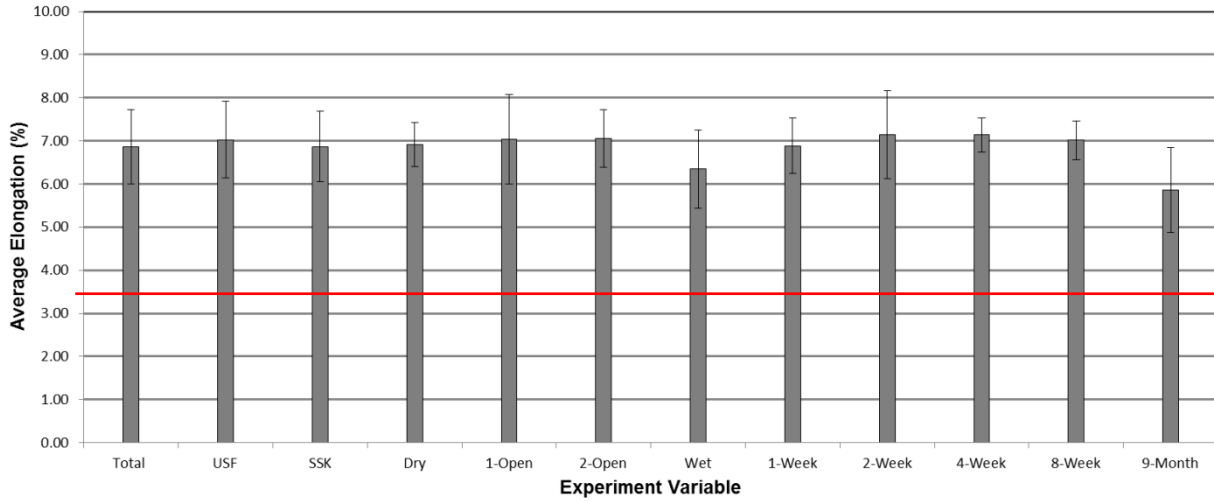


Figure 50 Average Elongation to Failure by Experiment Variable - Error Bars are 2 Standard Deviations Tail (Red Line Indicates ASTM A416 Minimum Requirement)

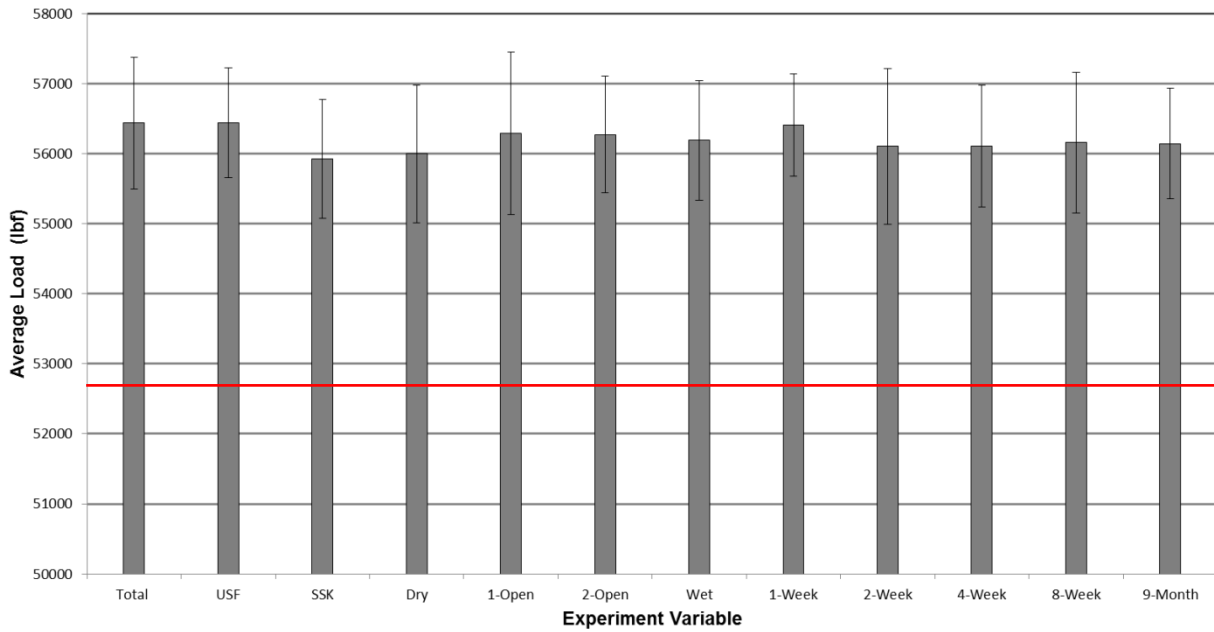


Figure 51 Average Load at 1% Extension by Experiment Variable - Error Bars are 2 Standard Deviations Tail (Red Line Indicates ASTM A416 Minimum Requirement)

Fracture Surface

Typical wire fracture surfaces are illustrated in Figures 52-55. The fracture shown in different perspectives in Figures 52 & 53, is from sample SW2D3b (referring to the labeling index in Figure 8) which is from a wet duct exposed for 2-Weeks in the SSK location. The other fracture shown in Figures 54 & 55 is from the same strand, but a different wire. Failure surfaces exhibited typical cap and cone structure as expected in a ductile failure. It is clearly shown in Figure 52 major elements of ductile failure: fibrous fracture in the center portion, the radial shear emanating outwards from the center, and shear lips around the perimeter. No indication of transverse cracking was observed on any of the wire fracture surfaces.



Figure 52 Typical Fracture Surface (1/4)



Figure 53 Typical Fracture Surface (2/4)



Figure 54 Typical Fracture Surface (3/4)



Figure 55 Typical Fracture Surface (4/4)

Metallography

Figures 56 through 70 depict the results from metallographic evaluation. Large and or sharp enough preexisting cracks or surface irregularities could cause the sample to break during the bending procedure, as discovered during exploratory testing with notches induced with a hacksaw blade. Small sharp notches on the surface, even those generated from wedge piece (chuck) grip marks, were also found to be enough to cause specimen fracture during bending. However, no specimen extracted from the even the most severely exposed strands failed during bending. Metallographic samples were polished to 1 μm diamond polish, examined, and then subsequently etched with Nital (1% nitric acid, 99% ethanol) then examined again. Cross sections were made longitudinally along the wire, parallel to the drawing axis and oriented to show the cross section of the bend. Note for scale: strand diameters are 5 mm.



Figure 56 9-Month SSK Wet Exposure Sample - Exterior of Bend Surface



Figure 57 9-Month SSK Wet Exposure Sample - Unetched (Field Width- 2 mm)



Figure 58 9-Month SSK Wet Exposure Sample - Etched with Nital (Field Width- 2 mm)

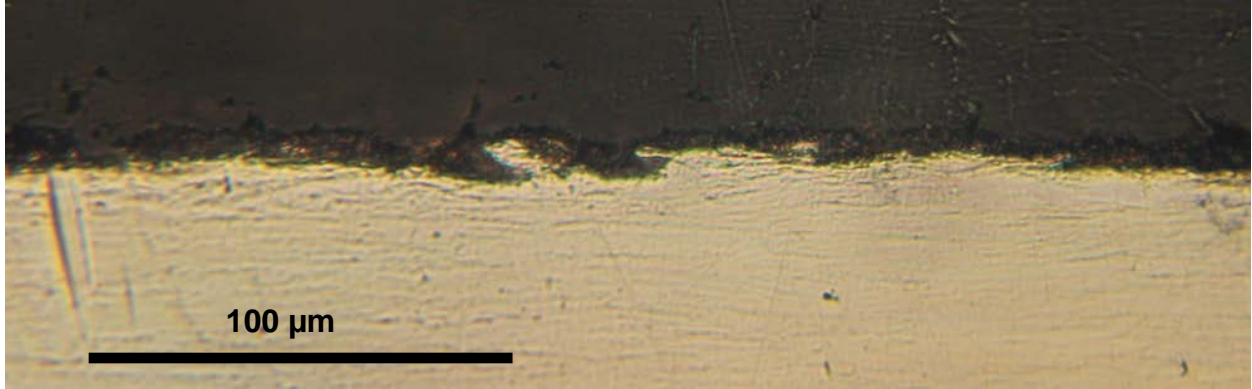


Figure 59 9-Month SSK Wet Exposure Sample - Unetched

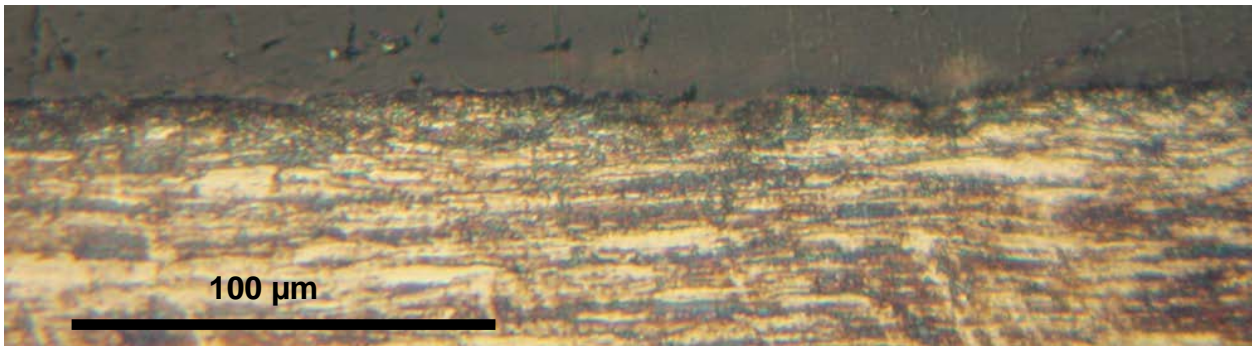


Figure 60 9-Month SSK Wet Exposure Sample – Etched with Nital



Figure 61 8-Week SSK 2-Open Exposure Sample - Exterior of Bend Surface



Figure 62 8-Week SSK 2-Open Exposure Sample - Unetched (Field Width- 2 mm)

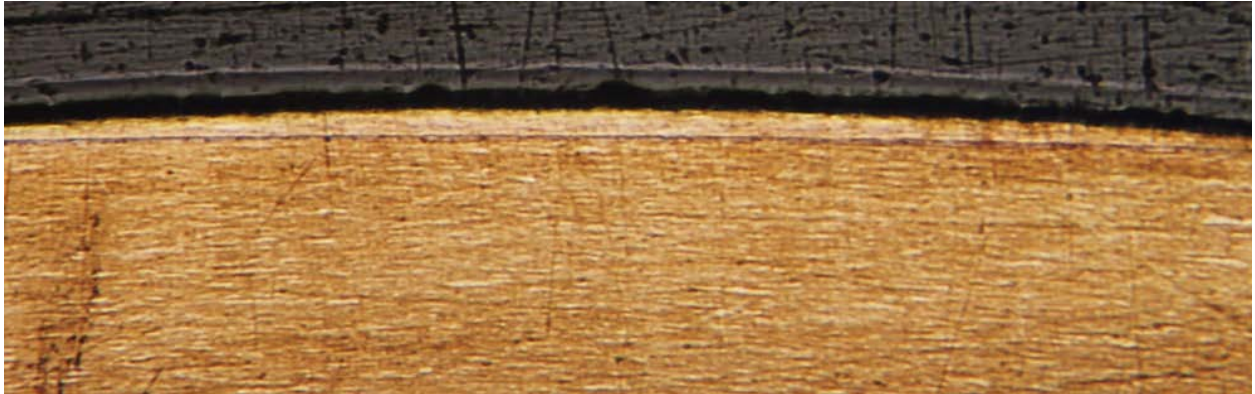


Figure 63 8-Week SSK 2-Open Exposure Sample - Etched with Nital (Field Width- 2 mm)

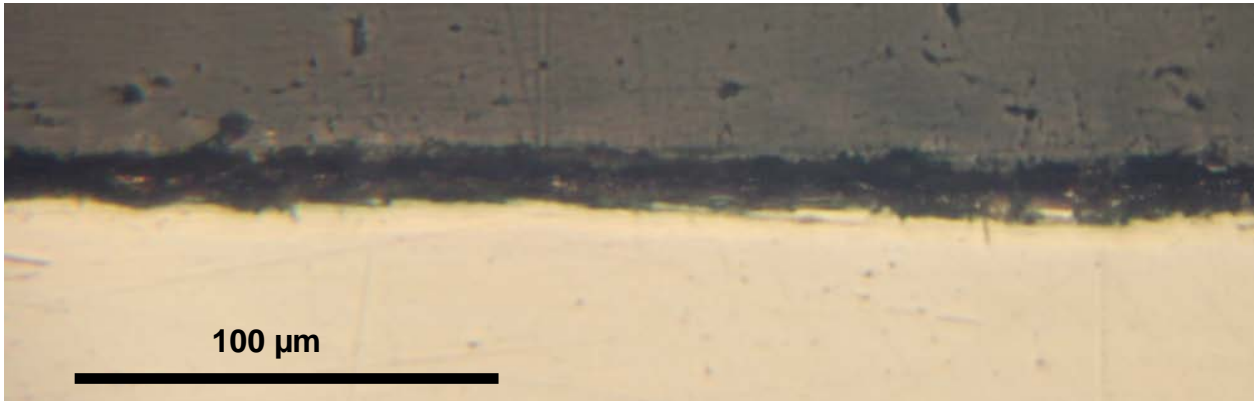


Figure 64 8-Week SSK 2-Open Exposure Sample - Unetched

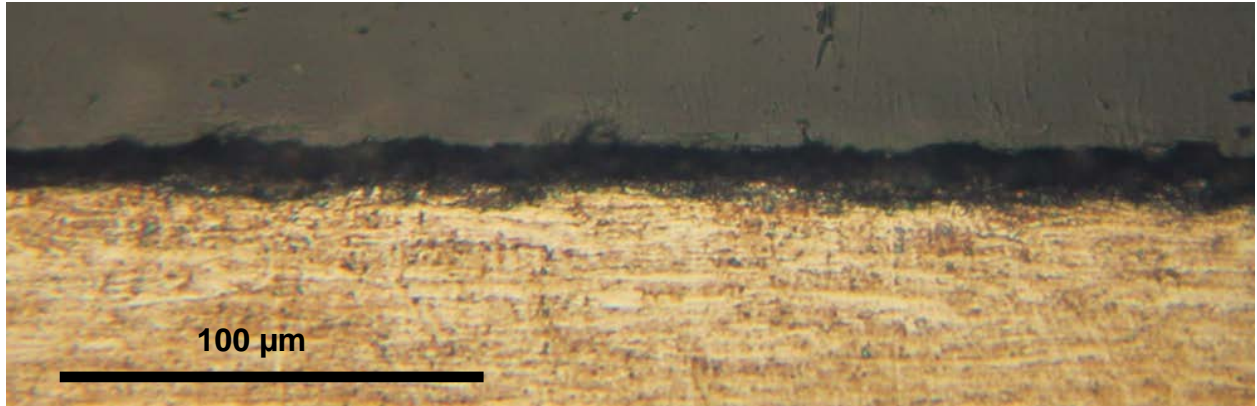


Figure 65 8-Week SSK 2-Open Exposure Sample - Etched with Nital



Figure 66 8-Week USF 2-Open Exposure Sample - Exterior of Bend Surface

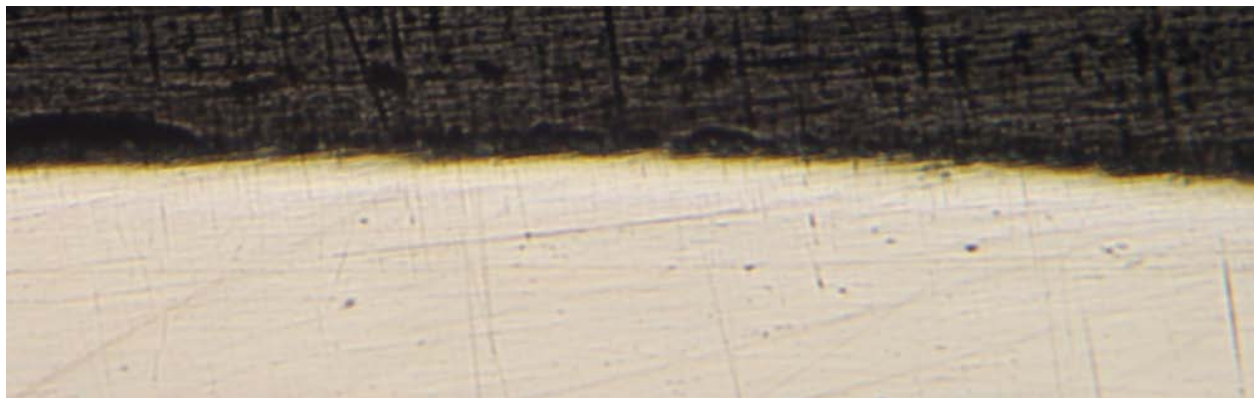


Figure 67 8-Week USF 2-Open Exposure Sample - Unetched (Field Width- 2 mm)



Figure 68 8-Week USF 2-Open Exposure Sample - Etched with Nital (Field Width- 2 mm)

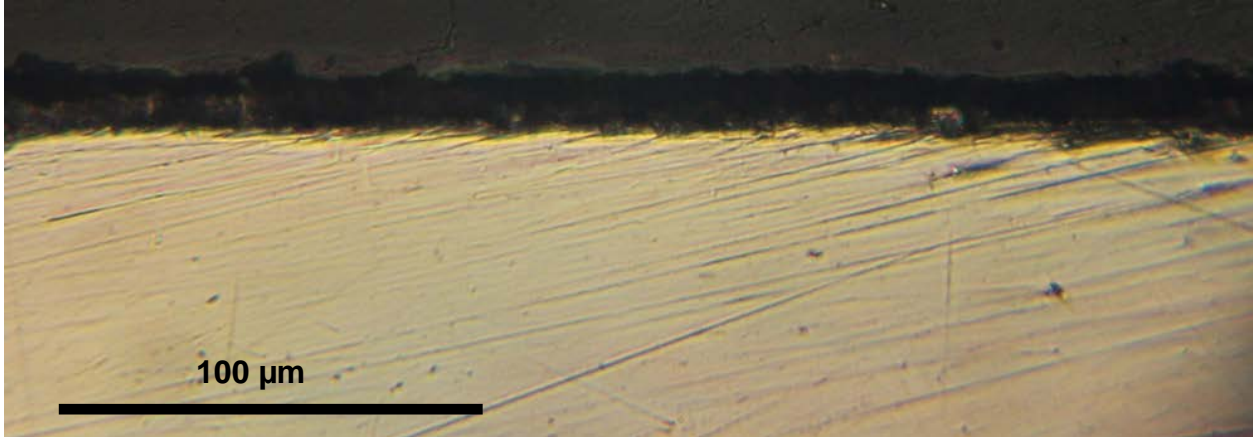


Figure 69 8-Week USF 2-Open Exposure Sample - Unetched

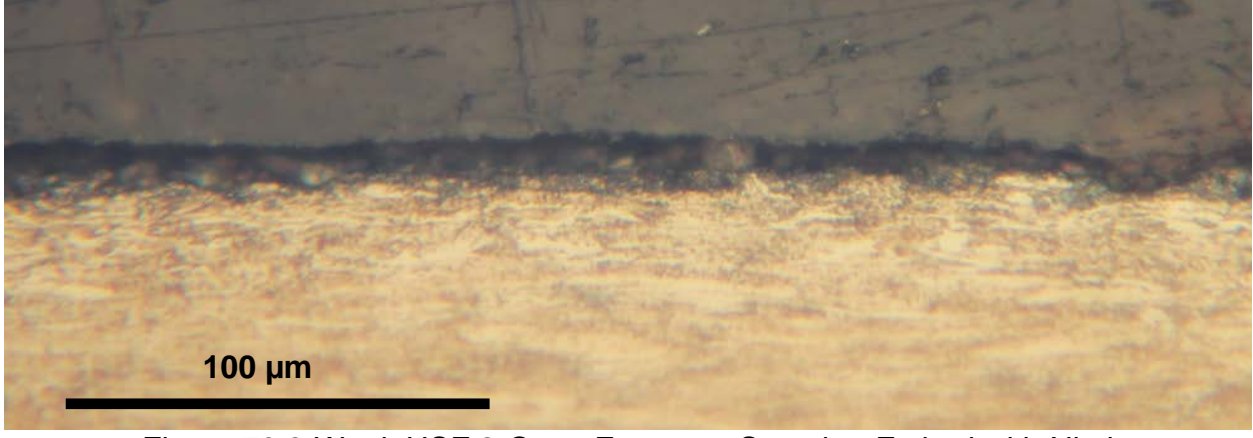


Figure 70 8-Week USF 2-Open Exposure Sample - Etched with Nital

DISCUSSION

Relative Humidity and Temperature

Temperature results from both locations are typical values expected for those locations. With the exceptions of spikes coincident with sample insertion/extraction events, typical temperatures ranged from highs around 35° C to lows in the mid to low 20s. This range is in contrast with temperatures rarely exceeding 30 C and lows reaching into the 10s in the previous investigation with the same assemblies. (Sagüés, Karins, & Lau, 2011)

Although slightly more pronounced in the SSK location, similar diurnal cycling and high and low values in RH occurred at both locations. Otherwise there was not a major variation in the RH results obtained from the SSK and the USF locations. High RH values were typically in the 80% to 90% range for closed and One-End Open ducts and about 95% for the Both Ends Open ducts. As expected, the variability of the diurnal cycles increased with the extent of interaction with the external air. Closed ducts showed the most insulation from the external air One-end open ducts showed closer behavior to that of the closed ducts. However this may be because the probes were placed in the closed end of these ducts. Two-end open ducts mimicked the external RH environment and recorded wide sweeping variability from day to night, as expected. Overall, the conditions were consistent with the high temperature, humidity and rainfall frequency prevalent at the test locations during summer months. These conditions are

of interest given that RH values above 80% are normally associated with a sustained water film forming on the surface of steel enabling corrosion. In the previous investigation at the same facility, RH in the dry and the open ducts approached but rarely exceeded 80%. (Sagüés, Karins, & Lau, 2011).

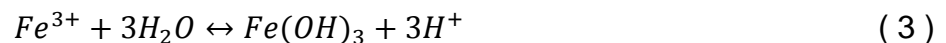
Probes in the wet and closed duct conditions recorded fully saturated air as expected. The probes were removed following an extraction where one of the wet condition probes initially would not transfer data, indicating internal circuitry damage of the probe. As the RH condition in all wet ducts showed no indication of change, the probes were removed to prevent further damage to their circuitry. The water reservoirs attached to the ducts (Figure 5) were inspected periodically to ensure the saturation condition was maintained. RH within these ducts maintained 100% through the entire duration of the experiment. RH variation in the sealed ducts appears consistent with changes in temperature condensing water, thus making that water removed from duct air as reflected by the lower RH.

It is of interest to compare the present results to those obtained during a late spring visit to a PT construction site. As part of an ongoing investigation, RH was monitored inside selected tendon ducts prior to strand placement from a PT structure under-construction in Tampa, Florida. The RH in the ducts sampled at high elevation in that structure consistently sustained values below 80% with an exception following a rain event. These results are in contrast with the somewhat higher RH values obtained within ducts from the present experiment. Several features may contribute to this disparity: elevation differences, duct size and length, constructed time, and sealing methods. At the site, temporary caps were used to seal the ducts from rain-water

intrusion, however, these seals are not air-tight and water vapor could easily escape over the construction period effectively 'drying out' the ducts. Ducts at the USF and SSK locations were sealed quite well and were only opened during daytime hours which coincided with high RH times of the outside air. Importantly, the ducts which were monitored at the construction site were cast within concrete elements, which may insulate the ducts within from the diurnal temperature cycle and cause RH to drop within the duct. That condition is not sampled by the present tests and is being presently incorporated in ongoing follow-up research

Water Availability

When considering corrosion in an enclosed air space, the availability of reacting species is of interest. In particular, it may be asked whether the water in the air within the ducts would be adequate to support a corrosion rate enough to enable a failure under sustained load on loss of cross section from uniform corrosion. For simplicity, we will assume only the formation of ferric (Iron (III)) hydroxide, while recognizing that other compounds may be also formed. The corresponding chemical equation is



Calculating the molar masses, a relationship between the amount of iron hydroxide formed and the amount of water consumed can be easily derived. That ratio was calculated to be 1.98 grams of $Fe(OH)_3$ produced for every gram of H_2O consumed. The water in the duct air at 30°C and 100% RH was calculated for the systems dimensions to be 0.982 grams. The volume and amount of iron to be consumed was also calculated by similar means as the rust, and consideration of the density of steel (7.87 g/cm^3), taken to be nearly all iron. An estimated timeframe for

strand corrosion to a critical section loss can be made by assuming that the corrosion rate is solely limited by the availability of water in the duct, and that all of the water in the duct air is recharged in a cyclical basis by some intrusion mechanism. The critical cross section is taken to be the area at which the strand can no longer take the required ASTM specified loading. The resulting amount of time needed to corrode to that critical cross section is found to be roughly six (6) years when assuming that water recharge is one day. However, if the corrosion were to be localized to a small segment or even a pit location, the critical condition at that rate of recharge could be reached in a conceivably much shorter time, in proportion to the degree of localization. Likewise, even much longer recharge cycles, as could be expected in very tight duct and anchor assemblies might introduce sufficient amounts of water to enable appreciable cross section loss in relatively short times if water availability were the limiting factor for corrosion development. Corrosion rates are limited too by other factors such as surface reaction kinetics, ignored by this analysis. Nevertheless, the calculations suggest that corrosion control aimed at eliminating water should address the disposition of any recharge water.

Visual Inspection

The strand segments depicted in Appendix 1 are an 8-inch section of each strand in the region with the greatest visual indication of corrosion damage. That selection was made as the strand is expected to fail in the most heavily corroded area. Sample wires used for bending and metallographic analysis showed that pitting was most prominent in the supplemental 9-month exposed strands in wet conditions. The other exposures did not show as noticeable damage as on these samples.

Environment

Strands extracted from the SSK environment generally had a duller exterior finish than those extracted from the USF location. Peppered red rust appeared on the surface of SSK strands where USF strands this appearance was fairly unaltered from the as-extracted condition. This difference in appearances was more evident after the strands were cleaned.

Duct Conditions

Closed duct strands showed very little corrosion on the strand, nearly indistinguishable from the as-received condition. It would be unlikely that strand would be considered for rejection in this condition. The wide variability of relative humidity between day and night, particularly pronounced in open ducts may be of interest. Moisture condensed on the strand can act as an electrolyte and cause shallow pitting.

Strands from the wet ducts showed considerably more conspicuous corrosion on the areas where water was intentionally splashed. However this corrosion was mostly superficial and following mechanical cleaning, the areas of conspicuous corrosion were nearly indistinguishable from the rest of the surface which has also undergone some surface corrosion. Wet duct strands in visual inspection appear to be more heavily corroded than those at the SSK condition, but it must be noted that SSK strands were transported to the laboratory using PVC tubing prior to photographing and those strands' corrosion products may have been mildly abraded off during transit. It must also be noted that as the 'wetted' sections of the wet ducts strands did not show more than superficial corrosion, which may have been due to the use of distilled water in the

experiment. Contaminated water, e.g. extra bleed water from nearby construction, might cause more damaging corrosion on the strand surface.

Exposure Length

Exposure length of strands did not seem to have a visually identifiable impact when compared to other variables. Even after the prolonged nine months of exposure of the supplemental samples, the cleaned strand surface was not visually dissimilar enough to distinguish it from other strands. Nevertheless, the exposure length was apparent on the corrosion propagation of the open duct strands, particularly on the 2-end open condition (not applied to the supplemental samples). After 8 weeks of exposure to the marine environment (SSK strands) the 2-end open strand had a dark red appearance generated from peppered red rust on the surface.

Tensile Testing

As can be appreciated for the global summary of data in Figure 37, the most striking feature of the tensile test results is that all samples properly tested (that is, without grip slipping) met or exceeded the specified strength requirement (red line). The lowest force datum in that figure corresponds to a 2-week, One-End Open exposure at SSK, but as indicated in the Results section this is likely the result of an undetected testing irregularity. The strength requirement was exceeded even by the visibly corroded supplemental 9-month wet exposure samples. It is noted however that 4 out of the 16 tensile test samples in that group were distinctly differentiated as the next lowest strength data, clearly identified in Figure 40 that compares the effect of exposure length. This differentiation is likely due to the pits observed on the surface of these strands (see Figure 30, Figure 31, and Figure 32).

Figures 38 to 40 show that other than the condition just noted for the supplemental samples, environment was the most prominent differentiating factor in terms of strength loss. As shown in Figure 38, the median load at failure for the seashore facility samples was distinctly lower than that of the inland exposure samples. The corresponding strength difference, however, was only 1% and both strength values still amply exceeded the ASTM requirement. This difference may tentatively be ascribed to salt spray from the nearby bay acting on the open-duct exposed strands, as well as briefly on all the other strands during the placement/extraction procedures. The deposited salt could promote the formation of small regions of electrolyte on the surface and initiating pitting or other forms of localized corrosion. The previously noted indications of somewhat greater visual appearance of surface distress in the SSK specimens (Visual Inspection section) are supportive of this interpretation. The associated enhanced pitting and local cross section loss would then be a possible explanation for the differentiation observed.

Total elongation at failure of all the strands tested (with one exception, for the same sample with the lowest tensile mentioned earlier) met or exceeded the minimum requirement (3.5%). The median value (7%) greatly exceeded the requirement. Elongation values showed no clear differentiation with respect to duct condition or environment. Duration of exposure of tests also did not appear to have an effect on ductility values, with the exception of the supplemental 9-Month exposure samples which showed as a group a marginal reduction (~1%) in median total elongation, and several values at the extreme low end of the elongation distribution. This comparative loss of ductility is likely associated with the loss of cross section and stress

concentration effects from the greater incidence of pitting present in these very long exposure specimens.

The values of load at 1% extension (Figures 45 to 48) followed trends consistent with those noted above and likely associated with the same factors.

It is noted that compliance with the mechanical specifications as evaluated by the tensile test is only one aspect of the many issues that may concern durability of a PT tendon, so the present results should be considered only in that light (Reis, 2007).

Metallography

The microstructure of the samples examined was consistent with that of heavily cold worked pearlitic steel. Grain boundaries, visible from etching, are longitudinal along the wire as expected. This structure is obtained from the drawing process (ASM Handbook Committee, 1973). Grain size is only a few micrometers in this orientation. For additional information on this particular steel's microstructure the reader is referred to Enos & Scully (2002).

The near-surface metallography revealed only minor corrosion-induced roughness, limited only to the supplemental 9-Month wet exposure samples and illustrated in Figure 56. The interface appeared mostly smooth for the samples examined that had been exposed during the regular test sequence, as illustrated in Figures 64 and 69.

The bending procedure was intended to open up any preexisting transversal cracks and provide an opportunity for initiation and expansion of cracks that could originate at the bottom of corrosion pits. Metallographic examination at high magnification showed no cracks exposed on any of the bend-tested specimens and no

evidence of preexisting transverse cracking was observed. As the strands were not stressed during exposure, the latter result was as expected since residual stresses from manufacturing alone are not anticipated to be important.

Discussion on Limit Conditions Associated with Corrosion

The following subsections discuss approaches that may serve as a basis for future examinations of the mechanical conditions resulting from corrosion progression in strands exposed during the pregrouting period. The treatments are tentative but serve as starting points for more sophisticated approaches to be elaborated in future work.

General (Uniform) Corrosion Approximation

Estimating the general corrosion on the strand under idealized conditions can provide insight onto the theoretical maximum amount of time the strand may be left in an ungrouted duct. Making a quantified estimation requires several assumptions:

- Corrosion is uniform along the entire strand
- Corrosion rate is constant
- Only outer wires experience corrosion, which takes place circumferentially (uniform radial loss). King wires are assumed to be obstructed by the outer wires and not affected by corrosion.
- The strand is assumed to have material properties as reported by the manufacturer in Appendix 2.

In the following it will be assumed that a strand with initial nominal 0.21775 in^2 cross sectional area will be tested after corrosion by applying the amount of force specified by ASTM A416 (ASTM International, 2006) as a load requirement (58.6 kip). It is further assumed that the steel has an ultimate strength equal to that determined in the

manufacturer test with results given in Appendix 2 (286.8 ksi). As the strand loses cross section by corrosion with the morphology indicated above, the cross section decreases until the stress reaches the ultimate strength. The amount of uniform corrosion penetration (radial loss) experienced by the outer wires at that moment is defined as the critical penetration depth “c”.

The approach of this calculation is to determine the critical penetration depth of the corrosion front on the circumference of the outer wires. Using the assumptions listed above, the formula for calculating the area of the outer wire is given by:

$$A_{outer} = \frac{\pi}{4}(d - 2c)^2 \quad (4)$$

where d is the initial diameter of the wire, and c is the penetration depth.

$$A_{limit\ state} = A_{king} + 6A_{outer} \quad (5)$$

Both the area of the king wire and the area of the limit state (area reduced enough to not meet breaking strength requirements per ASTM A416) are simply calculated to be the area of a circle. Using the information above, the critical penetration depth is:

$$c = \frac{1}{2} \left(d_{outer} - \sqrt{\frac{2F_{req}}{3\pi\sigma_{UTS}} - \frac{d_{king}^2}{6}} \right) \quad (6)$$

where F_{req} is the ASTM A416 Minimum breaking strength requirements, σ_{UTS} is the measured ultimate tensile strength of the material and d_{king} and d_{outer} are the measured diameters of the king and outer wires as given in the Methodology section.

The resulting critical corrosion penetration depth under the aforementioned assumptions is $c=0.093$ mm. Estimated corrosion rate (CR) values for atmospheric marine exposure is tabulated from Kennedy Space Center's (KSC) beachside research facility (Montgomery, Curran, Calle, & Kolody, 2012). The maximum corrosion rate reported at KSC was 0.55 mm/year for 1010 steel, and the minimum was 0.1 mm/year. This exposure is of similar conditions to the external environment at the SSK location; both locations are in Florida albeit opposite coasts. As an extreme upper bound of conditions, it is assumed that the strand is exposed directly to the external environment. Taking $c= 0.093$ mm, the time to reach the limit condition would be 2 months and 1 year for the maximum and minimum corrosion rates respectively of the range indicated above.

Further elaboration of this approach may serve as a baseline for comparison with the effects of localized corrosion, some of which are articulated in the next subsection.

Pitting

Some of the loss of strength and ductility noted, especially for the supplemental, very long exposure samples, in the Tensile Testing section may be attributed to the presence of pitting (as the term is understood in the previous discussions). Using similar geometric assumptions as in the general corrosion case and supposing a hemispherical pit, a critical pit depth to cause failure to meet specifications by a simple reduction in cross sectional area was found using the following derived expression.

$$d_{pit} = \sqrt{\left(\frac{d_{king}^2}{2} + 3(d_{outer}^2) - \frac{2F_{req}}{\pi\sigma_{UTS}}\right)} \quad (7)$$

where d_{pit} is the critical pit depth to cause failure by reduction in cross section.

The critical pit depth calculated was 2.3 mm. This estimate neglects any stress concentrations within the pit, so it is likely a pit smaller than this would cause failure to meet specified requirements. Changing the limit state of the required load to the lowest observed value (60.32 kips) rather than the ASTM required value, an estimated pit depth at the point of failure was calculated to be 1.75 mm, much above the maximum pit size measured which was $\sim 65 \mu\text{m}$, and only for the exceedingly long exposure conditions of the supplemental samples. It should be noted however that the probability of finding a pit of a given depth drastically increases with metal area at risk so that issue should be considered in detail when examining the consequences for long tendons. Furthermore, this rough analysis does not include factors of stress intensity, which could cause strand failure before reaching its full capacity (Stauder & Hartt, 1998) (Enos & Scully, 2002).

Comparison with Prior Study

The prevailing evidence obtained in the present study did not show major disparity with results acquired within the prior investigation (Sagüés, Karins, & Lau, 2011). RH and Temperature values were shown to be higher in the present work compared with that observed in the prior study, as expected given the seasonal difference. The prior investigation was conducted in the late fall and early winter months, where the present work was conducted in the late summer. In the previous study, shallow pitting was present after 8-weeks of exposure (longest tested duration) in ducts with wet conditions but with no correlated loss of mechanical properties. Corrosion development in this investigation showed similar morphology to that found

previously. Likewise, strands within the most aggressive environments in the same exposure schedule as in the previous work did not show any dramatic degradation in performance as tested.

The availability of the supplemental, very long exposure 9-month samples in this work showed that in that case there was some indication of reduction in mechanical performance associated with pitting, although standardized strength test requirements were still largely met even for those samples. It is noted however that strands in this group that showed visible pitting would be liable to rejection based on visual appearance alone (ASTM International, 2006) (Sason, 1992).

In summary, the principal conclusions of both studies concur with one another even though the exposure conditions in the present work were nominally somewhat more aggressive than in the former.

It is emphasized that the present and previous investigations do not address the stressed condition of the strand during the ungrouted period. Important deterioration mechanisms such as EAC and HE, not explored in the present work, may be activated and could potentially lead to serious degradation (Reis, 2007) (Sagüés A. A., 2007) (Enos & Scully, 2002) (Proverbio & Longo, 2003). The stressed condition needs investigation and is the subject of ongoing FDOT work in continuation of the present study.

CONCLUSIONS

- Tension testing of exposed strands in all conditions examined resulted in strength values that always met or exceeded the ASTM A416 specification. Ductility as measured by elongation to failure met or exceeded the ASTM A416 specification in all cases except one which may be ascribed to a test irregularity. It is emphasized that tensile tests are of limited scope and that broader analysis is needed when evaluating their significance on the durability of PT tendons.
- Bending tests and metallography did not reveal any evidence of cracking that could have initiated at locations of corrosion pits that resulted from even the most severe exposure conditions.
- The deepest pits observed (supplemental samples, 9 month exposure, wet conditions) were ~65 μm deep, not enough to reduce cross section to cause failure by simple overload. However, stress concentration and pitting statistics effects need consideration in future work.
- Corrosion damage on unstressed strands during ungrouted periods of durations in the order of those otherwise currently prescribed did not appear to seriously degrade mechanical performance as measured by standardized tests. However the presence of stress in the ungrouted period, as is normally the case, may activate other mechanisms (e.g., EAC) that require further investigation.

- The results of this study generally concur with those from a previous investigation performed in the same facility, even though the present tests were conducted in a warmer season and with extended evaluations.

FUTURE WORK

Tests of unstressed strands in ungrouted ducts have provided some of the needed information on general corrosion on the surface of the strand during construction. However, strands in the stressed condition are vulnerable to other mechanisms of degradation, such as environmentally assisted cracking. Using the results from the unstressed condition as a baseline for comparison, strands in the stressed condition will undergo similar and expanded testing and evaluation methods. Comparative metallography of stress and unstressed strands will aid in determining the presence and characteristics of stress induced degradation mechanism. Ducts placed in concrete will be used instead of isolated ducts to more realistically simulate construction practice. A quantification of salt precipitation at the specific service environments, not available in the current work, is of particular interest for future studies and will be conducted as an integral part of those investigations.

REFERENCES

- American Concrete Institute. (1990). *External Prestressing in Bridges*. (A. Naaman, & J. Breen, Eds.) Detroit, Michigan.
- American Society for Metals. (1984). *Hydrogen Embrittlement and Stress Corrosion Cracking*. (R. Gibala, & R. F. Hehemann, Eds.) Metals Park: American Society for Metals.
- Andrew, A. E. (1987). *Unbonded tendons in post-tensioned construction*. London, England: Thomas Telford.
- ASM Handbook Committee. (1972). *Metals Handbook* (8th ed., Vol. 7). (T. Lyman, Ed.) Metals Park, Ohio, USA: American Society for Metals.
- ASM Handbook Committee. (1973). *Metals Handbook* (8th ed., Vol. 8). Metals Park, Ohio, USA: American Society for Metals.
- ASM International. (1992). *Stress-Corrosion Cracking*. (R. H. Jones, Ed.) Materials Park, Ohio: ASM International.
- ASTM International. (2006). *A416*. ASTM.
- ASTM International. (2009). *A1061*.
- ASTM International. (2009). *Making and Using U-Bend Stress-Corrosion Test Specimens*. Conshohocken: ASTM Int'l.
- Barrett, C. R., Nix, W. D., & Tetelman, A. S. (1973). *The Principles of Engineering Materials*. Englewood, New Jersey: Prentice-Hall, Inc.
- Bertolini, L., & Carsana, M. (2011). High pH corrosion of prestressing steel in segregated grout. *Modelling of Corroding Concrete Structures*, 5, 147-158.
- Coronelli, D., Castel, A., Vu, N. A., & François, R. (2009). Corroded post-tensioned beams with bonded tendons and wire failure. *Engineering Structures*, 31, 1687-1697.
- Corrosion and Corrosion Control* (2nd ed.). (1971). John Wiley & Sons, Inc.

- Corven, J., & Moreton, A. (2004). *Post-Tensioning Tendon Installation and Grouting Manual*. Federal Highway Administration.
- Darmawan, M. S., & Stewart, M. G. (2007, March). Effect of pitting corrosion on capacity of prestressing wires. *Magazine of Concrete Research*, 59(2), 131-139.
- Enos, D. G., & Scully, J. R. (2002). A Critical-Strain Criterion for Hydrogen Embrittlement of Cold-Drawn, Ultrafine Pearlitic Steel. *Metallurgical and Materials Transactions*, 33A.
- Federal Highway Administration. (2012). *Post-Tensioning Tendon Installation and Grouting Manual*. Retrieved from <http://www.fhwa.dot.gov/bridge/pt/pt02.cfm>
- Fontana, M. G., & Greene, N. D. (1978). *Corrosion Engineering* (2nd ed.). (B. J. Clark, & F. A. Neal, Eds.) United States of America: McGraw-Hill, Inc.
- Gellings, P. J. (2005). *Introduction to Corrosion Prevention and Control*. Enschede, Netherlands.
- Gerwick, B. C. (1993). *Construction of Prestressed Concrete Structures* (2nd ed.). New York, New York: John Wiley & Sons, Inc.
- Ghods, P., Isgor, O. B., & Gu, G. P. (2010). Electrochemical Investigation of Chloride-Induced Depassivation of Black Steel Rebar Under Simulated Service Conditions. *Corrosion Science*, 1649-1659.
- Hartt, W. H. (2002). *Corrosion Evaluation of Post-Tensioned Tendons on the Mid Bay Bridge in Destin, Florida*. Tallahassee: Florida Department of Transportation.
- Hertzberg, R. W. (1996). *Deformation and Fracture Mechanics of Engineering Materials* (4th ed.). John Wiley & Sons Inc.
- Jaeger, B. J., Sansalone, M. J., & Poston, R. W. (1996). Detecting voids in grouted tendon ducts of post-tensioned concrete structures using the impact-echo method. *ACI Structural Journal*, 93(4), 428-438.
- Kovac, J., Leban, M., & Legat, A. (2007). Detection of SCC on prestressing steel wire by the simultaneous use of electrochemical noise and acoustic emission measurements. *Electrochimica Acta*, 52, 7607-7616.
- Leygraf, C., & Graedel, T. E. (2000). *Atmospheric Corrosion*. New York: John Wiley & Sons Inc.
- Mietz, J. (2000). Investigations on hydrogen-induced embrittlement of quenched and tempered prestressing steels. *Materials and Corrosion*, 51(2), 80-90.
- Mindess, S., Young, J. F., & Darwin, D. (2003). *Concrete* (2nd ed.). Upper Saddle River, New Jersey: Pearson Education, Inc. .

- Minh, H., Mutsuyoshi, H., & Niitani, K. (2007). Influence of grouting condition on crack and load-carrying capacity of post-tensioned concrete beam due to chloride-induced corrosion. *Construction and Building Materials*, 21, 1568-1575.
- Montgomery, E. L., Curran, J. C., Calle, L. M., & Kolody, M. R. (2012). Timescale Correlation between Marine Atmospheric Exposure and Accelerated Corrosion Testing - Part 2. *NACE Intl. Corrosion Conference & Expo*. Orlando.
- Nürnbergger, U. (2002). Corrosion induced failure mechanisms of prestressing steels. *Materials and Corrosion*, 53, 591-601.
- Pillai, R. G., Gardoni, P., Trejo, D., Hueste, M. D., & Reinschmidt, K. F. (2010). Probabilistic models for the tensile strength of corroding strands in posttensioned segmental concrete bridges. *Journal of Materials in Civil Engineering*, 967-977.
- Poupard, O., Ait-Mokhtar, A., & Dumargue, P. (2004). Corrosion by Chlorides in Reinforced Concrete: Determination of Chloride Concentration Threshold by Impedance Spectroscopy. *Cement and Concrete Research*, 991-1000.
- Prestressed Concrete Institute. (1972). *PCI Post-Tensioning Manual*. Chicago, Illinois: Prestressed Concrete Institute.
- Proverbio, E., & Longo, P. (2003). Failure mechanisms of high-strength steels in bicarbonate solutions under anodic polarization. *Corrosion Science*, 45, 2017-2030.
- Reed-Hill, R. E., & Abbaschian, R. (1992). *Physical Metallurgy Principles*. Boston: PWS-Kent.
- Reis, R. A. (2007). *Corrosion Evaluation and Tensile Results of Selected Post-Tensioning Strands at the SFOBB Skyway Seismic Replacement Project*. Sacramento: California Department of Transportation.
- Sagüés, A. A. (2007). *APPENDIX B (Sagues Materials Consulting, Inc. Trip Report) From Corrosion Evaluation and Tensile Results of Selected Post-Tensioning Strands at the SFOBB Skyway Seismic Replacement Project*. Phase III Report, Sacramento.
- Sagüés, A. A., Karins, F. C., & Lau, K. (2011). *Corrosion Characteristics of Post-Tensioning Strands in UngROUTED DUCTS*. Tallahassee: Florida Department of Transportation.
- Sason, A. S. (1992, May-June). Evaluation of Degree of Rusting on Prestressed Concrete Strand. *PCI Journal*, 25-30.
- Sedriks, A. J. (1990). *Stress Corrosion Cracking Test Methods*. Houston: National Association of Corrosion Engineers.

- Stauder, A.-L., & Hartt, W. H. (1998). Cathodic Protection of Pre-Tensioned Concrete: Part I - Brittle Fracture Propensity of Corrosion Damaged Prestressing Tendon Wire. *NACE Intl. Corrosion*. Houston.
- The Electrochemical Society. (1982). *Atmospheric Corrosion*. (W. H. Ailor, Ed.) New York: John Wiley & Sons, Inc.
- Threlkeld, J. L. (1962). *Thermal Environmental Engineering*. Englewood Cliffs, New Jersey: Prentice-Hall Inc.
- Threlkeld, J. L. (1962). *Thermal Environmental Engineering*. Englewood Cliffs: Prentice-Hall, Inc.
- Toribio, J., Kharin, V., & Vergara, D. (2011). Role of drawing-induced residual stresses and strains in the hydrogen embrittlement susceptibility of prestressing steels. *Corrosion Science*, 53, 3346-3355.
- Wang, H., Sagüés, A. A., & Powers, R. (2005). Corrosion of the Strand-Anchorage System in Post-Tensioned Grouted Assemblies. *NACE International*. Houston.

APPENDIX 1 PHOTOGRAPHIC EVALUATION

Typical Strand As Received



Figure A1.71 Typical As Received Condition of Strands Prior to Exposure

APPENDIX 1 (Continued)

Duct Condition Comparison - SSK Strands









































	Post Extraction	After Cleaning	
Dry Ducts			1 Week
			2 Weeks
			4 Weeks
			8 Weeks
			9 Months
1 End Open			1 Week
			2 Weeks
			4 Weeks
			8 Weeks
			9 Months
2 Ends Open			1 Week
			2 Weeks
			4 Weeks
			8 Weeks
			9 Months
Wet Ducts			1 Week
			2 Weeks
			4 Weeks
			8 Weeks
			9 Months

Figure A1.72 Duct Condition Comparison of Exposed SSK Strands

APPENDIX 1 (Continued)

Duct Condition Comparison – USF Strands









































	Post Extraction	After Cleaning	
Dry Ducts			1 Week
			2 Weeks
			4 Weeks
			8 Weeks
			9 Months
1 End Open			1 Week
			2 Weeks
			4 Weeks
			8 Weeks
			9 Months
2 Ends Open			1 Week
			2 Weeks
			4 Weeks
			8 Weeks
			9 Months
Wet Ducts			1 Week
			2 Weeks
			4 Weeks
			8 Weeks
			9 Months

Figure A1.73 Duct Condition Comparison of Exposed USF Strands

APPENDIX 1 (Continued)

Exposure Length Comparison – SSK Strands































	Post Extraction	After Cleaning	
1 Week			Dry
			Open 1
			Open 2
2 Weeks			Wet
			Dry
			Open 1
4 Weeks			Open 2
			Wet
			Dry
8 Weeks			Open 1
			Open 2
			Wet
9 Months			Dry
			Open 1
			Wet

Figure A1.74 Exposure Length Comparison of Exposed SSK Strands

APPENDIX 1 (Continued)

Exposure Length Comparison – USF Strands























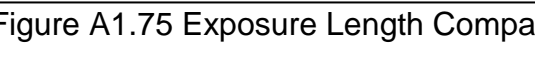
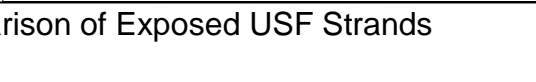






	Post Extraction	After Cleaning	
1 Week			Dry
			Open 1
			Open 2
2 Weeks			Wet
			Dry
			Open 1
4 Weeks			Open 2
			Wet
			Dry
8 Weeks			Open 1
			Open 2
			Wet
9 Months			Dry
			Open 1
			Wet

Figure A1.75 Exposure Length Comparison of Exposed USF Strands

APPENDIX 1 (Continued)

Environment Comparison – As Extracted

	USF Strands	SSK Strands	
1 Week			Dry
			Open 1
			Open 2
2 Weeks			Wet
			Dry
			Open 1
4 Weeks			Open 2
			Wet
			Dry
8 Weeks			Open 1
			Open 2
			Wet
9 Months			Dry
			Open 1
			Wet

Figure A1.76 Environment Comparison of Exposed Strand - As Extracted

APPENDIX 1 (Continued)

Environment Comparison – Cleaned



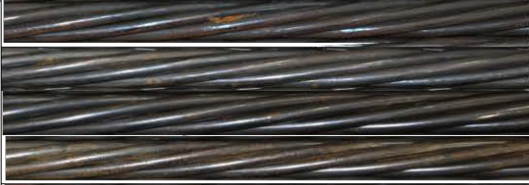







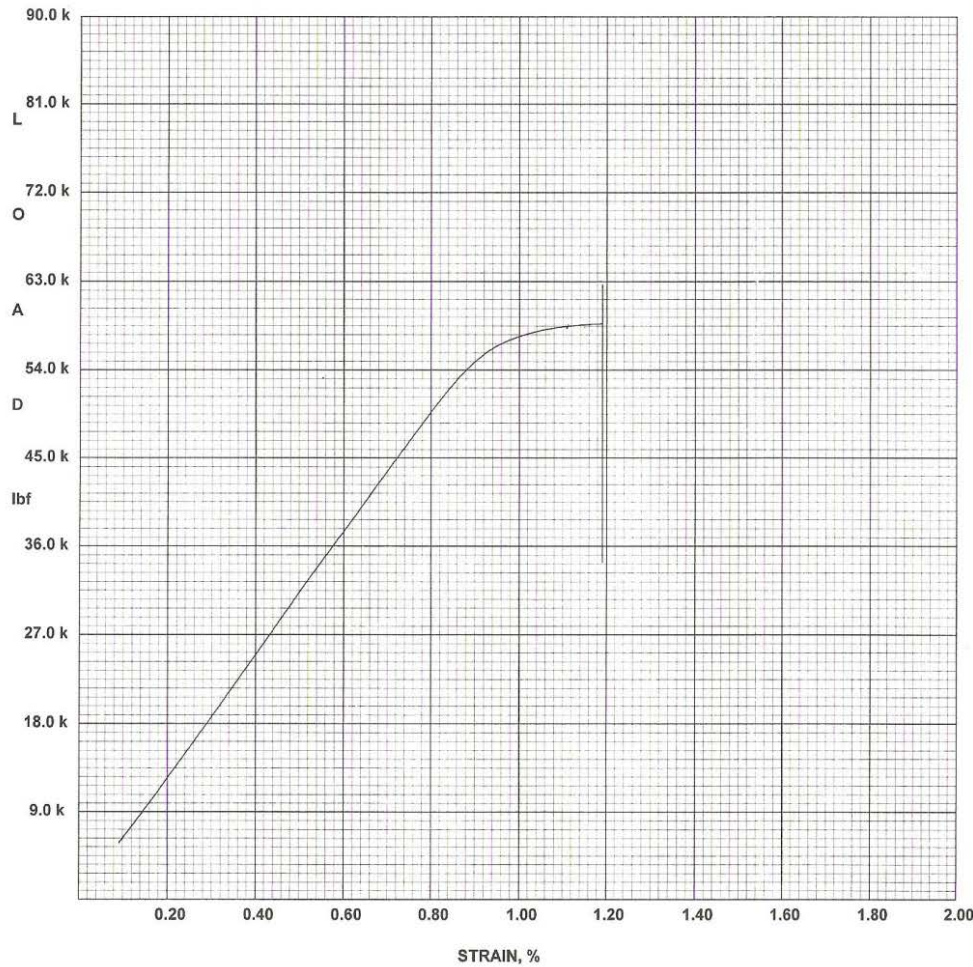
	USF Strands	SSK Strands	
1 Week			Dry Open 1 Open 2 Wet
2 Weeks			Dry Open 1 Open 2 Wet
4 Weeks			Dry Open 1 Open 2 Wet
8 Weeks			Dry Open 1 Open 2 Wet
9 Months			Dry Open 1 Wet

Figure A1.77 Environment Comparison of Exposed Strand – Cleaned

APPENDIX 2 STRAND MANUFACTURER STRENGTH REPORT

**Insteel Wire Products
Prestressed Concrete Strand**

.600" 270 7W LOW RELAXATION



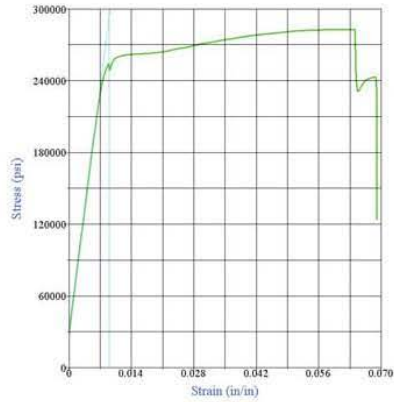
Test Number:	10069040
Tested By:	CER
Ultimate Breaking Strength, lbf:	62683
Ultimate Breaking Strength, kN:	279
Load @ 1% Extension, lbf:	57414
Load @ 1% Extension, kN:	255
Ultimate Elongation, %:	5.73
Representative Area, in ² :	0.217
Representative Area, mm ² :	140
Actual Area, in ² :	0.2185
Actual Area, mm ² :	140.9513
Avg Modulus of Elasticity, Mpsi:	29.0
Avg Modulus of Elasticity, MPa:	199947.6
Reference:	

Aug 19, 2011 9:37:44 AM
SN: 206250-R2 V7.02.07

APPENDIX 3 TENSILE TESTING DATA

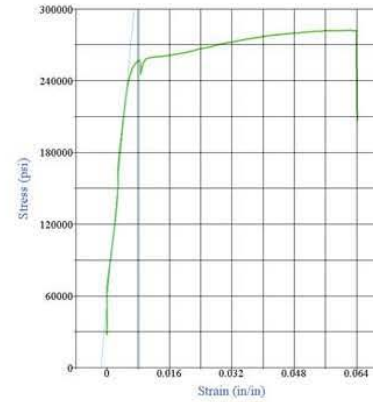
The following presents data from tensile testing. Strands which had slipped from the grips during testing are not reported. Recall from Figure 8 the strand identification code concerning sample labeling. Extensometer was removed from strand after 1% strain was reach and further strain measurements were obtained from grip separation values.

APPENDIX 3 (Continued)



Test Results
 Specimen Gage Length: **31.0000** in
 Area: **0.2180** in²
 Total Load: **61650** lbf
 Tensile Strength: **282810** psi
 Correlation Coefficient: **0.9999**
 Modulus of Elasticity: **29252200** psi
 Load at 1% EUL: **55510** lbf
 Stress at 1% EUL: **254650** psi
 Est. Elongation: **0.1**
 Total Elongation: **6.90** %
 Position at Break: **2.642** in

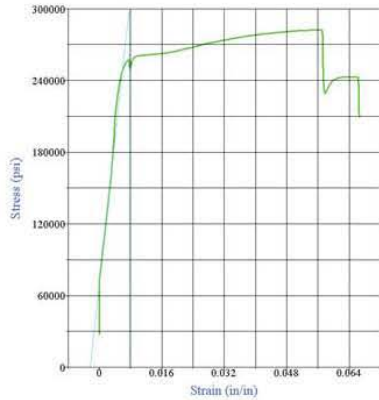
Test Summary
 Counter: **6668**
 Elapsed Time: **00:01:39**
 LIMS Number: **n/a**
 Project Number: **n/a**
 Sample Number: **SW1D1**
 Size: **.6**
 Grade: **270 K**
 Coil: **n/a**
 Operator: **MC**
 Condition of Sample: **Satisfactory**
 Comments:
 Procedure Name: **ASTM A416 - 7 wire strand - 40988**
 Start Date: **2/28/2012**
 Start Time: **3:53:51 PM**
 End Date: **2/28/2012**
 End Time: **3:58:30 PM**
 Workstation: **FLORIDA-DOT**
 Tested By: **tech**



Test Results
 Specimen Gage Length: **31.0000** in
 Area: **0.2180** in²
 Total Load: **61480** lbf
 Tensile Strength: **282020** psi
 Correlation Coefficient: **0.9780**
 Modulus of Elasticity: **35240900** psi
 Load at 1% EUL: **56030** lbf
 Stress at 1% EUL: **257020** psi
 Est. Elongation: **0.1**
 Total Elongation: **6.40** %
 Position at Break: **2.401** in

Test Summary
 Counter: **6666**
 Elapsed Time: **00:02:36**
 LIMS Number: **n/a**
 Project Number: **n/a**
 Sample Number: **SW1D2**
 Size: **.6**
 Grade: **270 K**
 Coil: **n/a**
 Operator: **MC**
 Condition of Sample: **Satisfactory**
 Comments:
 Procedure Name: **ASTM A416 - 7 wire strand - 40988**
 Start Date: **2/28/2012**
 Start Time: **2:40:26 PM**
 End Date: **2/28/2012**
 End Time: **2:43:02 PM**
 Workstation: **FLORIDA-DOT**
 Tested By: **tech**

APPENDIX 3 (Continued)



Test Results
 Specimen Gage Length: **31.0000** in
 Area: **0.2180** in²
 Total Load: **61520** lbf
 Tensile Strength: **282200** psi
 Correlation Coefficient: **0.9992**
 Modulus of Elasticity: **29995300** psi
 Load at 1% EUL: **56160** lbf
 Stress at 1% EUL: **257620** psi
 Est. Elongation: **0.1**
 Total Elongation: **6.64** %
 Position at Break: **2.487** in

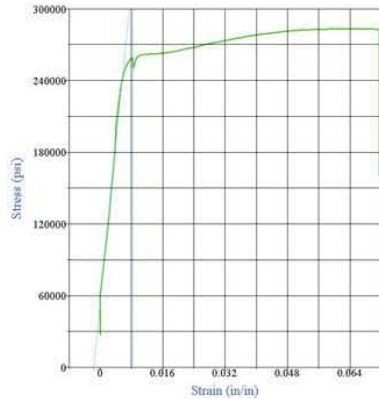
Test Summary
 Counter: **6661**
 Elapsed Time: **00:01:47**
 LIMS Number: **n/a**
 Project Number: **n/a**
 Sample Number: **SW1D3a**
 Size: **.6**
 Grade: **270 K**
 Coil: **n/a**
 Operator: **MC**
 Condition of Sample: **Satisfactory**
 Comments:
 Procedure Name: **ASTM A416 - 7 wire strand - 40988**
 Start Date: **2/28/2012**
 Start Time: **1:44:06 PM**
 End Date: **2/28/2012**
 End Time: **1:45:53 PM**
 Workstation: **FLORIDA-DOT**
 Tested By: **tech**



Test Results
 Specimen Gage Length: **31.0000** in
 Area: **0.2180** in²
 Total Load: **61650** lbf
 Tensile Strength: **282790** psi
 Correlation Coefficient: **0.9966**
 Modulus of Elasticity: **36273800** psi
 Load at 1% EUL: **56410** lbf
 Stress at 1% EUL: **258740** psi
 Est. Elongation: **0.1**
 Total Elongation: **7.10** %
 Position at Break: **2.707** in

Test Summary
 Counter: **6665**
 Elapsed Time: **00:01:56**
 LIMS Number: **n/a**
 Project Number: **n/a**
 Sample Number: **SW1D3a**
 Size: **.6**
 Grade: **270 K**
 Coil: **n/a**
 Operator: **MC**
 Condition of Sample: **Satisfactory**
 Comments:
 Procedure Name: **ASTM A416 - 7 wire strand - 40988**
 Start Date: **2/28/2012**
 Start Time: **2:27:10 PM**
 End Date: **2/28/2012**
 End Time: **2:29:06 PM**
 Workstation: **FLORIDA-DOT**
 Tested By: **tech**

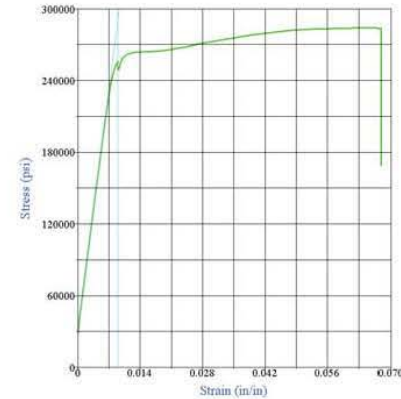
APPENDIX 3 (Continued)



Test Results
 Specimen Gage Length: **31.0000** in
 Area: **0.2180** in²
 Total Load: **61740** lbf
 Tensile Strength: **283220** psi
 Correlation Coefficient: **0.9990**
 Modulus of Elasticity: **32961800** psi
 Load at 1% EUL: **56440** lbf
 Stress at 1% EUL: **258880** psi
 Est. Elongation: **0.1**
 Total Elongation: **7.16** %
 Position at Break: **2.907** in

Test Summary

Counter: **6663**
 Elapsed Time: **00:01:54**
 LIMS Number: **n/a**
 Project Number: **n/a**
 Sample Number: **SW1D4**
 Size: **.6**
 Grade: **270 K**
 Coil: **n/a**
 Operator: **MC**
 Condition of Sample: **Satisfactory**
 Comments:
 Procedure Name: **ASTM A416 - 7 wire strand - 40988**
 Start Date: **2/28/2012**
 Start Time: **2:00:42 PM**
 End Date: **2/28/2012**
 End Time: **2:02:36 PM**
 Workstation: **FLORIDA-DOT**
 Tested By: **tech**

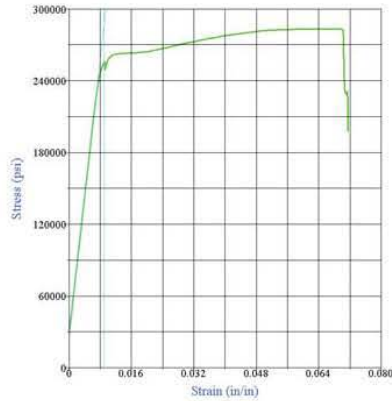


Test Results
 Specimen Gage Length: **31.0000** in
 Area: **0.2180** in²
 Total Load: **61910** lbf
 Tensile Strength: **283970** psi
 Correlation Coefficient: **1.0000**
 Modulus of Elasticity: **28932300** psi
 Load at 1% EUL: **55780** lbf
 Stress at 1% EUL: **255890** psi
 Est. Elongation: **0.1**
 Total Elongation: **6.78** %
 Position at Break: **2.551** in

Test Summary

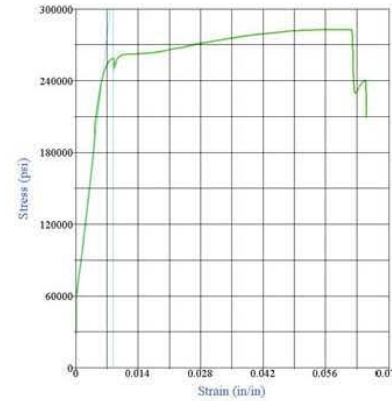
Counter: **6669**
 Elapsed Time: **00:02:00**
 LIMS Number: **n/a**
 Project Number: **n/a**
 Sample Number: **SW1D5**
 Size: **.6**
 Grade: **270 K**
 Coil: **n/a**
 Operator: **MC**
 Condition of Sample: **Satisfactory**
 Comments:
 Procedure Name: **ASTM A416 - 7 wire strand - 40988**
 Start Date: **2/29/2012**
 Start Time: **7:56:47 AM**
 End Date: **2/29/2012**
 End Time: **7:58:47 AM**
 Workstation: **FLORIDA-DOT**
 Tested By: **tech**

APPENDIX 3 (Continued)



Test Results
 Specimen Gage Length: 31.0000 in
 Area: 0.2180 in²
 Total Load: 61770 lbf
 Tensile Strength: 283350 psi
 Correlation Coefficient: 1.0000
 Modulus of Elasticity: 28835900 psi
 Load at 1% EUL: 55740 lbf
 Stress at 1% EUL: 255690 psi
 Est. Elongation: 0.1
 Total Elongation: 7.14 %
 Position at Break: 2.713 in

Test Summary
 Counter: 6667
 Elapsed Time: 00:01:46
 LIMS Number: n/a
 Project Number: n/a
 Sample Number: SW1D6
 Size: .6
 Grade: 270 K
 Coil: n/a
 Operator: MC
 Condition of Sample: Satisfactory
 Comments:
 Procedure Name: ASTM A416 - 7 wire strand - 40988
 Start Date: 2/28/2012
 Start Time: 3:47:50 PM
 End Date: 2/28/2012
 End Time: 3:49:36 PM
 Workstation: FLORIDA-DOT
 Tested By: tech



Test Results
 Specimen Gage Length: 31.0000 in
 Area: 0.2180 in²
 Total Load: 61680 lbf
 Tensile Strength: 322930 psi
 Correlation Coefficient: 0.9998
 Modulus of Elasticity: 32217000 psi
 Load at 1% EUL: 56440 lbf
 Stress at 1% EUL: 258900 psi
 Est. Elongation: 0.1
 Total Elongation: 6.50 %
 Position at Break: 2.569 in

Test Summary
 Counter: 6662
 Elapsed Time: 00:01:48
 LIMS Number: n/a
 Project Number: n/a
 Sample Number: SW1D7a
 Size: .6
 Grade: 270 K
 Coil: n/a
 Operator: MC
 Condition of Sample: Satisfactory
 Comments:
 Procedure Name: ASTM A416 - 7 wire strand - 40988
 Start Date: 2/28/2012
 Start Time: 1:55:35 PM
 End Date: 2/28/2012
 End Time: 1:57:23 PM
 Workstation: FLORIDA-DOT
 Tested By: tech

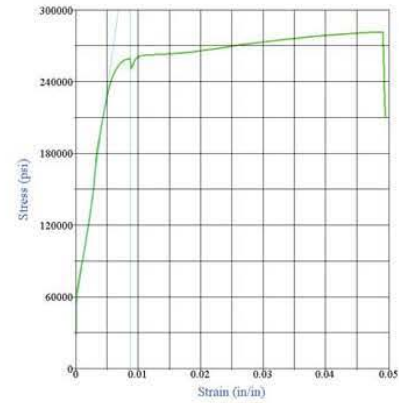
APPENDIX 3 (Continued)



Test Results
 Specimen Gage Length: **31.0000** in
 Area: **0.2180** in²
 Total Load: **61870** lbf
 Tensile Strength: **283820** psi
 Correlation Coefficient: **0.9933**
 Modulus of Elasticity: **35591400** psi
 Load at 1% EUL: **56980** lbf
 Stress at 1% EUL: **261390** psi
 Est. Elongation: **0.1**
 Total Elongation: **6.49** %
 Position at Break: **2.329** in

Test Summary

Counter: **6660**
 Elapsed Time: **00:02:08**
 LIMS Number: **n/a**
 Project Number: **n/a**
 Sample Number: **SW1D7b**
 Size: **.6**
 Grade: **270 K**
 Coil: **n/a**
 Operator: **MC**
 Condition of Sample: **Satisfactory**
 Comments:
 Procedure Name: **ASTM A416 - 7 wire strand - 40988**
 Start Date: **2/28/2012**
 Start Time: **1:35:38 PM**
 End Date: **2/28/2012**
 End Time: **1:37:46 PM**
 Workstation: **FLORIDA-DOT**
 Tested By: **tech**

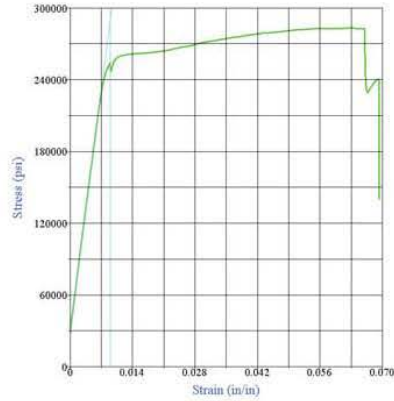


Test Results
 Specimen Gage Length: **31.0000** in
 Area: **0.2180** in²
 Total Load: **61370** lbf
 Tensile Strength: **281510** psi
 Correlation Coefficient: **0.9931**
 Modulus of Elasticity: **36867300** psi
 Load at 1% EUL: **56560** lbf
 Stress at 1% EUL: **259440** psi
 Est. Elongation: **0.1**
 Total Elongation: **4.93** %
 Position at Break: **1.965** in

Test Summary

Counter: **6659**
 Elapsed Time: **00:01:35**
 LIMS Number: **n/a**
 Project Number: **n/a**
 Sample Number: **SW1D8**
 Size: **.6**
 Grade: **270 K**
 Coil: **n/a**
 Operator: **MC**
 Condition of Sample: **Satisfactory**
 Comments:
 Procedure Name: **ASTM A416 - 7 wire strand - 40988**
 Start Date: **2/28/2012**
 Start Time: **1:29:45 PM**
 End Date: **2/28/2012**
 End Time: **1:31:20 PM**
 Workstation: **FLORIDA-DOT**
 Tested By: **tech**

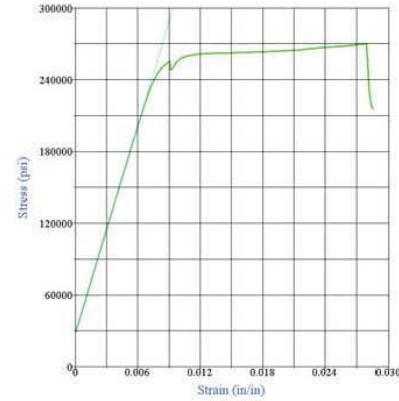
APPENDIX 3 (Continued)



Test Results
 Specimen Gage Length: 31.0000 in
 Area: 0.2180 in²
 Total Load: 61690 lbf
 Tensile Strength: 282970 psi
 Correlation Coefficient: 1.0000
 Modulus of Elasticity: 28873600 psi
 Load at 1% EUL: 55350 lbf
 Stress at 1% EUL: 253900 psi
 Est. Elongation: 0.1
 Total Elongation: 6.92 %
 Position at Break: 2.646 in

Test Summary

Counter: 6702
 Elapsed Time: 00:01:44
 LIMS Number: n/a
 Project Number: n/a
 Sample Number: SW2D1
 Size: .6
 Grade: 270 K
 Coil: n/a
 Operator: MC
 Condition of Sample: Satisfactory
 Comments:
 Procedure Name: ASTM A416 - 7 wire strand - 40988
 Start Date: 3/1/2012
 Start Time: 9:38:53 AM
 End Date: 3/1/2012
 End Time: 9:40:37 AM
 Workstation: FLORIDA-DOT
 Tested By: tech

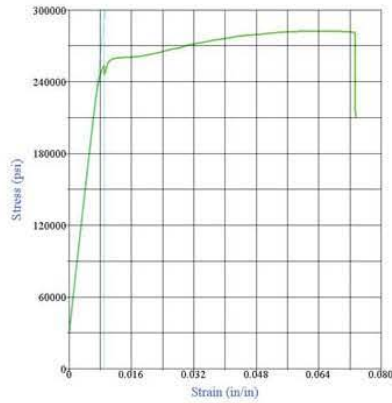


Test Results
 Specimen Gage Length: 31.0000 in
 Area: 0.2180 in²
 Total Load: 58900 lbf
 Tensile Strength: 270170 psi
 Correlation Coefficient: 1.0000
 Modulus of Elasticity: 28979300 psi
 Load at 1% EUL: 55640 lbf
 Stress at 1% EUL: 255210 psi
 Est. Elongation: 0.1
 Total Elongation: 2.85 %
 Position at Break: 1.427 in

Test Summary

Counter: 6705
 Elapsed Time: 00:01:14
 LIMS Number: n/a
 Project Number: n/a
 Sample Number: SW2D2
 Size: .6
 Grade: 270 K
 Coil: n/a
 Operator: MC
 Condition of Sample: Satisfactory
 Comments:
 Procedure Name: ASTM A416 - 7 wire strand - 40988
 Start Date: 3/1/2012
 Start Time: 10:26:08 AM
 End Date: 3/1/2012
 End Time: 10:27:22 AM
 Workstation: FLORIDA-DOT
 Tested By: tech

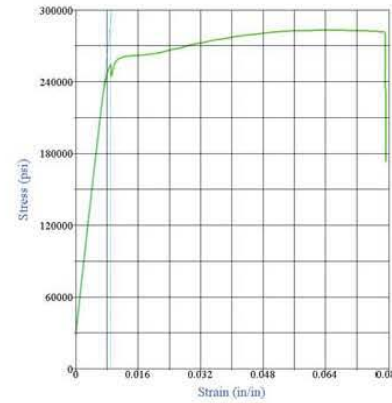
APPENDIX 3 (Continued)



Test Results
 Specimen Gauge Length: 31.0000 in
 Area: 0.2180 in²
 Total Load: 61550 lbf
 Tensile Strength: 282360 psi
 Correlation Coefficient: 1.0000
 Modulus of Elasticity: 28853300 psi
 Load at 1% EUL: 55250 lbf
 Stress at 1% EUL: 253460 psi
 Est. Elongation: 0.1
 Total Elongation: 7.32 %
 Position at Break: 2.889 in

Test Summary

Counter: 6703
 Elapsed Time: 00:01:52
 LIMS Number: n/a
 Project Number: n/a
 Sample Number: SW2D3a
 Size: .6
 Grade: 270 K
 Coil: n/a
 Operator: MC
 Condition of Sample: Satisfactory
 Comments:
 Procedure Name: ASTM A416 - 7 wire strand - 40988
 Start Date: 3/1/2012
 Start Time: 9:46:13 AM
 End Date: 3/1/2012
 End Time: 9:48:05 AM
 Workstation: FLORIDA-DOT
 Tested By: tech

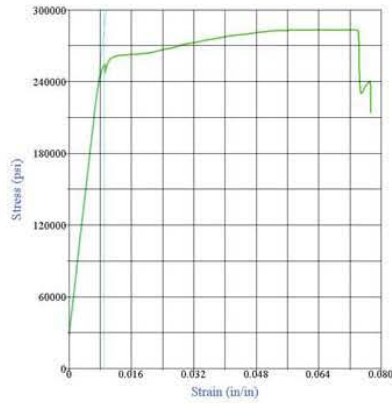


Test Results
 Specimen Gauge Length: 31.0000 in
 Area: 0.2180 in²
 Total Load: 61700 lbf
 Tensile Strength: 283020 psi
 Correlation Coefficient: 1.0000
 Modulus of Elasticity: 28810800 psi
 Load at 1% EUL: 55440 lbf
 Stress at 1% EUL: 254300 psi
 Est. Elongation: 0.1
 Total Elongation: 7.90 %
 Position at Break: 2.839 in

Test Summary

Counter: 6701
 Elapsed Time: 00:03:12
 LIMS Number: n/a
 Project Number: n/a
 Sample Number: SW2D3b
 Size: .6
 Grade: 270 K
 Coil: n/a
 Operator: MC
 Condition of Sample: Satisfactory
 Comments:
 Procedure Name: ASTM A416 - 7 wire strand - 40988
 Start Date: 3/1/2012
 Start Time: 9:30:08 AM
 End Date: 3/1/2012
 End Time: 9:33:20 AM
 Workstation: FLORIDA-DOT
 Tested By: tech

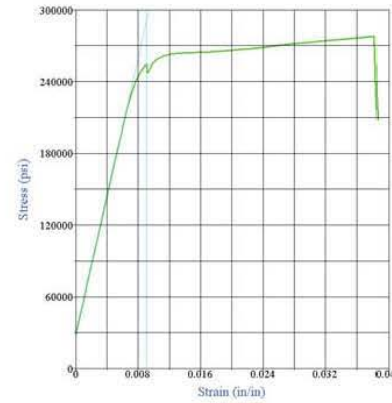
APPENDIX 3 (Continued)



Test Results
 Specimen Gage Length: 31.0000 in
 Area: 0.2180 in²
 Total Load: 61780 lbf
 Tensile Strength: 283410 psi
 Correlation Coefficient: 0.9999
 Modulus of Elasticity: 28447100 psi
 Load at 1% EUL: 55420 lbf
 Stress at 1% EUL: 254200 psi
 Est. Elongation: 0.1
 Total Elongation: 7.72 %
 Position at Break: 2.777 in

Test Summary

Counter: 6706
 Elapsed Time: 00:01:52
 LIMS Number: n/a
 Project Number: n/a
 Sample Number: SW2D4
 Size: .6
 Grade: 270 K
 Coil: n/a
 Operator: MC
 Condition of Sample: Satisfactory
 Comments:
 Procedure Name: ASTM A416 - 7 wire strand - 40988
 Start Date: 3/1/2012
 Start Time: 10:30:44 AM
 End Date: 3/1/2012
 End Time: 10:32:36 AM
 Workstation: FLORIDA-DOT
 Tested By: tech

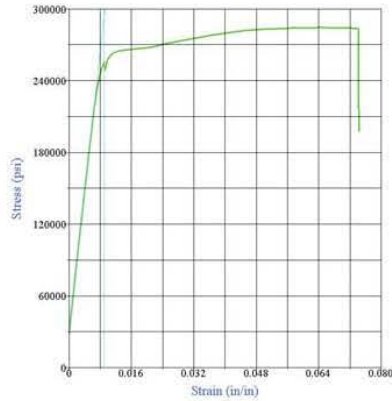


Test Results
 Specimen Gage Length: 31.0000 in
 Area: 0.2180 in²
 Total Load: 60510 lbf
 Tensile Strength: 277570 psi
 Correlation Coefficient: 1.0000
 Modulus of Elasticity: 28967800 psi
 Load at 1% EUL: 55430 lbf
 Stress at 1% EUL: 254250 psi
 Est. Elongation: 0.1
 Total Elongation: 3.85 %
 Position at Break: 1.771 in

Test Summary

Counter: 6709
 Elapsed Time: 00:01:34
 LIMS Number: n/a
 Project Number: n/a
 Sample Number: SW2D5
 Size: .6
 Grade: 270 K
 Coil: n/a
 Operator: MC
 Condition of Sample: Satisfactory
 Comments:
 Procedure Name: ASTM A416 - 7 wire strand - 40988
 Start Date: 3/1/2012
 Start Time: 11:41:18 AM
 End Date: 3/1/2012
 End Time: 11:42:52 AM
 Workstation: FLORIDA-DOT
 Tested By: tech

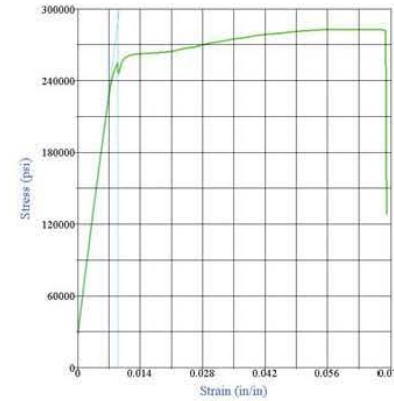
APPENDIX 3 (Continued)



Test Results
 Specimen Gage Length: **31.0000** in
 Area: **0.2180** in²
 Total Load: **61990** lbf
 Tensile Strength: **284330** psi
 Correlation Coefficient: **1.0000**
 Modulus of Elasticity: **29256600** psi
 Load at 1% EUL: **55610** lbf
 Stress at 1% EUL: **255080** psi
 Est. Elongation: **0.1**
 Total Elongation: **7.41** %
 Position at Break: **2.930** in

Test Summary

Counter: **6708**
 Elapsed Time: **00:01:51**
 LIMS Number: **n/a**
 Project Number: **n/a**
 Sample Number: **SW2D6**
 Size: **.6**
 Grade: **270 K**
 Coil: **n/a**
 Operator: **MC**
 Condition of Sample: **Satisfactory**
 Comments:
 Procedure Name: **ASTM A416 - 7 wire strand - 40988**
 Start Date: **3/1/2012**
 Start Time: **11:35:47 AM**
 End Date: **3/1/2012**
 End Time: **11:37:38 AM**
 Workstation: **FLORIDA-DOT**
 Tested By: **tech**

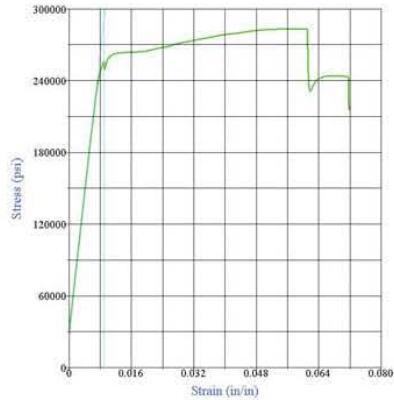


Test Results
 Specimen Gage Length: **31.0000** in
 Area: **0.2180** in²
 Total Load: **61680** lbf
 Tensile Strength: **282950** psi
 Correlation Coefficient: **1.0000**
 Modulus of Elasticity: **28849200** psi
 Load at 1% EUL: **55500** lbf
 Stress at 1% EUL: **254570** psi
 Est. Elongation: **0.1**
 Total Elongation: **6.88** %
 Position at Break: **2.536** in

Test Summary

Counter: **6704**
 Elapsed Time: **00:02:20**
 LIMS Number: **n/a**
 Project Number: **n/a**
 Sample Number: **SW2D7a**
 Size: **.6**
 Grade: **270 K**
 Coil: **n/a**
 Operator: **MC**
 Condition of Sample: **Satisfactory**
 Comments:
 Procedure Name: **ASTM A416 - 7 wire strand - 40988**
 Start Date: **3/1/2012**
 Start Time: **9:55:47 AM**
 End Date: **3/1/2012**
 End Time: **9:58:07 AM**
 Workstation: **FLORIDA-DOT**
 Tested By: **tech**

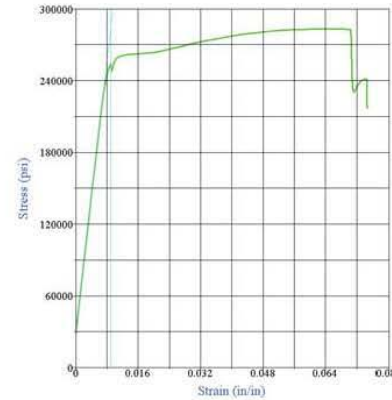
APPENDIX 3 (Continued)



Test Results
 Specimen Gage Length: **31.0000** in
 Area: **0.2180** in²
 Total Load: **61770** lbf
 Tensile Strength: **283350** psi
 Correlation Coefficient: **1.0000**
 Modulus of Elasticity: **29049700** psi
 Load at 1% EUL: **55770** lbf
 Stress at 1% EUL: **255810** psi
 Est. Elongation: **0.1**
 Total Elongation: **7.16** %
 Position at Break: **2.836** in

Test Summary

Counter: **6700**
 Elapsed Time: **00:01:43**
 LIMS Number: **n/a**
 Project Number: **n/a**
 Sample Number: **SW2D7b**
 Size: **.6**
 Grade: **270 K**
 Coil: **n/a**
 Operator: **MC**
 Condition of Sample: **Satisfactory**
 Comments:
 Procedure Name: **ASTM A416 - 7 wire strand - 40988**
 Start Date: **3/1/2012**
 Start Time: **9:13:57 AM**
 End Date: **3/1/2012**
 End Time: **9:15:40 AM**
 Workstation: **FLORIDA-DOT**
 Tested By: **tech**

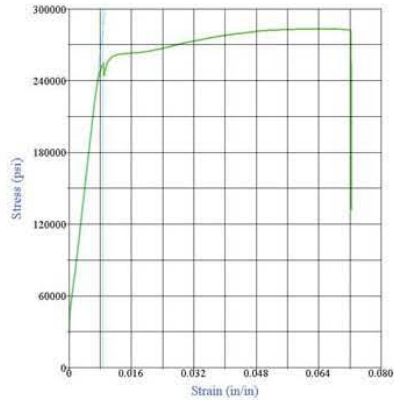


Test Results
 Specimen Gage Length: **31.0000** in
 Area: **0.2180** in²
 Total Load: **61720** lbf
 Tensile Strength: **283130** psi
 Correlation Coefficient: **0.9999**
 Modulus of Elasticity: **28547700** psi
 Load at 1% EUL: **55360** lbf
 Stress at 1% EUL: **253960** psi
 Est. Elongation: **0.1**
 Total Elongation: **7.46** %
 Position at Break: **2.869** in

Test Summary

Counter: **6707**
 Elapsed Time: **00:01:45**
 LIMS Number: **n/a**
 Project Number: **n/a**
 Sample Number: **SW2D8**
 Size: **.6**
 Grade: **270 K**
 Coil: **n/a**
 Operator: **MC**
 Condition of Sample: **Satisfactory**
 Comments:
 Procedure Name: **ASTM A416 - 7 wire strand - 40988**
 Start Date: **3/1/2012**
 Start Time: **11:29:13 AM**
 End Date: **3/1/2012**
 End Time: **11:30:58 AM**
 Workstation: **FLORIDA-DOT**
 Tested By: **tech**

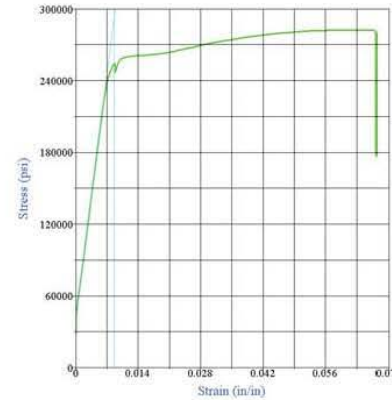
APPENDIX 3 (Continued)



Test Results
 Specimen Gage Length: **31.0000** in
 Area: **0.2180** in²
 Total Load: **61760** lbf
 Tensile Strength: **283290** psi
 Correlation Coefficient: **1.0000**
 Modulus of Elasticity: **28619900** psi
 Load at 1% EUL: **55520** lbf
 Stress at 1% EUL: **254690** psi
 Est. Elongation: **0.1**
 Total Elongation: **7.23** %
 Position at Break: **2.464** in

Test Summary

Counter: **6633**
 Elapsed Time: **00:03:21**
 LIMS Number: **n/a**
 Project Number: **n/a**
 Sample Number: **SW4D1**
 Size: **.6**
 Grade: **270 K**
 Coil: **n/a**
 Operator: **MC**
 Condition of Sample: **Satisfactory**
 Comments:
 Procedure Name: **ASTM A416 - 7 wire strand - 40988**
 Start Date: **2/27/2012**
 Start Time: **1:41:31 PM**
 End Date: **2/27/2012**
 End Time: **1:44:52 PM**
 Workstation: **FLORIDA-DOT**
 Tested By: **tech**

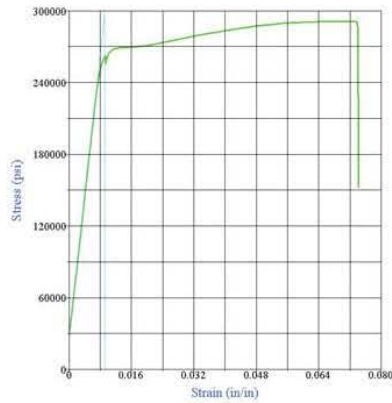


Test Results
 Specimen Gage Length: **31.0000** in
 Area: **0.2180** in²
 Total Load: **61540** lbf
 Tensile Strength: **282290** psi
 Correlation Coefficient: **1.0000**
 Modulus of Elasticity: **29450800** psi
 Load at 1% EUL: **55490** lbf
 Stress at 1% EUL: **254540** psi
 Est. Elongation: **0.1**
 Total Elongation: **6.72** %
 Position at Break: **2.269** in

Test Summary

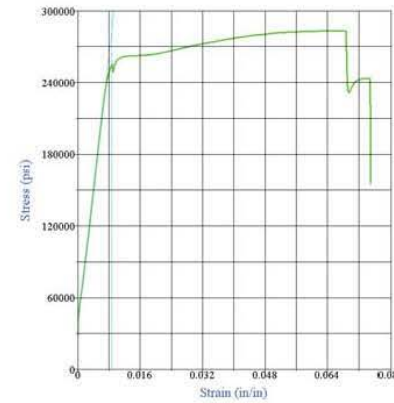
Counter: **6649**
 Elapsed Time: **00:01:49**
 LIMS Number: **n/a**
 Project Number: **n/a**
 Sample Number: **SW4D2**
 Size: **.6**
 Grade: **270 K**
 Coil: **n/a**
 Operator: **MC**
 Condition of Sample: **Satisfactory**
 Comments:
 Procedure Name: **ASTM A416 - 7 wire strand - 40988**
 Start Date: **2/28/2012**
 Start Time: **10:57:23 AM**
 End Date: **2/28/2012**
 End Time: **10:59:12 AM**
 Workstation: **FLORIDA-DOT**
 Tested By: **tech**

APPENDIX 3 (Continued)



Test Results
 Specimen Gage Length: **31.0000** in
 Area: **0.2120** in²
 Total Load: **61730** lbf
 Tensile Strength: **291170** psi
 Correlation Coefficient: **1.0000**
 Modulus of Elasticity: **29941400** psi
 Load at 1% EUL: **55570** lbf
 Stress at 1% EUL: **262130** psi
 Est. Elongation: **0.1**
 Total Elongation: **7.41** %
 Position at Break: **2.908** in

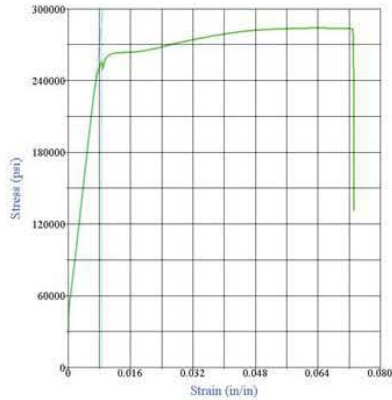
Test Summary
 Counter: **6636**
 Elapsed Time: **00:01:52**
 LIMS Number: **n/a**
 Project Number: **n/a**
 Sample Number: **SW4D3a**
 Size: **.6**
 Grade: **270 K**
 Coil: **n/a**
 Operator: **MC**
 Condition of Sample: **Satisfactory**
 Comments:
 Procedure Name: **ASTM A416 - 7 wire strand - 40988**
 Start Date: **2/28/2012**
 Start Time: **6:51:35 AM**
 End Date: **2/28/2012**
 End Time: **6:53:27 AM**
 Workstation: **FLORIDA-DOT**
 Tested By: **tech**



Test Results
 Specimen Gage Length: **31.0000** in
 Area: **0.2180** in²
 Total Load: **61740** lbf
 Tensile Strength: **283200** psi
 Correlation Coefficient: **1.0000**
 Modulus of Elasticity: **28501300** psi
 Load at 1% EUL: **55580** lbf
 Stress at 1% EUL: **254950** psi
 Est. Elongation: **0.1**
 Total Elongation: **7.49** %
 Position at Break: **2.759** in

Test Summary
 Counter: **6635**
 Elapsed Time: **00:01:55**
 LIMS Number: **n/a**
 Project Number: **n/a**
 Sample Number: **SW4D3b**
 Size: **.6**
 Grade: **270 K**
 Coil: **n/a**
 Operator: **MC**
 Condition of Sample: **Satisfactory**
 Comments:
 Procedure Name: **ASTM A416 - 7 wire strand - 40988**
 Start Date: **2/28/2012**
 Start Time: **6:44:38 AM**
 End Date: **2/28/2012**
 End Time: **6:46:33 AM**
 Workstation: **FLORIDA-DOT**
 Tested By: **tech**

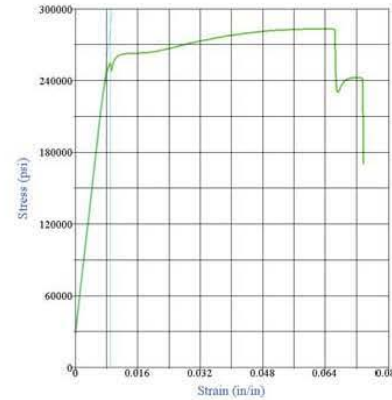
APPENDIX 3 (Continued)



Test Results
 Specimen Gage Length: **31.0000** in
 Area: **0.2180** in²
 Total Load: **61890** lbf
 Tensile Strength: **283890** psi
 Correlation Coefficient: **1.0000**
 Modulus of Elasticity: **28799400** psi
 Load at 1% EUL: **55780** lbf
 Stress at 1% EUL: **255860** psi
 Est. Elongation: **0.1**
 Total Elongation: **7.31** %
 Position at Break: **2.635** in

Test Summary

Counter: **6651**
 Elapsed Time: **00:01:45**
 LIMS Number: **n/a**
 Project Number: **n/a**
 Sample Number: **SW4D4**
 Size: **.6**
 Grade: **270 K**
 Coil: **n/a**
 Operator: **MC**
 Condition of Sample: **Satisfactory**
 Comments:
 Procedure Name: **ASTM A416 - 7 wire strand - 40988**
 Start Date: **2/28/2012**
 Start Time: **11:08:11 AM**
 End Date: **2/28/2012**
 End Time: **11:09:56 AM**
 Workstation: **FLORIDA-DOT**
 Tested By: **tech**

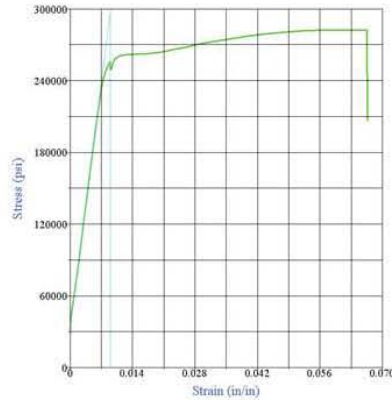


Test Results
 Specimen Gage Length: **31.0000** in
 Area: **0.2180** in²
 Total Load: **61750** lbf
 Tensile Strength: **283240** psi
 Correlation Coefficient: **1.0000**
 Modulus of Elasticity: **28525200** psi
 Load at 1% EUL: **55600** lbf
 Stress at 1% EUL: **255050** psi
 Est. Elongation: **0.1**
 Total Elongation: **7.37** %
 Position at Break: **1.682** in

Test Summary

Counter: **6644**
 Elapsed Time: **00:01:51**
 LIMS Number: **n/a**
 Project Number: **n/a**
 Sample Number: **SW4D7a**
 Size: **.6**
 Grade: **270 K**
 Coil: **n/a**
 Operator: **MC**
 Condition of Sample: **Satisfactory**
 Comments:
 Procedure Name: **ASTM A416 - 7 wire strand - 40988**
 Start Date: **2/28/2012**
 Start Time: **9:31:39 AM**
 End Date: **2/28/2012**
 End Time: **9:33:30 AM**
 Workstation: **FLORIDA-DOT**
 Tested By: **tech**

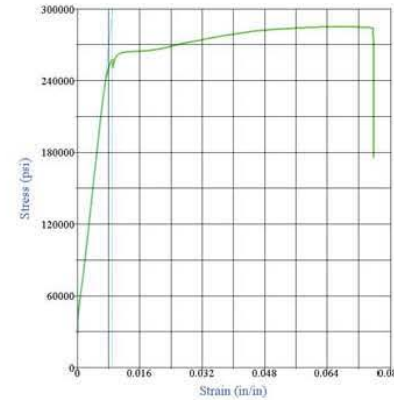
APPENDIX 3 (Continued)



Test Results
 Specimen Gage Length: **31.0000** in
 Area: **0.2180** in²
 Total Load: **61560** lbf
 Tensile Strength: **282400** psi
 Correlation Coefficient: **1.0000**
 Modulus of Elasticity: **29567500** psi
 Load at 1% EUL: **55650** lbf
 Stress at 1% EUL: **255270** psi
 Est. Elongation: **0.1**
 Total Elongation: **6.65** %
 Position at Break: **2.326** in

Test Summary

Counter: **6645**
 Elapsed Time: **00:01:37**
 LIMS Number: **n/a**
 Project Number: **n/a**
 Sample Number: **SW4D7b**
 Size: **.6**
 Grade: **270 K**
 Coil: **n/a**
 Operator: **MC**
 Condition of Sample: **Satisfactory**
 Comments:
 Procedure Name: **ASTM A416 - 7 wire strand - 40988**
 Start Date: **2/28/2012**
 Start Time: **10:33:07 AM**
 End Date: **2/28/2012**
 End Time: **10:34:44 AM**
 Workstation: **FLORIDA-DOT**
 Tested By: **tech**



Test Results
 Specimen Gage Length: **31.0000** in
 Area: **0.2180** in²
 Total Load: **62150** lbf
 Tensile Strength: **285090** psi
 Correlation Coefficient: **1.0000**
 Modulus of Elasticity: **29526800** psi
 Load at 1% EUL: **56180** lbf
 Stress at 1% EUL: **257710** psi
 Est. Elongation: **0.1**
 Total Elongation: **7.58** %
 Position at Break: **2.733** in

Test Summary

Counter: **6634**
 Elapsed Time: **00:01:51**
 LIMS Number: **n/a**
 Project Number: **n/a**
 Sample Number: **SW4D8**
 Size: **.6**
 Grade: **270 K**
 Coil: **n/a**
 Operator: **MC**
 Condition of Sample: **Satisfactory**
 Comments:
 Procedure Name: **ASTM A416 - 7 wire strand - 40988**
 Start Date: **2/27/2012**
 Start Time: **2:22:15 PM**
 End Date: **2/27/2012**
 End Time: **2:24:06 PM**
 Workstation: **FLORIDA-DOT**
 Tested By: **tech**

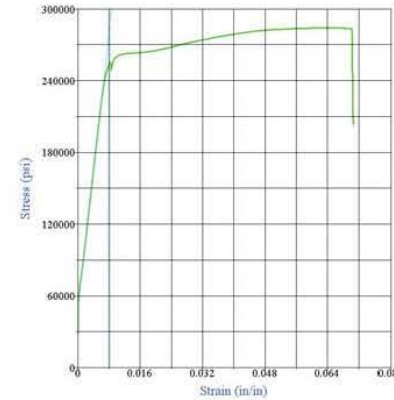
APPENDIX 3 (Continued)



Test Results
 Specimen Gage Length: **31.0000** in
 Area: **0.2180** in²
 Total Load: **61660** lbf
 Tensile Strength: **282820** psi
 Correlation Coefficient: **1.0000**
 Modulus of Elasticity: **28887100** psi
 Load at 1% EUL: **55620** lbf
 Stress at 1% EUL: **255140** psi
 Est. Elongation: **0.1**
 Total Elongation: **6.59** %
 Position at Break: **2.205** in

Test Summary

Counter: **6652**
 Elapsed Time: **00:01:44**
 LIMS Number: **n/a**
 Project Number: **n/a**
 Sample Number: **SW8D1**
 Size: **.6**
 Grade: **270 K**
 Coil: **n/a**
 Operator: **MC**
 Condition of Sample: **Satisfactory**
 Comments:
 Procedure Name: **ASTM A416 - 7 wire strand - 40988**
 Start Date: **2/28/2012**
 Start Time: **11:17:09 AM**
 End Date: **2/28/2012**
 End Time: **11:18:53 AM**
 Workstation: **FLORIDA-DOT**
 Tested By: **tech**

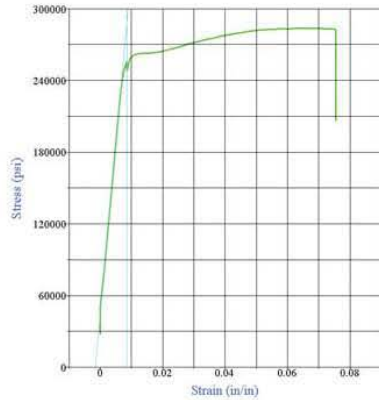


Test Results
 Specimen Gage Length: **31.0000** in
 Area: **0.2180** in²
 Total Load: **61920** lbf
 Tensile Strength: **284020** psi
 Correlation Coefficient: **1.0000**
 Modulus of Elasticity: **28795300** psi
 Load at 1% EUL: **55660** lbf
 Stress at 1% EUL: **255320** psi
 Est. Elongation: **0.1**
 Total Elongation: **7.04** %
 Position at Break: **2.452** in

Test Summary

Counter: **6650**
 Elapsed Time: **00:01:45**
 LIMS Number: **n/a**
 Project Number: **n/a**
 Sample Number: **SW8D2**
 Size: **.6**
 Grade: **270 K**
 Coil: **n/a**
 Operator: **MC**
 Condition of Sample: **Satisfactory**
 Comments:
 Procedure Name: **ASTM A416 - 7 wire strand - 40988**
 Start Date: **2/28/2012**
 Start Time: **11:03:21 AM**
 End Date: **2/28/2012**
 End Time: **11:05:06 AM**
 Workstation: **FLORIDA-DOT**
 Tested By: **tech**

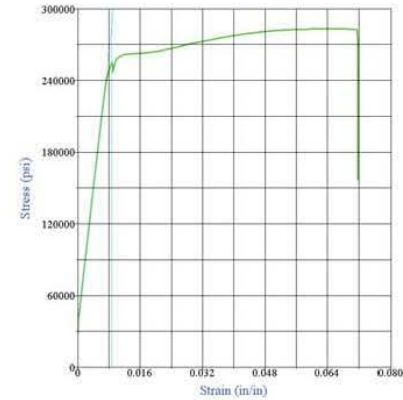
APPENDIX 3 (Continued)



Test Results
 Specimen Gage Length: **31.0000** in
 Area: **0.2180** in²
 Total Load: **61830** lbf
 Tensile Strength: **283630** psi
 Correlation Coefficient: **1.0000**
 Modulus of Elasticity: **28534100** psi
 Load at 1% EUL: **55610** lbf
 Stress at 1% EUL: **255110** psi
 Est. Elongation: **0.1**
 Total Elongation: **7.54** %
 Position at Break: **2.661** in

Test Summary

Counter: **6657**
 Elapsed Time: **00:01:53**
 LIMS Number: **n/a**
 Project Number: **n/a**
 Sample Number: **SW8D3a**
 Size: **.6**
 Grade: **270 K**
 Coil: **n/a**
 Operator: **MC**
 Condition of Sample: **Satisfactory**
 Comments:
 Procedure Name: **ASTM A416 - 7 wire strand - 40988**
 Start Date: **2/28/2012**
 Start Time: **1:16:56 PM**
 End Date: **2/28/2012**
 End Time: **1:18:49 PM**
 Workstation: **FLORIDA-DOT**
 Tested By: **tech**

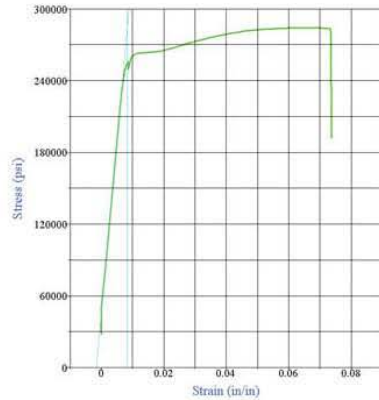


Test Results
 Specimen Gage Length: **31.0000** in
 Area: **0.2180** in²
 Total Load: **61730** lbf
 Tensile Strength: **283170** psi
 Correlation Coefficient: **1.0000**
 Modulus of Elasticity: **28660400** psi
 Load at 1% EUL: **55550** lbf
 Stress at 1% EUL: **254820** psi
 Est. Elongation: **0.1**
 Total Elongation: **7.17** %
 Position at Break: **2.760** in

Test Summary

Counter: **6656**
 Elapsed Time: **00:02:01**
 LIMS Number: **n/a**
 Project Number: **n/a**
 Sample Number: **SW8D3b**
 Size: **.6**
 Grade: **270 K**
 Coil: **n/a**
 Operator: **MC**
 Condition of Sample: **Satisfactory**
 Comments:
 Procedure Name: **ASTM A416 - 7 wire strand - 40988**
 Start Date: **2/28/2012**
 Start Time: **1:11:27 PM**
 End Date: **2/28/2012**
 End Time: **1:13:28 PM**
 Workstation: **FLORIDA-DOT**
 Tested By: **tech**

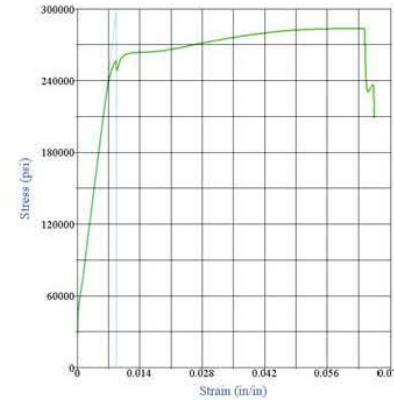
APPENDIX 3 (Continued)



Test Results
 Specimen Gage Length: **31.0000** in
 Area: **0.2180** in²
 Total Load: **61940** lbf
 Tensile Strength: **284120** psi
 Correlation Coefficient: **1.0000**
 Modulus of Elasticity: **28672600** psi
 Load at 1% EUL: **55730** lbf
 Stress at 1% EUL: **255650** psi
 Est. Elongation: **0.1**
 Total Elongation: **7.35** %
 Position at Break: **2.434** in

Test Summary

Counter: **6654**
 Elapsed Time: **00:01:47**
 LIMS Number: **n/a**
 Project Number: **n/a**
 Sample Number: **SW8D4**
 Size: **.6**
 Grade: **270 K**
 Coil: **n/a**
 Operator: **MC**
 Condition of Sample: **Satisfactory**
 Comments:
 Procedure Name: **ASTM A416 - 7 wire strand - 40988**
 Start Date: **2/28/2012**
 Start Time: **11:33:48 AM**
 End Date: **2/28/2012**
 End Time: **11:35:35 AM**
 Workstation: **FLORIDA-DOT**
 Tested By: **tech**

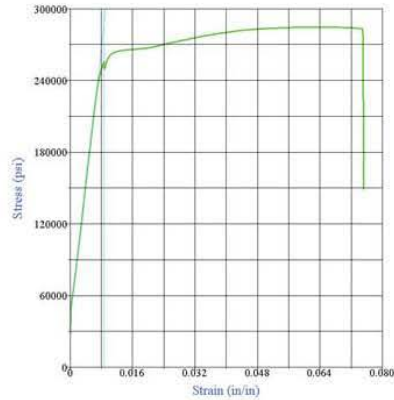


Test Results
 Specimen Gage Length: **31.0000** in
 Area: **0.2180** in²
 Total Load: **61870** lbf
 Tensile Strength: **283820** psi
 Correlation Coefficient: **0.9999**
 Modulus of Elasticity: **29624800** psi
 Load at 1% EUL: **56030** lbf
 Stress at 1% EUL: **257000** psi
 Est. Elongation: **0.1**
 Total Elongation: **6.64** %
 Position at Break: **2.410** in

Test Summary

Counter: **6655**
 Elapsed Time: **00:02:11**
 LIMS Number: **n/a**
 Project Number: **n/a**
 Sample Number: **SW8D5**
 Size: **.6**
 Grade: **270 K**
 Coil: **n/a**
 Operator: **MC**
 Condition of Sample: **Satisfactory**
 Comments:
 Procedure Name: **ASTM A416 - 7 wire strand - 40988**
 Start Date: **2/28/2012**
 Start Time: **1:05:27 PM**
 End Date: **2/28/2012**
 End Time: **1:07:38 PM**
 Workstation: **FLORIDA-DOT**
 Tested By: **tech**

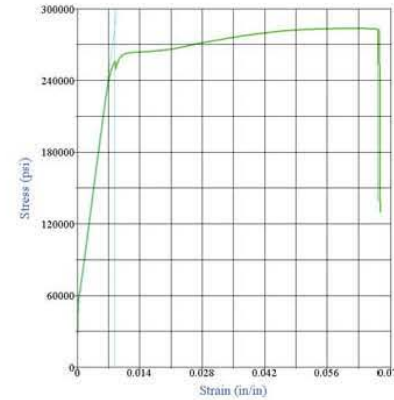
APPENDIX 3 (Continued)



Test Results
 Specimen Gage Length: **31.0000** in
 Area: **0.2180** in²
 Total Load: **62070** lbf
 Tensile Strength: **284720** psi
 Correlation Coefficient: **0.9999**
 Modulus of Elasticity: **28670100** psi
 Load at 1% EUL: **55650** lbf
 Stress at 1% EUL: **255270** psi
 Est. Elongation: **0.1**
 Total Elongation: **7.51** %
 Position at Break: **2.539** in

Test Summary

Counter: **6646**
 Elapsed Time: **00:01:42**
 LIMS Number: **n/a**
 Project Number: **n/a**
 Sample Number: **DW8D6**
 Size: **.6**
 Grade: **270 K**
 Coil: **n/a**
 Operator: **MC**
 Condition of Sample: **Satisfactory**
 Comments:
 Procedure Name: **ASTM A416 - 7 wire strand - 40988**
 Start Date: **2/28/2012**
 Start Time: **10:38:42 AM**
 End Date: **2/28/2012**
 End Time: **10:40:24 AM**
 Workstation: **FLORIDA-DOT**
 Tested By: **tech**

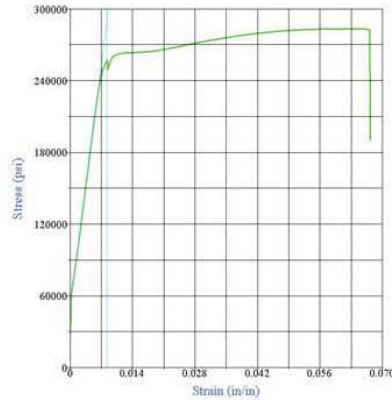


Test Results
 Specimen Gage Length: **31.0000** in
 Area: **0.2180** in²
 Total Load: **61830** lbf
 Tensile Strength: **283630** psi
 Correlation Coefficient: **1.0000**
 Modulus of Elasticity: **28583800** psi
 Load at 1% EUL: **55780** lbf
 Stress at 1% EUL: **255850** psi
 Est. Elongation: **0.1**
 Total Elongation: **6.75** %
 Position at Break: **2.451** in

Test Summary

Counter: **6647**
 Elapsed Time: **00:01:38**
 LIMS Number: **n/a**
 Project Number: **n/a**
 Sample Number: **SW8D7a**
 Size: **.6**
 Grade: **270 K**
 Coil: **n/a**
 Operator: **MC**
 Condition of Sample: **Satisfactory**
 Comments:
 Procedure Name: **ASTM A416 - 7 wire strand - 40988**
 Start Date: **2/28/2012**
 Start Time: **10:46:13 AM**
 End Date: **2/28/2012**
 End Time: **10:47:51 AM**
 Workstation: **FLORIDA-DOT**
 Tested By: **tech**

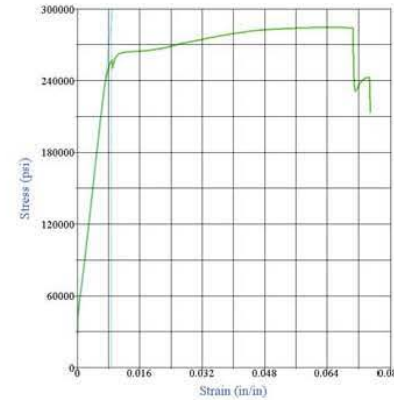
APPENDIX 3 (Continued)



Test Results
 Specimen Gage Length: **31.0000** in
 Area: **0.2180** in²
 Total Load: **61770** lbf
 Tensile Strength: **283330** psi
 Correlation Coefficient: **0.9999**
 Modulus of Elasticity: **29057600** psi
 Load at 1% EUL: **55940** lbf
 Stress at 1% EUL: **256610** psi
 Est. Elongation: **0.1**
 Total Elongation: **6.72** %
 Position at Break: **2.393** in

Test Summary

Counter: **6653**
 Elapsed Time: **00:01:43**
 LIMS Number: **n/a**
 Project Number: **n/a**
 Sample Number: **SW8D7b**
 Size: **.6**
 Grade: **270 K**
 Coil: **n/a**
 Operator: **MC**
 Condition of Sample: **Satisfactory**
 Comments:
 Procedure Name: **ASTM A416 - 7 wire strand - 40988**
 Start Date: **2/28/2012**
 Start Time: **11:23:53 AM**
 End Date: **2/28/2012**
 End Time: **11:25:36 AM**
 Workstation: **FLORIDA-DOT**
 Tested By: **tech**

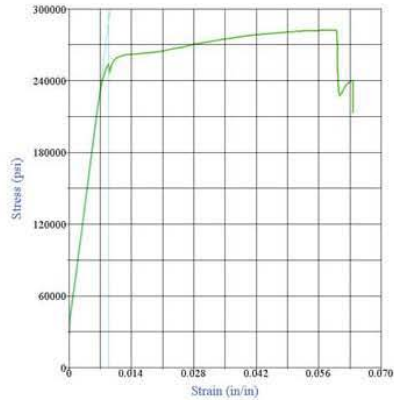


Test Results
 Specimen Gage Length: **31.0000** in
 Area: **0.2180** in²
 Total Load: **62030** lbf
 Tensile Strength: **284540** psi
 Correlation Coefficient: **1.0000**
 Modulus of Elasticity: **29004700** psi
 Load at 1% EUL: **56040** lbf
 Stress at 1% EUL: **257080** psi
 Est. Elongation: **0.1**
 Total Elongation: **7.49** %
 Position at Break: **2.800** in

Test Summary

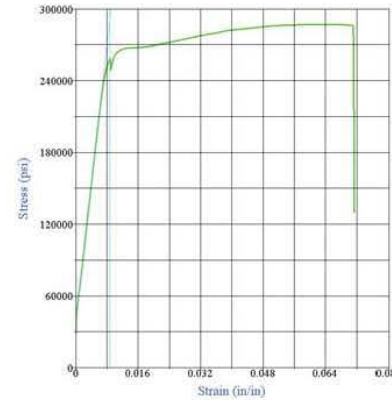
Counter: **6648**
 Elapsed Time: **00:01:46**
 LIMS Number: **n/a**
 Project Number: **n/a**
 Sample Number: **SW8D8**
 Size: **.6**
 Grade: **270 K**
 Coil: **n/a**
 Operator: **MC**
 Condition of Sample: **Satisfactory**
 Comments:
 Procedure Name: **ASTM A416 - 7 wire strand - 40988**
 Start Date: **2/28/2012**
 Start Time: **10:52:16 AM**
 End Date: **2/28/2012**
 End Time: **10:54:02 AM**
 Workstation: **FLORIDA-DOT**
 Tested By: **tech**

APPENDIX 3 (Continued)



Test Results
 Specimen Gage Length: **31.0000** in
 Area: **0.2180** in²
 Total Load: **61500** lbf
 Tensile Strength: **282110** psi
 Correlation Coefficient: **1.0000**
 Modulus of Elasticity: **28825100** psi
 Load at 1% EUL: **55350** lbf
 Stress at 1% EUL: **253880** psi
 Est. Elongation: **0.1**
 Total Elongation: **6.36** %
 Position at Break: **2.410** in

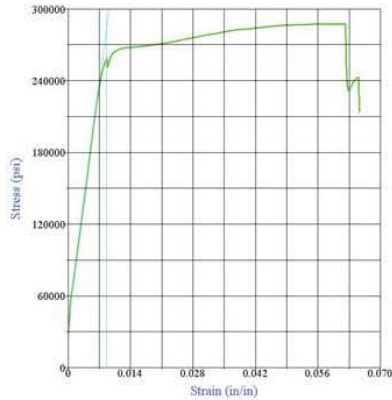
Test Summary
 Counter: **6609**
 Elapsed Time: **00:01:39**
 LIMS Number: **N/A**
 Project Number: **N/A**
 Sample Number: **SM9D1**
 Size: **.6**
 Grade: **270 K**
 Coil: **N/A**
 Operator: **N/A**
 Condition of Sample: **Satisfactory**
 Comments:
 Procedure Name: **ASTM A416 - 7 wire strand - 40988**
 Start Date: **2/23/2012**
 Start Time: **9:47:33 AM**
 End Date: **2/23/2012**
 End Time: **9:49:12 AM**
 Workstation: **FLORIDA-DOT**
 Tested By: **tech**



Test Results
 Specimen Gage Length: **31.0000** in
 Area: **0.2180** in²
 Total Load: **62540** lbf
 Tensile Strength: **286870** psi
 Correlation Coefficient: **1.0000**
 Modulus of Elasticity: **29121600** psi
 Load at 1% EUL: **56100** lbf
 Stress at 1% EUL: **258230** psi
 Est. Elongation: **0.1**
 Total Elongation: **7.12** %
 Position at Break: **2.801** in

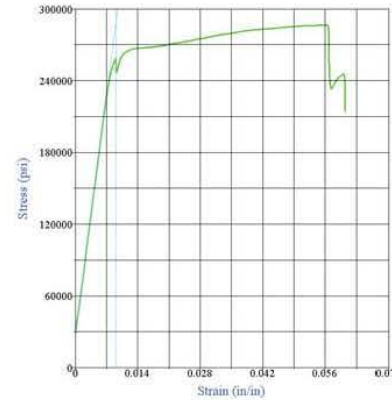
Test Summary
 Counter: **6612**
 Elapsed Time: **00:02:23**
 LIMS Number: **N/A**
 Project Number: **N/A**
 Sample Number: **SM9D2**
 Size: **.6**
 Grade: **270 K**
 Coil: **N/A**
 Operator: **N/A**
 Condition of Sample: **Satisfactory**
 Comments:
 Procedure Name: **ASTM A416 - 7 wire strand - 40988**
 Start Date: **2/23/2012**
 Start Time: **10:22:56 AM**
 End Date: **2/23/2012**
 End Time: **10:25:19 AM**
 Workstation: **FLORIDA-DOT**
 Tested By: **tech**

APPENDIX 3 (Continued)



Test Results
 Specimen Gage Length: **31.0000** in
 Area: **0.2180** in²
 Total Load: **62690** lbf
 Tensile Strength: **287560** psi
 Correlation Coefficient: **0.9999**
 Modulus of Elasticity: **28515000** psi
 Load at 1% EUL: **56330** lbf
 Stress at 1% EUL: **258390** psi
 Est. Elongation: **0.1**
 Total Elongation: **6.51** %
 Position at Break: **2.235** in

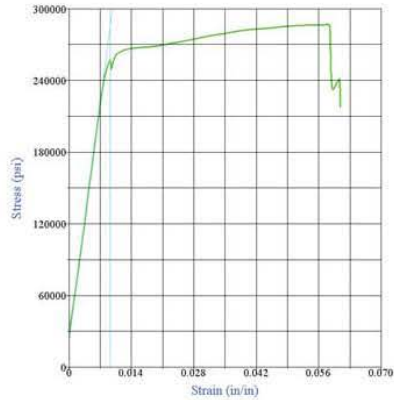
Test Summary
 Counter: **6614**
 Elapsed Time: **00:01:41**
 LIMS Number: **N/A**
 Project Number: **N/A**
 Sample Number: **SM9D3a**
 Size: **.6**
 Grade: **270 K**
 Coil: **N/A**
 Operator: **MC**
 Condition of Sample: **Satisfactory**
 Comments:
 Procedure Name: **ASTM A416 - 7 wire strand - 40988**
 Start Date: **2/23/2012**
 Start Time: **10:45:52 AM**
 End Date: **2/23/2012**
 End Time: **10:47:33 AM**
 Workstation: **FLORIDA-DOT**
 Tested By: **tech**



Test Results
 Specimen Gage Length: **31.0000** in
 Area: **0.2180** in²
 Total Load: **62420** lbf
 Tensile Strength: **286310** psi
 Correlation Coefficient: **0.9999**
 Modulus of Elasticity: **28834900** psi
 Load at 1% EUL: **56320** lbf
 Stress at 1% EUL: **258350** psi
 Est. Elongation: **0.1**
 Total Elongation: **6.04** %
 Position at Break: **2.115** in

Test Summary
 Counter: **6619**
 Elapsed Time: **00:03:38**
 LIMS Number: **N/A**
 Project Number: **N/A**
 Sample Number: **SM9D3a**
 Size: **.6**
 Grade: **270 K**
 Coil: **N/A**
 Operator: **MC**
 Condition of Sample: **Satisfactory**
 Comments:
 Procedure Name: **ASTM A416 - 7 wire strand - 40988**
 Start Date: **2/23/2012**
 Start Time: **1:19:03 PM**
 End Date: **2/23/2012**
 End Time: **1:22:41 PM**
 Workstation: **FLORIDA-DOT**
 Tested By: **tech**

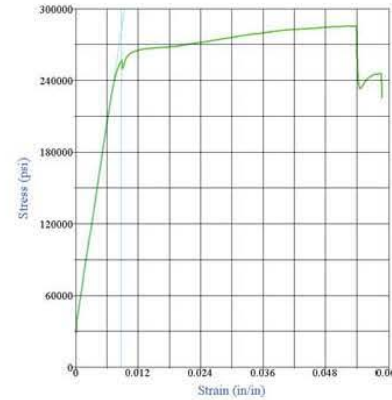
APPENDIX 3 (Continued)



Test Results
 Specimen Gage Length: **31.0000** in
 Area: **0.2180** in²
 Total Load: **62490** lbf
 Tensile Strength: **286640** psi
 Correlation Coefficient: **0.9999**
 Modulus of Elasticity: **28619700** psi
 Load at 1% EUL: **56100** lbf
 Stress at 1% EUL: **257360** psi
 Est. Elongation: **0.1**
 Total Elongation: **6.07** %
 Position at Break: **2.121** in

Test Summary

Counter: **6616**
 Elapsed Time: **00:01:46**
 LIMS Number: **N/A**
 Project Number: **N/A**
 Sample Number: **SM9D4a**
 Size: **.6**
 Grade: **270 K**
 Coil: **N/A**
 Operator: **MC**
 Condition of Sample: **Satisfactory**
 Comments:
 Procedure Name: **ASTM A416 - 7 wire strand - 40988**
 Start Date: **2/23/2012**
 Start Time: **11:12:59 AM**
 End Date: **2/23/2012**
 End Time: **11:14:45 AM**
 Workstation: **FLORIDA-DOT**
 Tested By: **tech**

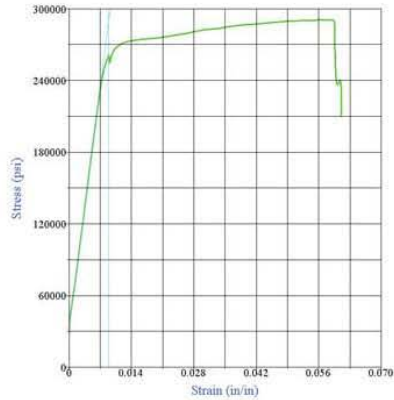


Test Results
 Specimen Gage Length: **31.0000** in
 Area: **0.2180** in²
 Total Load: **62550** lbf
 Tensile Strength: **285550** psi
 Correlation Coefficient: **0.9998**
 Modulus of Elasticity: **28297900** psi
 Load at 1% EUL: **55980** lbf
 Stress at 1% EUL: **256800** psi
 Est. Elongation: **0.1**
 Total Elongation: **5.85** %
 Position at Break: **2.165** in

Test Summary

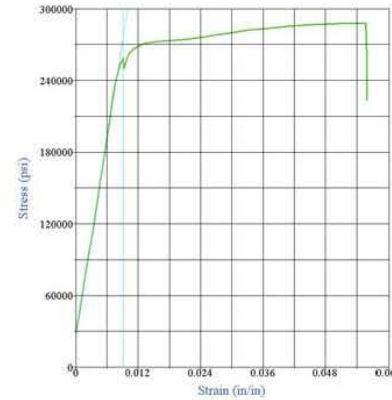
Counter: **6618**
 Elapsed Time: **00:01:36**
 LIMS Number: **N/A**
 Project Number: **N/A**
 Sample Number: **SM9D4b**
 Size: **.6**
 Grade: **270 K**
 Coil: **N/A**
 Operator: **MC**
 Condition of Sample: **Satisfactory**
 Comments:
 Procedure Name: **ASTM A416 - 7 wire strand - 40988**
 Start Date: **2/23/2012**
 Start Time: **11:32:30 AM**
 End Date: **2/23/2012**
 End Time: **11:34:06 AM**
 Workstation: **FLORIDA-DOT**
 Tested By: **tech**

APPENDIX 3 (Continued)



Test Results
 Specimen Gage Length: **31.0000** in
 Area: **0.2180** in²
 Total Load: **63320** lbf
 Tensile Strength: **290450** psi
 Correlation Coefficient: **1.0000**
 Modulus of Elasticity: **29022400** psi
 Load at 1% EUL: **56890** lbf
 Stress at 1% EUL: **260950** psi
 Est. Elongation: **0.1**
 Total Elongation: **6.10** %
 Position at Break: **2.286** in

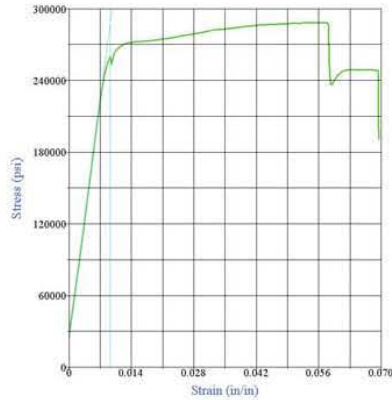
Test Summary
 Counter: **6610**
 Elapsed Time: **00:01:34**
 LIMS Number: **N/A**
 Project Number: **N/A**
 Sample Number: **SM9D5**
 Size: **.6**
 Grade: **270 K**
 Coil: **N/A**
 Operator: **MC**
 Condition of Sample: **Satisfactory**
 Comments:
 Procedure Name: **ASTM A416 - 7 wire strand - 40988**
 Start Date: **2/23/2012**
 Start Time: **10:08:40 AM**
 End Date: **2/23/2012**
 End Time: **10:10:14 AM**
 Workstation: **FLORIDA-DOT**
 Tested By: **tech**



Test Results
 Specimen Gage Length: **31.0000** in
 Area: **0.2180** in²
 Total Load: **62790** lbf
 Tensile Strength: **288000** psi
 Correlation Coefficient: **0.9995**
 Modulus of Elasticity: **27544100** psi
 Load at 1% EUL: **56370** lbf
 Stress at 1% EUL: **258600** psi
 Est. Elongation: **0.1**
 Total Elongation: **5.59** %
 Position at Break: **2.052** in

Test Summary
 Counter: **6608**
 Elapsed Time: **00:01:55**
 LIMS Number: **N/A**
 Project Number: **N/A**
 Sample Number: **SM9D6**
 Size: **.6**
 Grade: **270 K**
 Coil: **N/A**
 Operator: **MC**
 Condition of Sample: **Satisfactory**
 Comments:
 Procedure Name: **ASTM A416 - 7 wire strand - 40988**
 Start Date: **2/23/2012**
 Start Time: **9:18:30 AM**
 End Date: **2/23/2012**
 End Time: **9:20:25 AM**
 Workstation: **FLORIDA-DOT**
 Tested By: **tech**

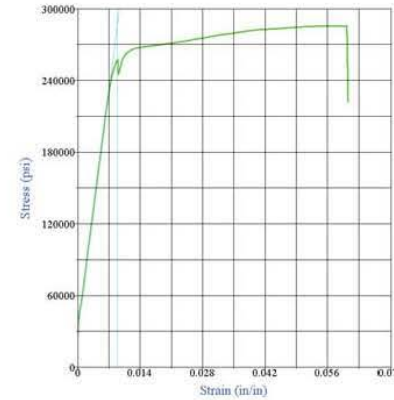
APPENDIX 3 (Continued)



Test Results
 Specimen Gage Length: **31.0000** in
 Area: **0.2180** in²
 Total Load: **62870** lbf
 Tensile Strength: **288380** psi
 Correlation Coefficient: **0.9999**
 Modulus of Elasticity: **28842700** psi
 Load at 1% EUL: **56670** lbf
 Stress at 1% EUL: **259940** psi
 Est. Elongation: **0.1**
 Total Elongation: **6.93** %
 Position at Break: **2.505** in

Test Summary

Counter: **6617**
 Elapsed Time: **00:01:44**
 LIMS Number: **N/A**
 Project Number: **N/A**
 Sample Number: **SM9D7b**
 Size: **.6**
 Grade: **270 K**
 Coil: **N/A**
 Operator: **MC**
 Condition of Sample: **Satisfactory**
 Comments:
 Procedure Name: **ASTM A416 - 7 wire strand - 40988**
 Start Date: **2/23/2012**
 Start Time: **11:21:10 AM**
 End Date: **2/23/2012**
 End Time: **11:22:54 AM**
 Workstation: **FLORIDA-DOT**
 Tested By: **tech**

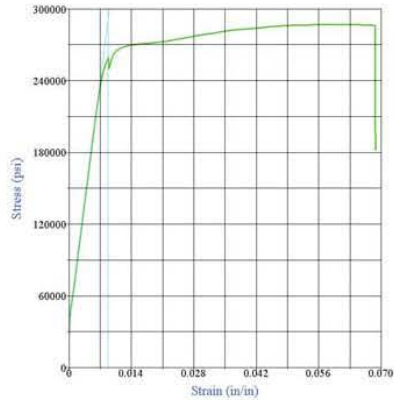


Test Results
 Specimen Gage Length: **31.0000** in
 Area: **0.2180** in²
 Total Load: **62280** lbf
 Tensile Strength: **285710** psi
 Correlation Coefficient: **1.0000**
 Modulus of Elasticity: **28725600** psi
 Load at 1% EUL: **56130** lbf
 Stress at 1% EUL: **257460** psi
 Est. Elongation: **0.1**
 Total Elongation: **6.04** %
 Position at Break: **2.356** in

Test Summary

Counter: **6611**
 Elapsed Time: **00:03:36**
 LIMS Number: **N/A**
 Project Number: **N/A**
 Sample Number: **SM9D8A**
 Size: **.6**
 Grade: **270 K**
 Coil: **N/A**
 Operator: **MC**
 Condition of Sample: **Satisfactory**
 Comments:
 Procedure Name: **ASTM A416 - 7 wire strand - 40988**
 Start Date: **2/23/2012**
 Start Time: **10:15:27 AM**
 End Date: **2/23/2012**
 End Time: **10:19:03 AM**
 Workstation: **FLORIDA-DOT**
 Tested By: **tech**

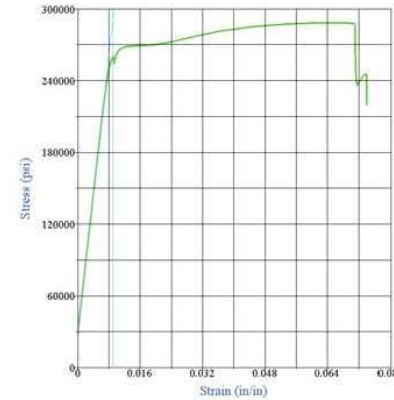
APPENDIX 3 (Continued)



Test Results
 Specimen Gage Length: **31.0000** in
 Area: **0.2180** in²
 Total Load: **62520** lbf
 Tensile Strength: **286790** psi
 Correlation Coefficient: **1.0000**
 Modulus of Elasticity: **29275100** psi
 Load at 1% EUL: **56460** lbf
 Stress at 1% EUL: **258980** psi
 Est. Elongation: **0.1**
 Total Elongation: **6.86** %
 Position at Break: **2.405** in

Test Summary

Counter: **6613**
 Elapsed Time: **00:01:57**
 LIMS Number: **N/A**
 Project Number: **N/A**
 Sample Number: **SM9D8a**
 Size: **.6**
 Grade: **270 K**
 Coil: **N/A**
 Operator: **MC**
 Condition of Sample: **Satisfactory**
 Comments:
 Procedure Name: **ASTM A416 - 7 wire strand - 40988**
 Start Date: **2/23/2012**
 Start Time: **10:34:04 AM**
 End Date: **2/23/2012**
 End Time: **10:36:01 AM**
 Workstation: **FLORIDA-DOT**
 Tested By: **tech**

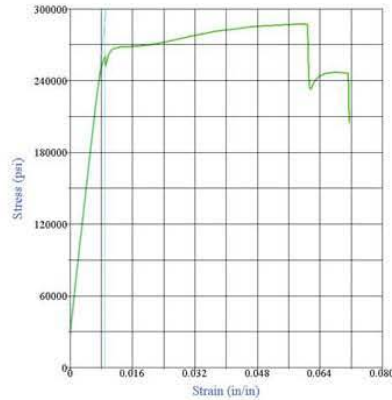


Test Results
 Specimen Gage Length: **31.0000** in
 Area: **0.2180** in²
 Total Load: **62880** lbf
 Tensile Strength: **288420** psi
 Correlation Coefficient: **1.0000**
 Modulus of Elasticity: **29157500** psi
 Load at 1% EUL: **56630** lbf
 Stress at 1% EUL: **259790** psi
 Est. Elongation: **0.1**
 Total Elongation: **7.39** %
 Position at Break: **2.744** in

Test Summary

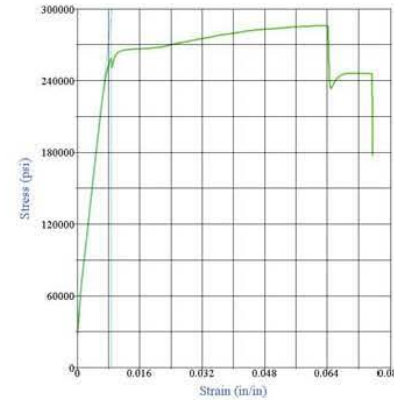
Counter: **6716**
 Elapsed Time: **00:01:43**
 LIMS Number: **n/a**
 Project Number: **n/a**
 Sample Number: **UW1D1**
 Size: **.6**
 Grade: **270 K**
 Coil: **n/a**
 Operator: **MC**
 Condition of Sample: **Satisfactory**
 Comments:
 Procedure Name: **ASTM A416 - 7 wire strand - 40988**
 Start Date: **3/5/2012**
 Start Time: **11:22:56 AM**
 End Date: **3/5/2012**
 End Time: **11:24:39 AM**
 Workstation: **FLORIDA-DOT**
 Tested By: **tech**

APPENDIX 3 (Continued)



Test Results
 Specimen Gage Length: 31.0000 in
 Area: 0.2180 in²
 Total Load: 62640 lbf
 Tensile Strength: 287330 psi
 Correlation Coefficient: 1.0000
 Modulus of Elasticity: 28932300 psi
 Load at 1% EUL: 56660 lbf
 Stress at 1% EUL: 259920 psi
 Est. Elongation: 0.1
 Total Elongation: 7.13 %
 Position at Break: 2.703 in

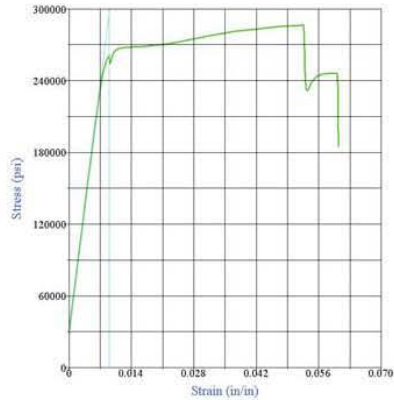
Test Summary
 Counter: 6719
 Elapsed Time: 00:02:00
 LIMS Number: n/a
 Project Number: n/a
 Sample Number: UW1D2
 Size: .6
 Grade: 270 K
 Coil: n/a
 Operator: MIC
 Condition of Sample: Satisfactory
 Comments:
 Procedure Name: ASTM A416 - 7 wire strand - 40988
 Start Date: 3/5/2012
 Start Time: 1:07:28 PM
 End Date: 3/5/2012
 End Time: 1:09:28 PM
 Workstation: FLORIDA-DOT
 Tested By: tech



Test Results
 Specimen Gage Length: 31.0000 in
 Area: 0.2180 in²
 Total Load: 62340 lbf
 Tensile Strength: 285970 psi
 Correlation Coefficient: 1.0000
 Modulus of Elasticity: 29223100 psi
 Load at 1% EUL: 56410 lbf
 Stress at 1% EUL: 258760 psi
 Est. Elongation: 0.1
 Total Elongation: 7.55 %
 Position at Break: 2.971 in

Test Summary
 Counter: 6711
 Elapsed Time: 00:02:11
 LIMS Number: n/a
 Project Number: n/a
 Sample Number: UW1D3a
 Size: .6
 Grade: 270 K
 Coil: n/a
 Operator: MIC
 Condition of Sample: Satisfactory
 Comments:
 Procedure Name: ASTM A416 - 7 wire strand - 40988
 Start Date: 3/1/2012
 Start Time: 2:48:45 PM
 End Date: 3/1/2012
 End Time: 2:50:56 PM
 Workstation: FLORIDA-DOT
 Tested By: tech

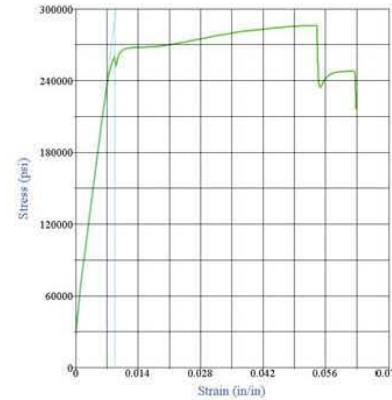
APPENDIX 3 (Continued)



Test Results
 Specimen Gage Length: **31.0000** in
 Area: **0.2180** in²
 Total Load: **62420** lbf
 Tensile Strength: **286310** psi
 Correlation Coefficient: **0.9999**
 Modulus of Elasticity: **29555700** psi
 Load at 1% EUL: **56830** lbf
 Stress at 1% EUL: **260670** psi
 Est. Elongation: **0.1**
 Total Elongation: **6.03** %
 Position at Break: **2.212** in

Test Summary

Counter: **6715**
 Elapsed Time: **00:01:37**
 LIMS Number: **n/a**
 Project Number: **n/a**
 Sample Number: **UW1D3b**
 Size: **.6**
 Grade: **270 K**
 Coil: **n/a**
 Operator: **MC**
 Condition of Sample: **Satisfactory**
 Comments:
 Procedure Name: **ASTM A416 - 7 wire strand - 40988**
 Start Date: **3/5/2012**
 Start Time: **11:14:57 AM**
 End Date: **3/5/2012**
 End Time: **11:16:34 AM**
 Workstation: **FLORIDA-DOT**
 Tested By: **tech**

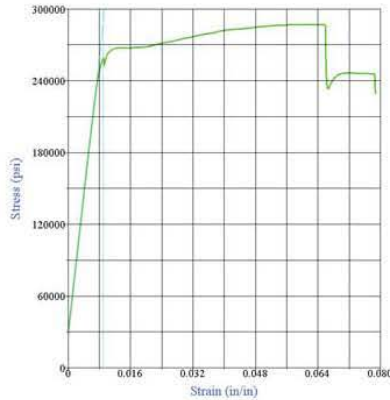


Test Results
 Specimen Gage Length: **31.0000** in
 Area: **0.2180** in²
 Total Load: **62380** lbf
 Tensile Strength: **286130** psi
 Correlation Coefficient: **1.0000**
 Modulus of Elasticity: **29036000** psi
 Load at 1% EUL: **56690** lbf
 Stress at 1% EUL: **260040** psi
 Est. Elongation: **0.1**
 Total Elongation: **6.27** %
 Position at Break: **2.273** in

Test Summary

Counter: **6718**
 Elapsed Time: **00:01:58**
 LIMS Number: **n/a**
 Project Number: **n/a**
 Sample Number: **UW1D4**
 Size: **.6**
 Grade: **270 K**
 Coil: **n/a**
 Operator: **MC**
 Condition of Sample: **Satisfactory**
 Comments:
 Procedure Name: **ASTM A416 - 7 wire strand - 40988**
 Start Date: **3/5/2012**
 Start Time: **12:59:30 PM**
 End Date: **3/5/2012**
 End Time: **1:01:28 PM**
 Workstation: **FLORIDA-DOT**
 Tested By: **tech**

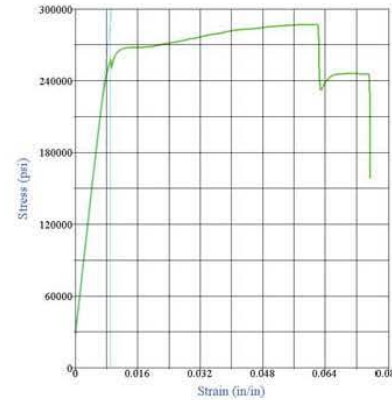
APPENDIX 3 (Continued)



Test Results
 Specimen Gage Length: **31.0000** in
 Area: **0.2180** in²
 Total Load: **62560** lbf
 Tensile Strength: **286960** psi
 Correlation Coefficient: **1.0000**
 Modulus of Elasticity: **28934500** psi
 Load at 1% EUL: **56430** lbf
 Stress at 1% EUL: **258840** psi
 Est. Elongation: **0.1**
 Total Elongation: **7.85** %
 Position at Break: **3.202** in

Test Summary

Counter: **6713**
 Elapsed Time: **00:01:50**
 LIMS Number: **n/a**
 Project Number: **n/a**
 Sample Number: **UW1D5**
 Size: **.6**
 Grade: **270 K**
 Coil: **n/a**
 Operator: **MC**
 Condition of Sample: **Satisfactory**
 Comments:
 Procedure Name: **ASTM A416 - 7 wire strand - 40988**
 Start Date: **3/1/2012**
 Start Time: **3:06:13 PM**
 End Date: **3/1/2012**
 End Time: **3:08:03 PM**
 Workstation: **FLORIDA-DOT**
 Tested By: **tech**

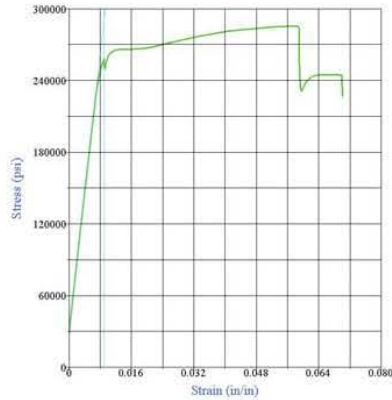


Test Results
 Specimen Gage Length: **31.0000** in
 Area: **0.2180** in²
 Total Load: **62540** lbf
 Tensile Strength: **286870** psi
 Correlation Coefficient: **1.0000**
 Modulus of Elasticity: **29003200** psi
 Load at 1% EUL: **56060** lbf
 Stress at 1% EUL: **257140** psi
 Est. Elongation: **0.1**
 Total Elongation: **7.54** %
 Position at Break: **3.084** in

Test Summary

Counter: **6712**
 Elapsed Time: **00:02:00**
 LIMS Number: **n/a**
 Project Number: **n/a**
 Sample Number: **UW1D6**
 Size: **.6**
 Grade: **270 K**
 Coil: **n/a**
 Operator: **MC**
 Condition of Sample: **Satisfactory**
 Comments:
 Procedure Name: **ASTM A416 - 7 wire strand - 40988**
 Start Date: **3/1/2012**
 Start Time: **2:56:20 PM**
 End Date: **3/1/2012**
 End Time: **2:58:20 PM**
 Workstation: **FLORIDA-DOT**
 Tested By: **tech**

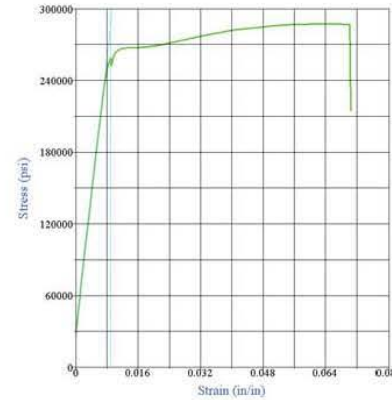
APPENDIX 3 (Continued)



Test Results
 Specimen Gage Length: **31.0000** in
 Area: **0.2180** in²
 Total Load: **62230** lbf
 Tensile Strength: **285460** psi
 Correlation Coefficient: **1.0000**
 Modulus of Elasticity: **28955700** psi
 Load at 1% EUL: **56220** lbf
 Stress at 1% EUL: **257900** psi
 Est. Elongation: **0.1**
 Total Elongation: **6.99** %
 Position at Break: **2.476** in

Test Summary

Counter: **6717**
 Elapsed Time: **00:02:01**
 LIMS Number: **n/a**
 Project Number: **n/a**
 Sample Number: **UW1D7b**
 Size: **.6**
 Grade: **270 K**
 Coil: **n/a**
 Operator: **MC**
 Condition of Sample: **Satisfactory**
 Comments:
 Procedure Name: **ASTM A416 - 7 wire strand - 40988**
 Start Date: **3/5/2012**
 Start Time: **12:52:30 PM**
 End Date: **3/5/2012**
 End Time: **12:54:31 PM**
 Workstation: **FLORIDA-DOT**
 Tested By: **tech**

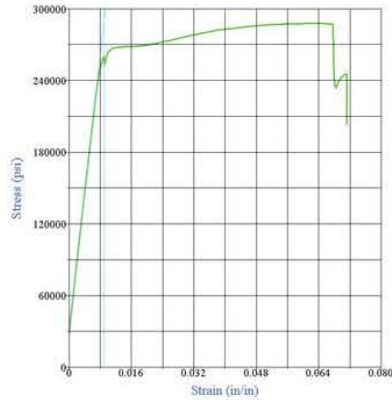


Test Results
 Specimen Gage Length: **31.0000** in
 Area: **0.2180** in²
 Total Load: **62630** lbf
 Tensile Strength: **287290** psi
 Correlation Coefficient: **0.9999**
 Modulus of Elasticity: **28423000** psi
 Load at 1% EUL: **56360** lbf
 Stress at 1% EUL: **258540** psi
 Est. Elongation: **0.1**
 Total Elongation: **7.03** %
 Position at Break: **2.778** in

Test Summary

Counter: **6710**
 Elapsed Time: **00:01:47**
 LIMS Number: **n/a**
 Project Number: **n/a**
 Sample Number: **UW1D8**
 Size: **.6**
 Grade: **270 K**
 Coil: **n/a**
 Operator: **MC**
 Condition of Sample: **Satisfactory**
 Comments:
 Procedure Name: **ASTM A416 - 7 wire strand - 40988**
 Start Date: **3/1/2012**
 Start Time: **11:46:31 AM**
 End Date: **3/1/2012**
 End Time: **11:48:18 AM**
 Workstation: **FLORIDA-DOT**
 Tested By: **tech**

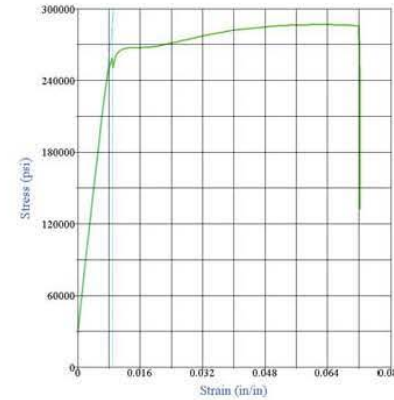
APPENDIX 3 (Continued)



Test Results
 Specimen Gage Length: **31.0000** in
 Area: **0.2180** in²
 Total Load: **62710** lbf
 Tensile Strength: **287650** psi
 Correlation Coefficient: **1.0000**
 Modulus of Elasticity: **28902000** psi
 Load at 1% EUL: **56680** lbf
 Stress at 1% EUL: **260010** psi
 Est. Elongation: **0.1**
 Total Elongation: **7.11** %
 Position at Break: **2.507** in

Test Summary

Counter: **6695**
 Elapsed Time: **00:01:42**
 LIMS Number: **n/a**
 Project Number: **n/a**
 Sample Number: **UW2D1**
 Size: **.6**
 Grade: **270 K**
 Coil: **n/a**
 Operator: **MC**
 Condition of Sample: **Satisfactory**
 Comments:
 Procedure Name: **ASTM A416 - 7 wire strand - 40988**
 Start Date: **2/29/2012**
 Start Time: **2:44:57 PM**
 End Date: **2/29/2012**
 End Time: **2:46:39 PM**
 Workstation: **FLORIDA-DOT**
 Tested By: **tech**

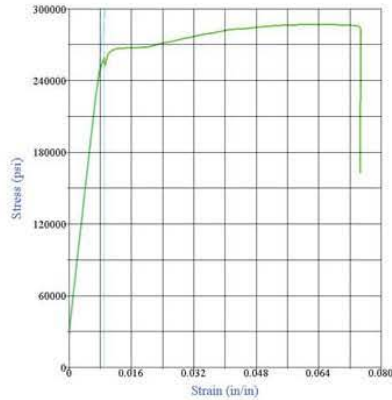


Test Results
 Specimen Gage Length: **31.0000** in
 Area: **0.2180** in²
 Total Load: **62500** lbf
 Tensile Strength: **286690** psi
 Correlation Coefficient: **0.9999**
 Modulus of Elasticity: **28576600** psi
 Load at 1% EUL: **56360** lbf
 Stress at 1% EUL: **258530** psi
 Est. Elongation: **0.1**
 Total Elongation: **7.22** %
 Position at Break: **2.609** in

Test Summary

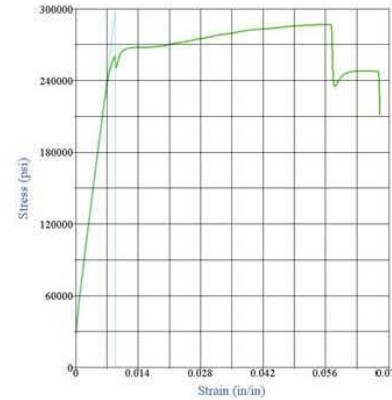
Counter: **6692**
 Elapsed Time: **00:01:51**
 LIMS Number: **n/a**
 Project Number: **n/a**
 Sample Number: **UW2D2**
 Size: **.6**
 Grade: **270 K**
 Coil: **n/a**
 Operator: **MC**
 Condition of Sample: **Satisfactory**
 Comments:
 Procedure Name: **ASTM A416 - 7 wire strand - 40988**
 Start Date: **2/29/2012**
 Start Time: **1:39:24 PM**
 End Date: **2/29/2012**
 End Time: **1:41:15 PM**
 Workstation: **FLORIDA-DOT**
 Tested By: **tech**

APPENDIX 3 (Continued)



Test Results
 Specimen Gage Length: **31.0000** in
 Area: **0.2180** in²
 Total Load: **62510** lbf
 Tensile Strength: **286760** psi
 Correlation Coefficient: **1.0000**
 Modulus of Elasticity: **28956100** psi
 Load at 1% EUL: **56440** lbf
 Stress at 1% EUL: **258880** psi
 Est. Elongation: **0.1**
 Total Elongation: **7.47** %
 Position at Break: **2.855** in

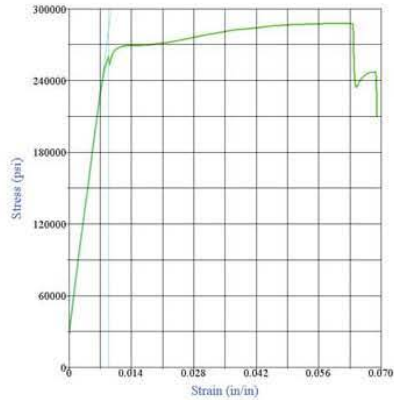
Test Summary
 Counter: **6698**
 Elapsed Time: **00:01:48**
 LIMS Number: **n/a**
 Project Number: **n/a**
 Sample Number: **UW2D3a**
 Size: **.6**
 Grade: **270 K**
 Coil: **n/a**
 Operator: **MC**
 Condition of Sample: **Satisfactory**
 Comments:
 Procedure Name: **ASTM A416 - 7 wire strand - 40988**
 Start Date: **3/1/2012**
 Start Time: **8:56:40 AM**
 End Date: **3/1/2012**
 End Time: **8:58:28 AM**
 Workstation: **FLORIDA-DOT**
 Tested By: **tech**



Test Results
 Specimen Gage Length: **31.0000** in
 Area: **0.2180** in²
 Total Load: **62510** lbf
 Tensile Strength: **286750** psi
 Correlation Coefficient: **1.0000**
 Modulus of Elasticity: **29650500** psi
 Load at 1% EUL: **56750** lbf
 Stress at 1% EUL: **260300** psi
 Est. Elongation: **0.1**
 Total Elongation: **6.78** %
 Position at Break: **2.628** in

Test Summary
 Counter: **6699**
 Elapsed Time: **00:03:01**
 LIMS Number: **n/a**
 Project Number: **n/a**
 Sample Number: **UW2D3b**
 Size: **.6**
 Grade: **270 K**
 Coil: **n/a**
 Operator: **MC**
 Condition of Sample: **Satisfactory**
 Comments:
 Procedure Name: **ASTM A416 - 7 wire strand - 40988**
 Start Date: **3/1/2012**
 Start Time: **9:04:28 AM**
 End Date: **3/1/2012**
 End Time: **9:07:29 AM**
 Workstation: **FLORIDA-DOT**
 Tested By: **tech**

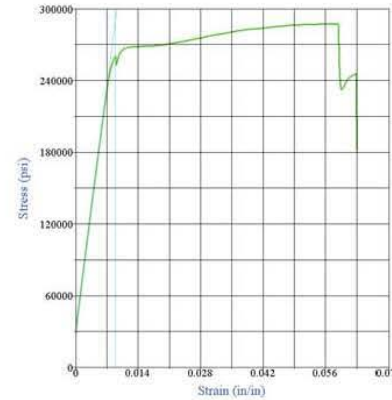
APPENDIX 3 (Continued)



Test Results
 Specimen Gage Length: **31.0000** in
 Area: **0.2180** in²
 Total Load: **62740** lbf
 Tensile Strength: **287820** psi
 Correlation Coefficient: **1.0000**
 Modulus of Elasticity: **28214700** psi
 Load at 1% EUL: **56600** lbf
 Stress at 1% EUL: **259650** psi
 Est. Elongation: **0.1**
 Total Elongation: **6.89** %
 Position at Break: **2.561** in

Test Summary

Counter: **6691**
 Elapsed Time: **00:01:45**
 LIMS Number: **n/a**
 Project Number: **n/a**
 Sample Number: **UW2D4**
 Size: **.6**
 Grade: **270 K**
 Coil: **n/a**
 Operator: **MC**
 Condition of Sample: **Satisfactory**
 Comments:
 Procedure Name: **ASTM A416 - 7 wire strand - 40988**
 Start Date: **2/29/2012**
 Start Time: **1:28:50 PM**
 End Date: **2/29/2012**
 End Time: **1:30:35 PM**
 Workstation: **FLORIDA-DOT**
 Tested By: **tech**

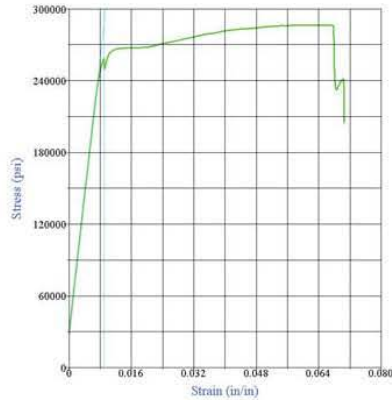


Test Results
 Specimen Gage Length: **31.0000** in
 Area: **0.2180** in²
 Total Load: **62650** lbf
 Tensile Strength: **287360** psi
 Correlation Coefficient: **1.0000**
 Modulus of Elasticity: **29015200** psi
 Load at 1% EUL: **56790** lbf
 Stress at 1% EUL: **260490** psi
 Est. Elongation: **0.1**
 Total Elongation: **6.29** %
 Position at Break: **2.284** in

Test Summary

Counter: **6690**
 Elapsed Time: **00:01:48**
 LIMS Number: **n/a**
 Project Number: **n/a**
 Sample Number: **UW2D5**
 Size: **.6**
 Grade: **270 K**
 Coil: **n/a**
 Operator: **MC**
 Condition of Sample: **Satisfactory**
 Comments:
 Procedure Name: **ASTM A416 - 7 wire strand - 40988**
 Start Date: **2/29/2012**
 Start Time: **1:19:47 PM**
 End Date: **2/29/2012**
 End Time: **1:21:35 PM**
 Workstation: **FLORIDA-DOT**
 Tested By: **tech**

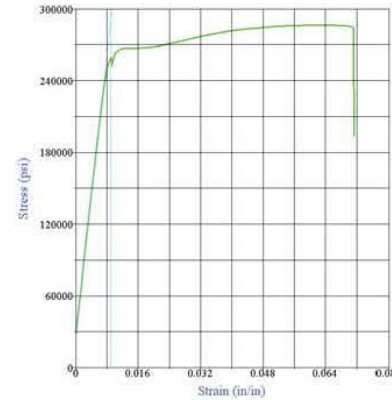
APPENDIX 3 (Continued)



Test Results
 Specimen Gage Length: **31.0000** in
 Area: **0.2180** in²
 Total Load: **62450** lbf
 Tensile Strength: **286480** psi
 Correlation Coefficient: **0.9999**
 Modulus of Elasticity: **28642600** psi
 Load at 1% EUL: **56400** lbf
 Stress at 1% EUL: **258700** psi
 Est. Elongation: **0.1**
 Total Elongation: **7.04** %
 Position at Break: **2.482** in

Test Summary

Counter: **6696**
 Elapsed Time: **00:02:22**
 LIMS Number: **n/a**
 Project Number: **n/a**
 Sample Number: **UW2D6**
 Size: **.6**
 Grade: **270 K**
 Coil: **n/a**
 Operator: **MC**
 Condition of Sample: **Satisfactory**
 Comments:
 Procedure Name: **ASTM A416 - 7 wire strand - 40988**
 Start Date: **3/1/2012**
 Start Time: **8:37:30 AM**
 End Date: **3/1/2012**
 End Time: **8:39:52 AM**
 Workstation: **FLORIDA-DOT**
 Tested By: **tech**

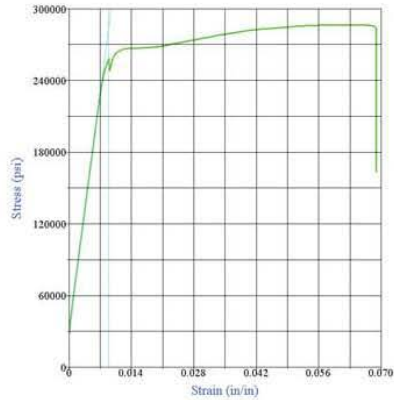


Test Results
 Specimen Gage Length: **31.0000** in
 Area: **0.2180** in²
 Total Load: **62430** lbf
 Tensile Strength: **286370** psi
 Correlation Coefficient: **0.9999**
 Modulus of Elasticity: **29182700** psi
 Load at 1% EUL: **56520** lbf
 Stress at 1% EUL: **259250** psi
 Est. Elongation: **0.1**
 Total Elongation: **7.12** %
 Position at Break: **2.549** in

Test Summary

Counter: **6694**
 Elapsed Time: **00:01:44**
 LIMS Number: **n/a**
 Project Number: **n/a**
 Sample Number: **UW2D7a**
 Size: **.6**
 Grade: **270 K**
 Coil: **n/a**
 Operator: **MC**
 Condition of Sample: **Satisfactory**
 Comments:
 Procedure Name: **ASTM A416 - 7 wire strand - 40988**
 Start Date: **2/29/2012**
 Start Time: **2:28:42 PM**
 End Date: **2/29/2012**
 End Time: **2:30:26 PM**
 Workstation: **FLORIDA-DOT**
 Tested By: **tech**

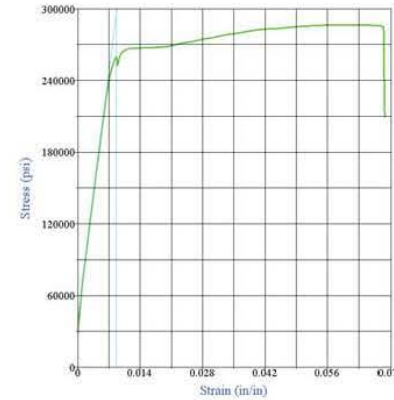
APPENDIX 3 (Continued)



Test Results
 Specimen Gage Length: **31.0000** in
 Area: **0.2180** in²
 Total Load: **62460** lbf
 Tensile Strength: **286530** psi
 Correlation Coefficient: **1.0000**
 Modulus of Elasticity: **28382600** psi
 Load at 1% EUL: **56180** lbf
 Stress at 1% EUL: **257700** psi
 Est. Elongation: **0.1**
 Total Elongation: **6.89** %
 Position at Break: **2.626** in

Test Summary

Counter: **6693**
 Elapsed Time: **00:02:59**
 LIMS Number: **n/a**
 Project Number: **n/a**
 Sample Number: **UW2D7b**
 Size: **.6**
 Grade: **270 K**
 Coil: **n/a**
 Operator: **MC**
 Condition of Sample: **Satisfactory**
 Comments:
 Procedure Name: **ASTM A416 - 7 wire strand - 40988**
 Start Date: **2/29/2012**
 Start Time: **1:50:07 PM**
 End Date: **2/29/2012**
 End Time: **1:53:06 PM**
 Workstation: **FLORIDA-DOT**
 Tested By: **tech**

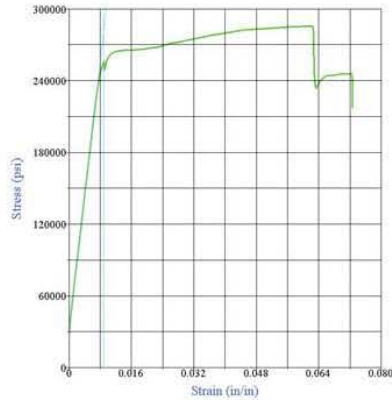


Test Results
 Specimen Gage Length: **31.0000** in
 Area: **0.2180** in²
 Total Load: **62460** lbf
 Tensile Strength: **286530** psi
 Correlation Coefficient: **1.0000**
 Modulus of Elasticity: **29645400** psi
 Load at 1% EUL: **56670** lbf
 Stress at 1% EUL: **259930** psi
 Est. Elongation: **0.1**
 Total Elongation: **6.84** %
 Position at Break: **2.541** in

Test Summary

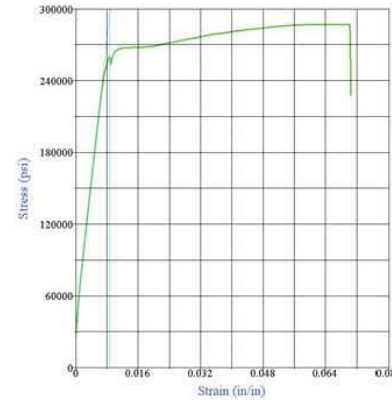
Counter: **6697**
 Elapsed Time: **00:01:48**
 LIMS Number: **n/a**
 Project Number: **n/a**
 Sample Number: **UW2D8**
 Size: **.6**
 Grade: **270 K**
 Coil: **n/a**
 Operator: **MC**
 Condition of Sample: **Satisfactory**
 Comments:
 Procedure Name: **ASTM A416 - 7 wire strand - 40988**
 Start Date: **3/1/2012**
 Start Time: **8:51:20 AM**
 End Date: **3/1/2012**
 End Time: **8:53:08 AM**
 Workstation: **FLORIDA-DOT**
 Tested By: **tech**

APPENDIX 3 (Continued)



Test Results
 Specimen Gage Length: **31.0000** in
 Area: **0.2180** in²
 Total Load: **62230** lbf
 Tensile Strength: **285440** psi
 Correlation Coefficient: **1.0000**
 Modulus of Elasticity: **28171600** psi
 Load at 1% EUL: **55730** lbf
 Stress at 1% EUL: **255650** psi
 Est. Elongation: **0.1**
 Total Elongation: **7.25** %
 Position at Break: **2.795** in

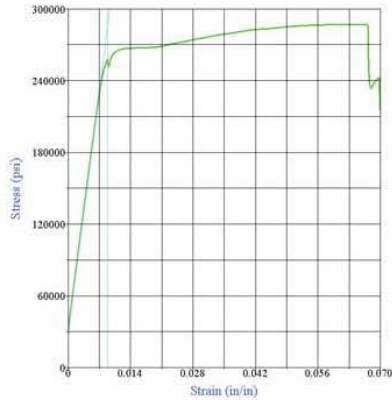
Test Summary
 Counter: **6685**
 Elapsed Time: **00:02:00**
 LIMS Number: **n/a**
 Project Number: **n/a**
 Sample Number: **UW4D1**
 Size: **.6**
 Grade: **270 K**
 Coil: **n/a**
 Operator: **MC**
 Condition of Sample: **Satisfactory**
 Comments:
 Procedure Name: **ASTM A416 - 7 wire strand - 40988**
 Start Date: **2/29/2012**
 Start Time: **11:30:42 AM**
 End Date: **2/29/2012**
 End Time: **11:32:42 AM**
 Workstation: **FLORIDA-DOT**
 Tested By: **tech**



Test Results
 Specimen Gage Length: **31.0000** in
 Area: **0.2180** in²
 Total Load: **62580** lbf
 Tensile Strength: **287050** psi
 Correlation Coefficient: **0.9999**
 Modulus of Elasticity: **29627100** psi
 Load at 1% EUL: **56680** lbf
 Stress at 1% EUL: **259980** psi
 Est. Elongation: **0.1**
 Total Elongation: **7.04** %
 Position at Break: **2.960** in

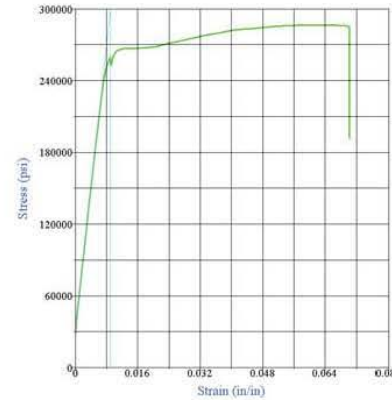
Test Summary
 Counter: **6686**
 Elapsed Time: **00:01:52**
 LIMS Number: **n/a**
 Project Number: **n/a**
 Sample Number: **UW4D2**
 Size: **.6**
 Grade: **270 K**
 Coil: **n/a**
 Operator: **MC**
 Condition of Sample: **Satisfactory**
 Comments:
 Procedure Name: **ASTM A416 - 7 wire strand - 40988**
 Start Date: **2/29/2012**
 Start Time: **11:39:40 AM**
 End Date: **2/29/2012**
 End Time: **11:41:32 AM**
 Workstation: **FLORIDA-DOT**
 Tested By: **tech**

APPENDIX 3 (Continued)



Test Results
 Specimen Gage Length: **31.0000** in
 Area: **0.2180** in²
 Total Load: **62540** lbf
 Tensile Strength: **286890** psi
 Correlation Coefficient: **1.0000**
 Modulus of Elasticity: **28476900** psi
 Load at 1% EUL: **56190** lbf
 Stress at 1% EUL: **257740** psi
 Est. Elongation: **0.1**
 Total Elongation: **6.97** %
 Position at Break: **2.574** in

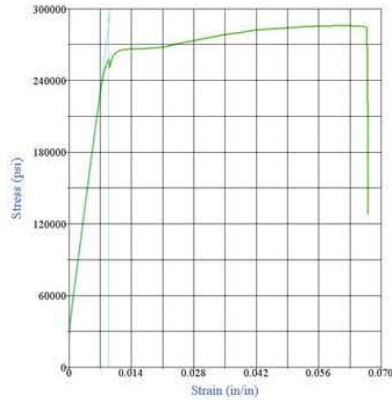
Test Summary
 Counter: **6682**
 Elapsed Time: **00:01:45**
 LIMS Number: **n/a**
 Project Number: **n/a**
 Sample Number: **UW4D3a**
 Size: **.6**
 Grade: **270 K**
 Coil: **n/a**
 Operator: **MC**
 Condition of Sample: **Satisfactory**
 Comments:
 Procedure Name: **ASTM A416 - 7 wire strand - 40988**
 Start Date: **2/29/2012**
 Start Time: **11:09:27 AM**
 End Date: **2/29/2012**
 End Time: **11:11:12 AM**
 Workstation: **FLORIDA-DOT**
 Tested By: **tech**



Test Results
 Specimen Gage Length: **31.0000** in
 Area: **0.2180** in²
 Total Load: **62450** lbf
 Tensile Strength: **286470** psi
 Correlation Coefficient: **0.9999**
 Modulus of Elasticity: **29721400** psi
 Load at 1% EUL: **56580** lbf
 Stress at 1% EUL: **259540** psi
 Est. Elongation: **0.1**
 Total Elongation: **7.01** %
 Position at Break: **2.662** in

Test Summary
 Counter: **6688**
 Elapsed Time: **00:01:43**
 LIMS Number: **n/a**
 Project Number: **n/a**
 Sample Number: **UW4D3b**
 Size: **.6**
 Grade: **270 K**
 Coil: **n/a**
 Operator: **MC**
 Condition of Sample: **Satisfactory**
 Comments:
 Procedure Name: **ASTM A416 - 7 wire strand - 40988**
 Start Date: **2/29/2012**
 Start Time: **1:01:53 PM**
 End Date: **2/29/2012**
 End Time: **1:03:36 PM**
 Workstation: **FLORIDA-DOT**
 Tested By: **tech**

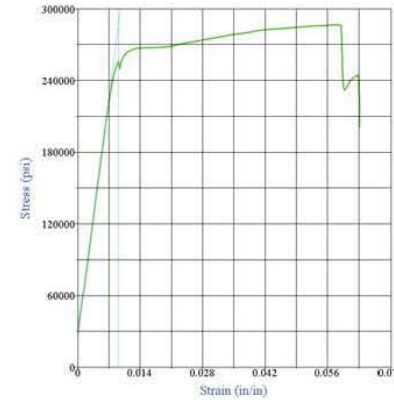
APPENDIX 3 (Continued)



Test Results
 Specimen Gage Length: **31.0000** in
 Area: **0.2180** in²
 Total Load: **62310** lbf
 Tensile Strength: **285830** psi
 Correlation Coefficient: **1.0000**
 Modulus of Elasticity: **28649800** psi
 Load at 1% EUL: **56150** lbf
 Stress at 1% EUL: **257570** psi
 Est. Elongation: **0.1**
 Total Elongation: **6.69** %
 Position at Break: **2.444** in

Test Summary

Counter: **6687**
 Elapsed Time: **00:01:41**
 LIMS Number: **n/a**
 Project Number: **n/a**
 Sample Number: **UW4D4**
 Size: **.6**
 Grade: **270 K**
 Coil: **n/a**
 Operator: **MC**
 Condition of Sample: **Satisfactory**
 Comments:
 Procedure Name: **ASTM A416 - 7 wire strand - 40988**
 Start Date: **2/29/2012**
 Start Time: **12:53:09 PM**
 End Date: **2/29/2012**
 End Time: **12:54:50 PM**
 Workstation: **FLORIDA-DOT**
 Tested By: **tech**

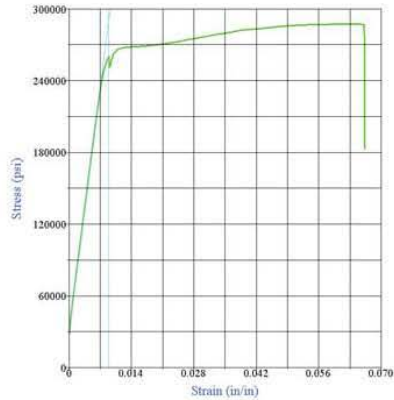


Test Results
 Specimen Gage Length: **31.0000** in
 Area: **0.2180** in²
 Total Load: **62440** lbf
 Tensile Strength: **286400** psi
 Correlation Coefficient: **1.0000**
 Modulus of Elasticity: **28678400** psi
 Load at 1% EUL: **55850** lbf
 Stress at 1% EUL: **256210** psi
 Est. Elongation: **0.1**
 Total Elongation: **6.31** %
 Position at Break: **2.417** in

Test Summary

Counter: **6684**
 Elapsed Time: **00:01:53**
 LIMS Number: **n/a**
 Project Number: **n/a**
 Sample Number: **UW4D5**
 Size: **.6**
 Grade: **270 K**
 Coil: **n/a**
 Operator: **MC**
 Condition of Sample: **Satisfactory**
 Comments:
 Procedure Name: **ASTM A416 - 7 wire strand - 40988**
 Start Date: **2/29/2012**
 Start Time: **11:20:31 AM**
 End Date: **2/29/2012**
 End Time: **11:22:24 AM**
 Workstation: **FLORIDA-DOT**
 Tested By: **tech**

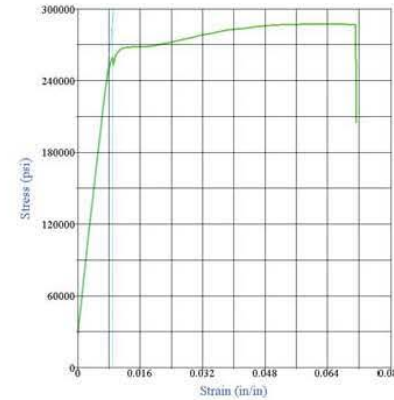
APPENDIX 3 (Continued)



Test Results
 Specimen Gage Length: **31.0000** in
 Area: **0.2180** in²
 Total Load: **62630** lbf
 Tensile Strength: **287300** psi
 Correlation Coefficient: **1.0000**
 Modulus of Elasticity: **29010500** psi
 Load at 1% EUL: **56670** lbf
 Stress at 1% EUL: **259950** psi
 Est. Elongation: **0.1**
 Total Elongation: **6.62** %
 Position at Break: **2.593** in

Test Summary

Counter: **6680**
 Elapsed Time: **00:02:36**
 LIMS Number: **n/a**
 Project Number: **n/a**
 Sample Number: **UW4D6**
 Size: **.6**
 Grade: **270 K**
 Coil: **n/a**
 Operator: **MC**
 Condition of Sample: **Satisfactory**
 Comments:
 Procedure Name: **ASTM A416 - 7 wire strand - 40988**
 Start Date: **2/29/2012**
 Start Time: **10:50:21 AM**
 End Date: **2/29/2012**
 End Time: **10:52:57 AM**
 Workstation: **FLORIDA-DOT**
 Tested By: **tech**

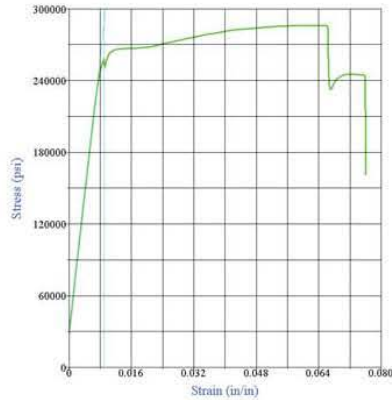


Test Results
 Specimen Gage Length: **31.0000** in
 Area: **0.2180** in²
 Total Load: **62640** lbf
 Tensile Strength: **287340** psi
 Correlation Coefficient: **0.9999**
 Modulus of Elasticity: **28805600** psi
 Load at 1% EUL: **56560** lbf
 Stress at 1% EUL: **259460** psi
 Est. Elongation: **0.1**
 Total Elongation: **7.12** %
 Position at Break: **2.652** in

Test Summary

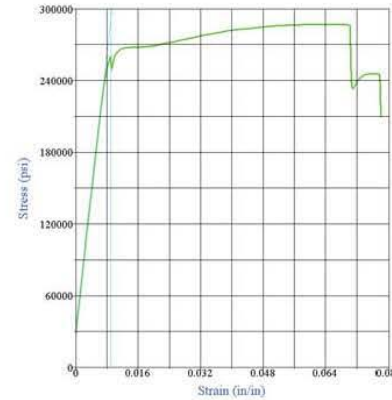
Counter: **6689**
 Elapsed Time: **00:01:43**
 LIMS Number: **n/a**
 Project Number: **n/a**
 Sample Number: **UW4D7a**
 Size: **.6**
 Grade: **270 K**
 Coil: **n/a**
 Operator: **MC**
 Condition of Sample: **Satisfactory**
 Comments:
 Procedure Name: **ASTM A416 - 7 wire strand - 40988**
 Start Date: **2/29/2012**
 Start Time: **1:12:04 PM**
 End Date: **2/29/2012**
 End Time: **1:13:47 PM**
 Workstation: **FLORIDA-DOT**
 Tested By: **tech**

APPENDIX 3 (Continued)



Test Results
 Specimen Gage Length: **31.0000** in
 Area: **0.2180** in²
 Total Load: **62390** lbf
 Tensile Strength: **286200** psi
 Correlation Coefficient: **1.0000**
 Modulus of Elasticity: **28700200** psi
 Load at 1% EUL: **56240** lbf
 Stress at 1% EUL: **257960** psi
 Est. Elongation: **0.1**
 Total Elongation: **7.59** %
 Position at Break: **2.960** in

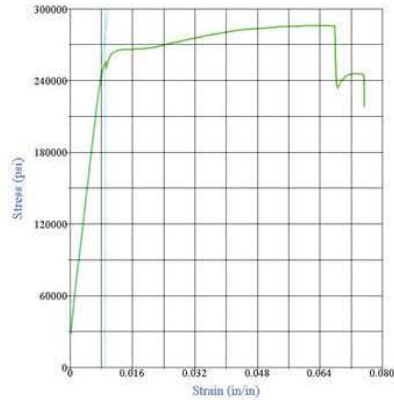
Test Summary
 Counter: **6683**
 Elapsed Time: **00:01:56**
 LIMS Number: **n/a**
 Project Number: **n/a**
 Sample Number: **UW4D7b**
 Size: **.6**
 Grade: **270 K**
 Coil: **n/a**
 Operator: **MC**
 Condition of Sample: **Satisfactory**
 Comments:
 Procedure Name: **ASTM A416 - 7 wire strand - 40988**
 Start Date: **2/29/2012**
 Start Time: **11:14:19 AM**
 End Date: **2/29/2012**
 End Time: **11:16:15 AM**
 Workstation: **FLORIDA-DOT**
 Tested By: **tech**



Test Results
 Specimen Gage Length: **31.0000** in
 Area: **0.2180** in²
 Total Load: **62530** lbf
 Tensile Strength: **286850** psi
 Correlation Coefficient: **0.9998**
 Modulus of Elasticity: **29118200** psi
 Load at 1% EUL: **56680** lbf
 Stress at 1% EUL: **259980** psi
 Est. Elongation: **0.1**
 Total Elongation: **7.77** %
 Position at Break: **2.854** in

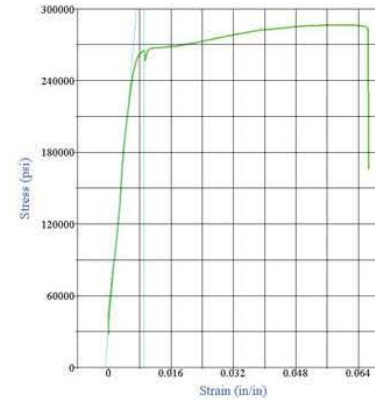
Test Summary
 Counter: **6681**
 Elapsed Time: **00:04:01**
 LIMS Number: **n/a**
 Project Number: **n/a**
 Sample Number: **UW4D8**
 Size: **.6**
 Grade: **270 K**
 Coil: **n/a**
 Operator: **MC**
 Condition of Sample: **Satisfactory**
 Comments:
 Procedure Name: **ASTM A416 - 7 wire strand - 40988**
 Start Date: **2/29/2012**
 Start Time: **11:00:31 AM**
 End Date: **2/29/2012**
 End Time: **11:04:32 AM**
 Workstation: **FLORIDA-DOT**
 Tested By: **tech**

APPENDIX 3 (Continued)



Test Results
 Specimen Gage Length: **31.0000** in
 Area: **0.2180** in²
 Total Load: **62330** lbf
 Tensile Strength: **285940** psi
 Correlation Coefficient: **1.0000**
 Modulus of Elasticity: **28011000** psi
 Load at 1% EUL: **55770** lbf
 Stress at 1% EUL: **255820** psi
 Est. Elongation: **0.1**
 Total Elongation: **7.52** %
 Position at Break: **2.882** in

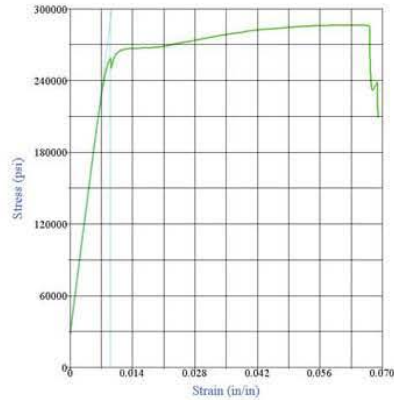
Test Summary
 Counter: **6675**
 Elapsed Time: **00:01:50**
 LIMS Number: **n/a**
 Project Number: **n/a**
 Sample Number: **UW8D1**
 Size: **.6**
 Grade: **270 K**
 Coil: **n/a**
 Operator: **MC**
 Condition of Sample: **Satisfactory**
 Comments:
 Procedure Name: **ASTM A416 - 7 wire strand - 40988**
 Start Date: **2/29/2012**
 Start Time: **9:07:26 AM**
 End Date: **2/29/2012**
 End Time: **9:09:16 AM**
 Workstation: **FLORIDA-DOT**
 Tested By: **tech**



Test Results
 Specimen Gage Length: **31.0000** in
 Area: **0.2180** in²
 Total Load: **62450** lbf
 Tensile Strength: **286470** psi
 Correlation Coefficient: **0.9939**
 Modulus of Elasticity: **37219700** psi
 Load at 1% EUL: **57790** lbf
 Stress at 1% EUL: **265110** psi
 Est. Elongation: **0.1**
 Total Elongation: **6.65** %
 Position at Break: **2.561** in

Test Summary
 Counter: **6664**
 Elapsed Time: **00:01:48**
 LIMS Number: **n/a**
 Project Number: **n/a**
 Sample Number: **UW8D2**
 Size: **.6**
 Grade: **270 K**
 Coil: **n/a**
 Operator: **MC**
 Condition of Sample: **Satisfactory**
 Comments:
 Procedure Name: **ASTM A416 - 7 wire strand - 40988**
 Start Date: **2/28/2012**
 Start Time: **2:09:39 PM**
 End Date: **2/28/2012**
 End Time: **2:11:27 PM**
 Workstation: **FLORIDA-DOT**
 Tested By: **tech**

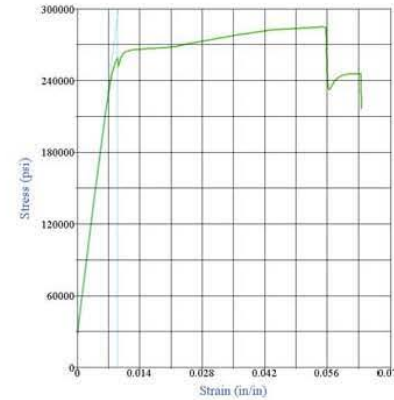
APPENDIX 3 (Continued)



Test Results
 Specimen Gage Length: **31.0000** in
 Area: **0.2180** in²
 Total Load: **62430** lbf
 Tensile Strength: **286390** psi
 Correlation Coefficient: **1.0000**
 Modulus of Elasticity: **28980800** psi
 Load at 1% EUL: **56350** lbf
 Stress at 1% EUL: **258490** psi
 Est. Elongation: **0.1**
 Total Elongation: **6.88** %
 Position at Break: **2.549** in

Test Summary

Counter: **6676**
 Elapsed Time: **00:02:04**
 LIMS Number: **n/a**
 Project Number: **n/a**
 Sample Number: **UW8D3a**
 Size: **.6**
 Grade: **270 K**
 Coil: **n/a**
 Operator: **MC**
 Condition of Sample: **Satisfactory**
 Comments:
 Procedure Name: **ASTM A416 - 7 wire strand - 40988**
 Start Date: **2/29/2012**
 Start Time: **9:27:12 AM**
 End Date: **2/29/2012**
 End Time: **9:29:16 AM**
 Workstation: **FLORIDA-DOT**
 Tested By: **tech**

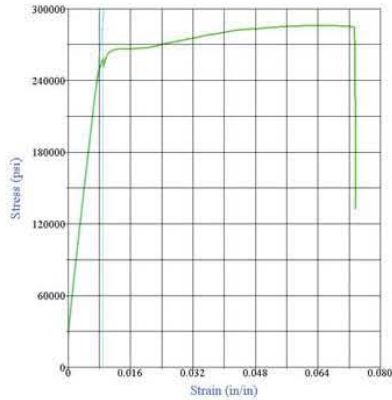


Test Results
 Specimen Gage Length: **31.0000** in
 Area: **0.2180** in²
 Total Load: **62100** lbf
 Tensile Strength: **284870** psi
 Correlation Coefficient: **0.9999**
 Modulus of Elasticity: **29364100** psi
 Load at 1% EUL: **56390** lbf
 Stress at 1% EUL: **258670** psi
 Est. Elongation: **0.1**
 Total Elongation: **6.35** %
 Position at Break: **2.619** in

Test Summary

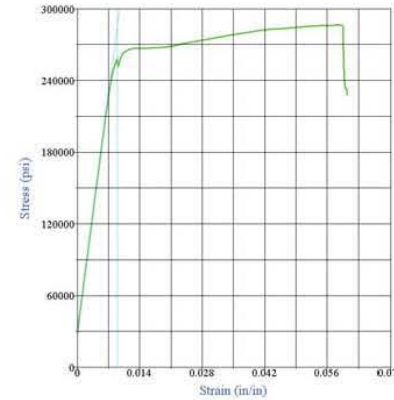
Counter: **6679**
 Elapsed Time: **00:01:49**
 LIMS Number: **n/a**
 Project Number: **n/a**
 Sample Number: **UW8D3b**
 Size: **.6**
 Grade: **270 K**
 Coil: **n/a**
 Operator: **MC**
 Condition of Sample: **Satisfactory**
 Comments:
 Procedure Name: **ASTM A416 - 7 wire strand - 40988**
 Start Date: **2/29/2012**
 Start Time: **10:40:17 AM**
 End Date: **2/29/2012**
 End Time: **10:42:06 AM**
 Workstation: **FLORIDA-DOT**
 Tested By: **tech**

APPENDIX 3 (Continued)



Test Results
 Specimen Gage Length: **31.0000** in
 Area: **0.2180** in²
 Total Load: **62340** lbf
 Tensile Strength: **285960** psi
 Correlation Coefficient: **1.0000**
 Modulus of Elasticity: **28770400** psi
 Load at 1% EUL: **56240** lbf
 Stress at 1% EUL: **257960** psi
 Est. Elongation: **0.1**
 Total Elongation: **7.35** %
 Position at Break: **2.799** in

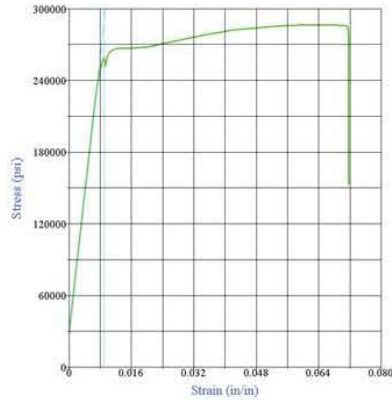
Test Summary
 Counter: **6674**
 Elapsed Time: **00:01:55**
 LIMS Number: **n/a**
 Project Number: **n/a**
 Sample Number: **UW8D4**
 Size: **.6**
 Grade: **270 K**
 Coil: **n/a**
 Operator: **MC**
 Condition of Sample: **Satisfactory**
 Comments:
 Procedure Name: **ASTM A416 - 7 wire strand - 40988**
 Start Date: **2/29/2012**
 Start Time: **8:55:29 AM**
 End Date: **2/29/2012**
 End Time: **8:57:24 AM**
 Workstation: **FLORIDA-DOT**
 Tested By: **tech**



Test Results
 Specimen Gage Length: **31.0000** in
 Area: **0.2180** in²
 Total Load: **62400** lbf
 Tensile Strength: **286250** psi
 Correlation Coefficient: **1.0000**
 Modulus of Elasticity: **28467100** psi
 Load at 1% EUL: **56270** lbf
 Stress at 1% EUL: **258130** psi
 Est. Elongation: **0.1**
 Total Elongation: **6.03** %
 Position at Break: **2.428** in

Test Summary
 Counter: **6673**
 Elapsed Time: **00:01:42**
 LIMS Number: **n/a**
 Project Number: **n/a**
 Sample Number: **UW8D5**
 Size: **.6**
 Grade: **270 K**
 Coil: **n/a**
 Operator: **MC**
 Condition of Sample: **Satisfactory**
 Comments:
 Procedure Name: **ASTM A416 - 7 wire strand - 40988**
 Start Date: **2/29/2012**
 Start Time: **8:49:46 AM**
 End Date: **2/29/2012**
 End Time: **8:51:28 AM**
 Workstation: **FLORIDA-DOT**
 Tested By: **tech**

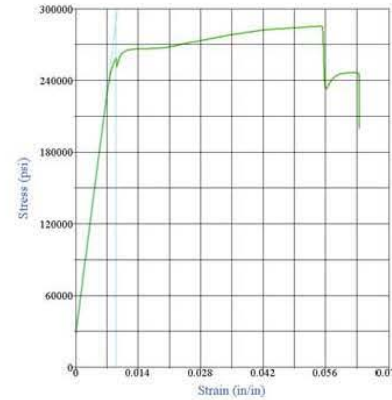
APPENDIX 3 (Continued)



Test Results
 Specimen Gage Length: **31.0000** in
 Area: **0.2180** in²
 Total Load: **62450** lbf
 Tensile Strength: **286450** psi
 Correlation Coefficient: **1.0000**
 Modulus of Elasticity: **28910300** psi
 Load at 1% EUL: **56480** lbf
 Stress at 1% EUL: **259060** psi
 Est. Elongation: **0.1**
 Total Elongation: **7.16** %
 Position at Break: **2.606** in

Test Summary

Counter: **6672**
 Elapsed Time: **00:01:59**
 LIMS Number: **n/a**
 Project Number: **n/a**
 Sample Number: **UW8D6**
 Size: **.6**
 Grade: **270 K**
 Coil: **n/a**
 Operator: **MC**
 Condition of Sample: **Satisfactory**
 Comments:
 Procedure Name: **ASTM A416 - 7 wire strand - 40988**
 Start Date: **2/29/2012**
 Start Time: **8:36:22 AM**
 End Date: **2/29/2012**
 End Time: **8:38:21 AM**
 Workstation: **FLORIDA-DOT**
 Tested By: **tech**

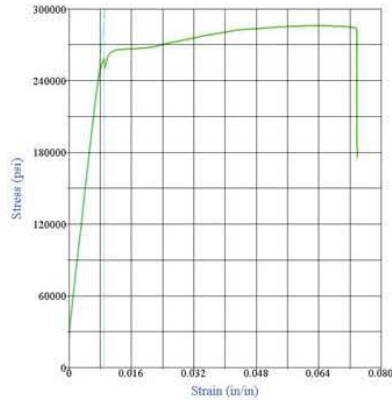


Test Results
 Specimen Gage Length: **31.0000** in
 Area: **0.2180** in²
 Total Load: **62200** lbf
 Tensile Strength: **285310** psi
 Correlation Coefficient: **1.0000**
 Modulus of Elasticity: **28888800** psi
 Load at 1% EUL: **56360** lbf
 Stress at 1% EUL: **258540** psi
 Est. Elongation: **0.1**
 Total Elongation: **6.35** %
 Position at Break: **2.429** in

Test Summary

Counter: **6671**
 Elapsed Time: **00:01:44**
 LIMS Number: **n/a**
 Project Number: **n/a**
 Sample Number: **UW8D7a**
 Size: **.6**
 Grade: **270 K**
 Coil: **n/a**
 Operator: **MC**
 Condition of Sample: **Satisfactory**
 Comments:
 Procedure Name: **ASTM A416 - 7 wire strand - 40988**
 Start Date: **2/29/2012**
 Start Time: **8:08:59 AM**
 End Date: **2/29/2012**
 End Time: **8:10:43 AM**
 Workstation: **FLORIDA-DOT**
 Tested By: **tech**

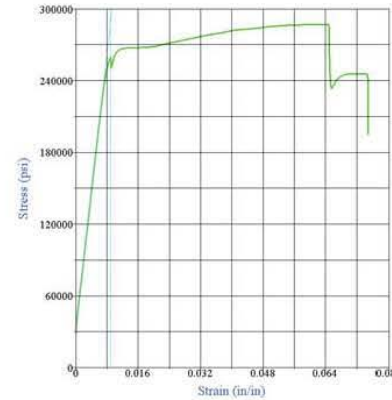
APPENDIX 3 (Continued)



Test Results
 Specimen Gage Length: **31.0000** in
 Area: **0.2180** in²
 Total Load: **62320** lbf
 Tensile Strength: **285880** psi
 Correlation Coefficient: **0.9999**
 Modulus of Elasticity: **28875500** psi
 Load at 1% EUL: **56320** lbf
 Stress at 1% EUL: **258350** psi
 Est. Elongation: **0.1**
 Total Elongation: **7.37** %
 Position at Break: **2.886** in

Test Summary

Counter: **6677**
 Elapsed Time: **00:02:09**
 LIMS Number: **n/a**
 Project Number: **n/a**
 Sample Number: **UW8D7b**
 Size: **.6**
 Grade: **270 K**
 Coil: **n/a**
 Operator: **MC**
 Condition of Sample: **Satisfactory**
 Comments:
 Procedure Name: **ASTM A416 - 7 wire strand - 40988**
 Start Date: **2/29/2012**
 Start Time: **9:33:11 AM**
 End Date: **2/29/2012**
 End Time: **9:35:20 AM**
 Workstation: **FLORIDA-DOT**
 Tested By: **tech**

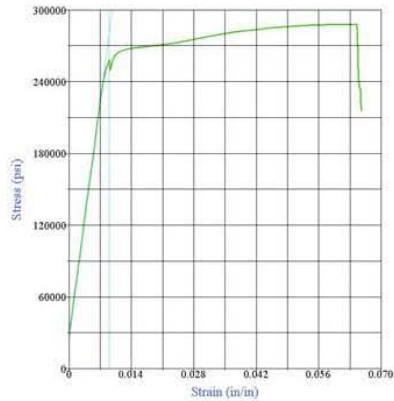


Test Results
 Specimen Gage Length: **31.0000** in
 Area: **0.2180** in²
 Total Load: **62550** lbf
 Tensile Strength: **286940** psi
 Correlation Coefficient: **1.0000**
 Modulus of Elasticity: **28889600** psi
 Load at 1% EUL: **56540** lbf
 Stress at 1% EUL: **259360** psi
 Est. Elongation: **0.1**
 Total Elongation: **7.48** %
 Position at Break: **2.785** in

Test Summary

Counter: **6678**
 Elapsed Time: **00:02:37**
 LIMS Number: **n/a**
 Project Number: **n/a**
 Sample Number: **UW8D8**
 Size: **.6**
 Grade: **270 K**
 Coil: **n/a**
 Operator: **MC**
 Condition of Sample: **Satisfactory**
 Comments:
 Procedure Name: **ASTM A416 - 7 wire strand - 40988**
 Start Date: **2/29/2012**
 Start Time: **10:20:14 AM**
 End Date: **2/29/2012**
 End Time: **10:22:51 AM**
 Workstation: **FLORIDA-DOT**
 Tested By: **tech**

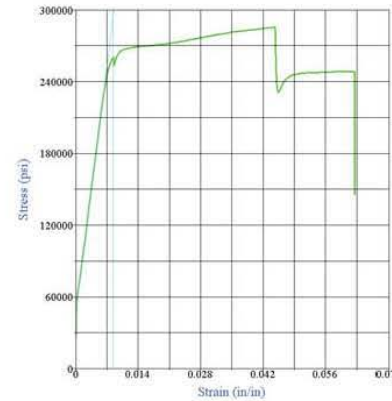
APPENDIX 3 (Continued)



Test Results
 Specimen Gage Length: 31.0000 in
 Area: 0.2180 in²
 Total Load: 62750 lbf
 Tensile Strength: 287860 psi
 Correlation Coefficient: 0.9997
 Modulus of Elasticity: 28074400 psi
 Load at 1% EUL: 56230 lbf
 Stress at 1% EUL: 257940 psi
 Est. Elongation: 0.1
 Total Elongation: 6.54 %
 Position at Break: -6.165 in

Test Summary

Counter: 6623
 Elapsed Time: 00:02:03
 LIMS Number: n/a
 Project Number: n/a
 Sample Number: UM9D4
 Size: .6
 Grade: 270 K
 Coil: n/a
 Operator: MC
 Condition of Sample: Satisfactory
 Comments:
 Procedure Name: ASTM A416 - 7 wire strand - 40988
 Start Date: 2/27/2012
 Start Time: 10:50:50 AM
 End Date: 2/27/2012
 End Time: 10:52:53 AM
 Workstation: FLORIDA-DOT
 Tested By: tech

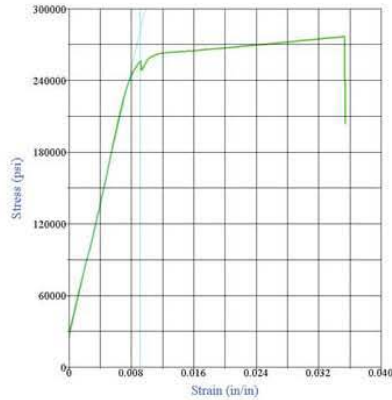


Test Results
 Specimen Gage Length: 31.0000 in
 Area: 0.2180 in²
 Total Load: 62250 lbf
 Tensile Strength: 285540 psi
 Correlation Coefficient: 0.9999
 Modulus of Elasticity: 29372800 psi
 Load at 1% EUL: 56780 lbf
 Stress at 1% EUL: 260440 psi
 Est. Elongation: 0.1
 Total Elongation: 6.25 %
 Position at Break: -6.125 in

Test Summary

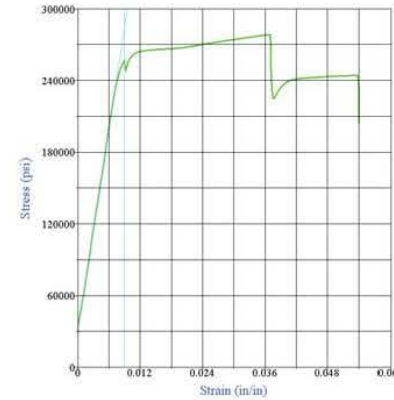
Counter: 6627
 Elapsed Time: 00:01:42
 LIMS Number: n/a
 Project Number: n/a
 Sample Number: UM9D2
 Size: .6
 Grade: 270 K
 Coil: n/a
 Operator: MC
 Condition of Sample: Satisfactory
 Comments:
 Procedure Name: ASTM A416 - 7 wire strand - 40988
 Start Date: 2/27/2012
 Start Time: 11:15:20 AM
 End Date: 2/27/2012
 End Time: 11:17:02 AM
 Workstation: FLORIDA-DOT
 Tested By: tech

APPENDIX 3 (Continued)



Test Results
 Specimen Gage Length: **31.0000** in
 Area: **0.2180** in²
 Total Load: **60320** lbf
 Tensile Strength: **276720** psi
 Correlation Coefficient: **0.9994**
 Modulus of Elasticity: **28292500** psi
 Load at 1% EUL: **55830** lbf
 Stress at 1% EUL: **256100** psi
 Est. Elongation: **0.1**
 Total Elongation: **3.53** %
 Position at Break: **1.418** in

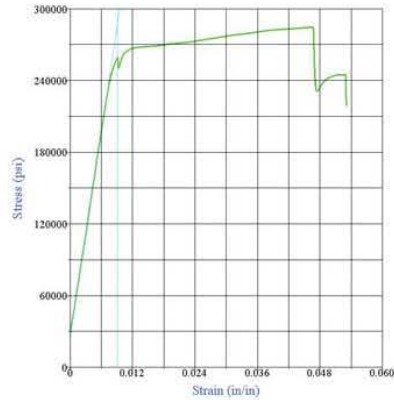
Test Summary
 Counter: **6631**
 Elapsed Time: **00:01:35**
 LIMS Number: **n/a**
 Project Number: **n/a**
 Sample Number: **UM19D3a**
 Size: **.6**
 Grade: **270 K**
 Coil: **n/a**
 Operator: **MC**
 Condition of Sample: **Satisfactory**
 Comments:
 Procedure Name: **ASTM A416 - 7 wire strand - 40988**
 Start Date: **2/27/2012**
 Start Time: **1:30:58 PM**
 End Date: **2/27/2012**
 End Time: **1:32:33 PM**
 Workstation: **FLORIDA-DOT**
 Tested By: **tech**



Test Results
 Specimen Gage Length: **31.0000** in
 Area: **0.2180** in²
 Total Load: **60680** lbf
 Tensile Strength: **278330** psi
 Correlation Coefficient: **0.9998**
 Modulus of Elasticity: **28385800** psi
 Load at 1% EUL: **55900** lbf
 Stress at 1% EUL: **256420** psi
 Est. Elongation: **0.1**
 Total Elongation: **5.40** %
 Position at Break: **-6.374** in

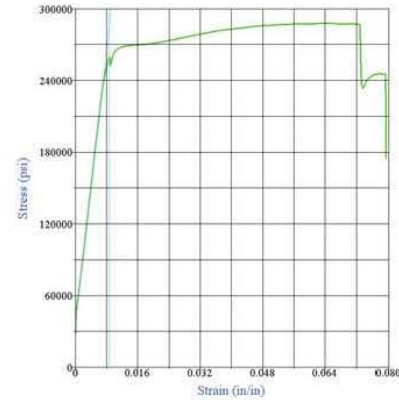
Test Summary
 Counter: **6626**
 Elapsed Time: **00:01:50**
 LIMS Number: **n/a**
 Project Number: **n/a**
 Sample Number: **UM19D3b**
 Size: **.6**
 Grade: **270 K**
 Coil: **n/a**
 Operator: **MC**
 Condition of Sample: **Satisfactory**
 Comments:
 Procedure Name: **ASTM A416 - 7 wire strand - 40988**
 Start Date: **2/27/2012**
 Start Time: **11:09:26 AM**
 End Date: **2/27/2012**
 End Time: **11:11:16 AM**
 Workstation: **FLORIDA-DOT**
 Tested By: **tech**

APPENDIX 3 (Continued)



Test Results
 Specimen Gage Length: **31.0000** in
 Area: **0.2180** in²
 Total Load: **62020** lbf
 Tensile Strength: **284500** psi
 Correlation Coefficient: **0.9999**
 Modulus of Elasticity: **28822700** psi
 Load at 1% EUL: **56470** lbf
 Stress at 1% EUL: **259030** psi
 Est. Elongation: **0.1**
 Total Elongation: **5.29** %
 Position at Break: **2.059** in

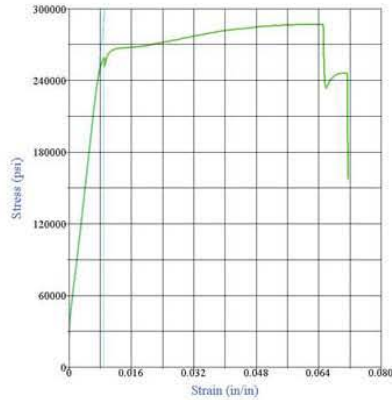
Test Summary
 Counter: **6620**
 Elapsed Time: **00:02:01**
 LIMS Number: **N/A**
 Project Number: **N/A**
 Sample Number: **UM19D4a**
 Size: **.6**
 Grade: **270 K**
 Coil: **N/A**
 Operator: **MC**
 Condition of Sample: **Satisfactory**
 Comments:
 Procedure Name: **ASTM A416 - 7 wire strand - 40988**
 Start Date: **2/23/2012**
 Start Time: **1:30:06 PM**
 End Date: **2/23/2012**
 End Time: **1:32:07 PM**
 Workstation: **FLORIDA-DOT**
 Tested By: **tech**



Test Results
 Specimen Gage Length: **31.0000** in
 Area: **0.2180** in²
 Total Load: **62710** lbf
 Tensile Strength: **287640** psi
 Correlation Coefficient: **1.0000**
 Modulus of Elasticity: **28699900** psi
 Load at 1% EUL: **56520** lbf
 Stress at 1% EUL: **259270** psi
 Est. Elongation: **0.1**
 Total Elongation: **7.92** %
 Position at Break: **-5.561** in

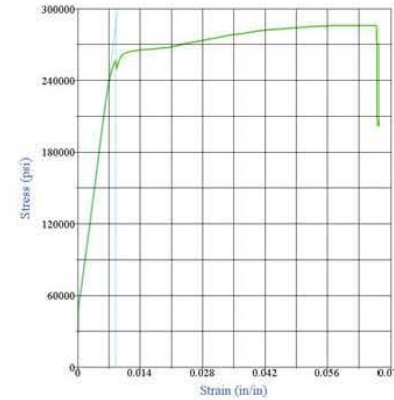
Test Summary
 Counter: **6629**
 Elapsed Time: **00:02:01**
 LIMS Number: **n/a**
 Project Number: **n/a**
 Sample Number: **UM19D4b**
 Size: **.6**
 Grade: **270 K**
 Coil: **n/a**
 Operator: **MC**
 Condition of Sample: **Satisfactory**
 Comments:
 Procedure Name: **ASTM A416 - 7 wire strand - 40988**
 Start Date: **2/27/2012**
 Start Time: **11:40:38 AM**
 End Date: **2/27/2012**
 End Time: **11:42:39 AM**
 Workstation: **FLORIDA-DOT**
 Tested By: **tech**

APPENDIX 3 (Continued)



Test Results
 Specimen Gage Length: **31.0000** in
 Area: **0.2180** in²
 Total Load: **62580** lbf
 Tensile Strength: **287060** psi
 Correlation Coefficient: **0.9999**
 Modulus of Elasticity: **28818700** psi
 Load at 1% EUL: **56450** lbf
 Stress at 1% EUL: **258930** psi
 Est. Elongation: **0.1**
 Total Elongation: **7.13** %
 Position at Break: **-8.741** in

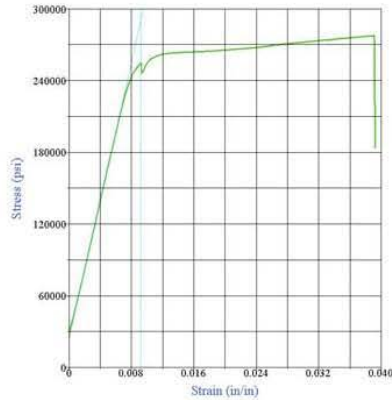
Test Summary
 Counter: **6628**
 Elapsed Time: **00:01:52**
 LIMS Number: **n/a**
 Project Number: **n/a**
 Sample Number: **UM19D5**
 Size: **.6**
 Grade: **270 K**
 Coil: **n/a**
 Operator: **MC**
 Condition of Sample: **Satisfactory**
 Comments:
 Procedure Name: **ASTM A416 - 7 wire strand - 40988**
 Start Date: **2/27/2012**
 Start Time: **11:29:17 AM**
 End Date: **2/27/2012**
 End Time: **11:31:09 AM**
 Workstation: **FLORIDA-DOT**
 Tested By: **tech**



Test Results
 Specimen Gage Length: **31.0000** in
 Area: **0.2180** in²
 Total Load: **62380** lbf
 Tensile Strength: **286140** psi
 Correlation Coefficient: **0.9999**
 Modulus of Elasticity: **28554900** psi
 Load at 1% EUL: **55940** lbf
 Stress at 1% EUL: **256620** psi
 Est. Elongation: **0.1**
 Total Elongation: **6.71** %
 Position at Break: **2.457** in

Test Summary
 Counter: **6621**
 Elapsed Time: **00:01:45**
 LIMS Number: **N/A**
 Project Number: **N/A**
 Sample Number: **UM19D7**
 Size: **.6**
 Grade: **270 K**
 Coil: **N/A**
 Operator: **MC**
 Condition of Sample: **Satisfactory**
 Comments:
 Procedure Name: **ASTM A416 - 7 wire strand - 40988**
 Start Date: **2/23/2012**
 Start Time: **1:39:24 PM**
 End Date: **2/23/2012**
 End Time: **1:41:09 PM**
 Workstation: **FLORIDA-DOT**
 Tested By: **tech**

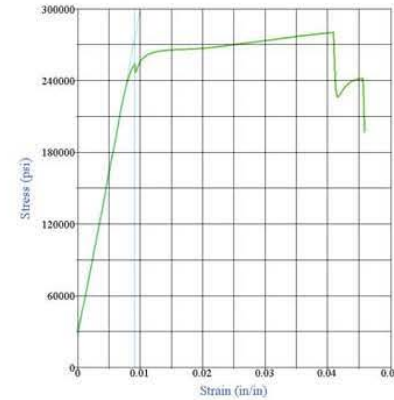
APPENDIX 3 (Continued)



Test Results
 Specimen Gage Length: **31.0000** in
 Area: **0.2180** in²
 Total Load: **60500** lbf
 Tensile Strength: **277510** psi
 Correlation Coefficient: **1.0000**
 Modulus of Elasticity: **28944800** psi
 Load at 1% EUL: **55510** lbf
 Stress at 1% EUL: **254640** psi
 Est. Elongation: **0.1**
 Total Elongation: **3.91** %
 Position at Break: **1.606** in

Test Summary

Counter: **6632**
 Elapsed Time: **00:01:51**
 LIMS Number: **n/a**
 Project Number: **n/a**
 Sample Number: **UM19D7a**
 Size: **.6**
 Grade: **270 K**
 Coil: **n/a**
 Operator: **MC**
 Condition of Sample: **Satisfactory**
 Comments:
 Procedure Name: **ASTM A416 - 7 wire strand - 40988**
 Start Date: **2/27/2012**
 Start Time: **1:37:34 PM**
 End Date: **2/27/2012**
 End Time: **1:39:25 PM**
 Workstation: **FLORIDA-DOT**
 Tested By: **tech**

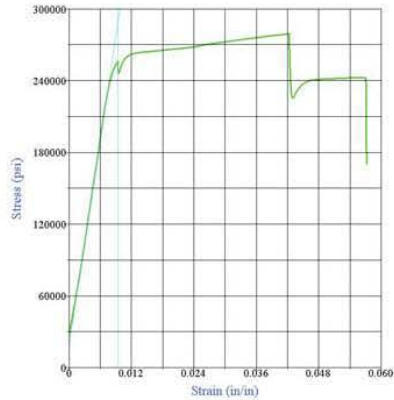


Test Results
 Specimen Gage Length: **31.0000** in
 Area: **0.2180** in²
 Total Load: **61090** lbf
 Tensile Strength: **280240** psi
 Correlation Coefficient: **0.9999**
 Modulus of Elasticity: **27416700** psi
 Load at 1% EUL: **55310** lbf
 Stress at 1% EUL: **253700** psi
 Est. Elongation: **0.1**
 Total Elongation: **4.58** %
 Position at Break: **-6.407** in

Test Summary

Counter: **6624**
 Elapsed Time: **00:01:41**
 LIMS Number: **n/a**
 Project Number: **n/a**
 Sample Number: **UM19D7b**
 Size: **.6**
 Grade: **270 K**
 Coil: **n/a**
 Operator: **MC**
 Condition of Sample: **Satisfactory**
 Comments:
 Procedure Name: **ASTM A416 - 7 wire strand - 40988**
 Start Date: **2/27/2012**
 Start Time: **10:56:23 AM**
 End Date: **2/27/2012**
 End Time: **10:58:04 AM**
 Workstation: **FLORIDA-DOT**
 Tested By: **tech**

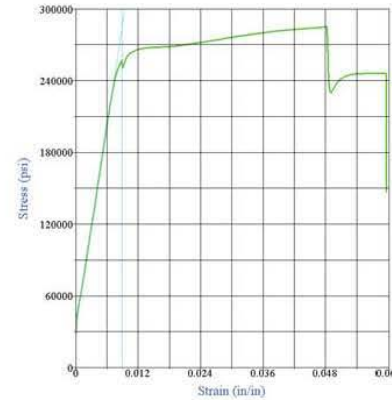
APPENDIX 3 (Continued)



Test Results
 Specimen Gage Length: **31.0000** in
 Area: **0.2180** in²
 Total Load: **60840** lbf
 Tensile Strength: **279100** psi
 Correlation Coefficient: **1.0000**
 Modulus of Elasticity: **28887700** psi
 Load at 1% EUL: **55850** lbf
 Stress at 1% EUL: **256170** psi
 Est. Elongation: **0.1**
 Total Elongation: **5.71** %
 Position at Break: **2.308** in

Test Summary

Counter: **6630**
 Elapsed Time: **00:03:17**
 LIMS Number: **n/a**
 Project Number: **n/a**
 Sample Number: **UM19D8a**
 Size: **.6**
 Grade: **270 K**
 Coil: **n/a**
 Operator: **MC**
 Condition of Sample: **Satisfactory**
 Comments:
 Procedure Name: **ASTM A416 - 7 wire strand - 40988**
 Start Date: **2/27/2012**
 Start Time: **1:21:51 PM**
 End Date: **2/27/2012**
 End Time: **1:25:08 PM**
 Workstation: **FLORIDA-DOT**
 Tested By: **tech**



Test Results
 Specimen Gage Length: **31.0000** in
 Area: **0.2180** in²
 Total Load: **62130** lbf
 Tensile Strength: **285010** psi
 Correlation Coefficient: **0.9999**
 Modulus of Elasticity: **28270900** psi
 Load at 1% EUL: **56010** lbf
 Stress at 1% EUL: **256910** psi
 Est. Elongation: **0.1**
 Total Elongation: **5.95** %
 Position at Break: **-6.323** in

Test Summary

Counter: **6625**
 Elapsed Time: **00:01:39**
 LIMS Number: **n/a**
 Project Number: **n/a**
 Sample Number: **UM19D8b**
 Size: **.6**
 Grade: **270 K**
 Coil: **n/a**
 Operator: **MC**
 Condition of Sample: **Satisfactory**
 Comments:
 Procedure Name: **ASTM A416 - 7 wire strand - 40988**
 Start Date: **2/27/2012**
 Start Time: **11:00:42 AM**
 End Date: **2/27/2012**
 End Time: **11:02:21 AM**
 Workstation: **FLORIDA-DOT**
 Tested By: **tech**